

SATELLITE PERSPECTIVES ON THE SPATIAL EXTENT OF NEW SNOWFALL
IN THE SOUTHERN APPALACHIAN MOUNTAINS

A Thesis
by
JOHNATHAN WENDELL SUGG

Submitted to the Graduate School
at Appalachian State University
in partial fulfillment of the requirements for the degree of
MASTER OF ARTS

May 2013
Department of Geography and Planning

SATELLITE PERSPECTIVES ON THE SPATIAL EXTENT OF NEW SNOWFALL
IN THE SOUTHERN APPALACHIAN MOUNTAINS

A Thesis
by
JOHNATHAN WENDELL SUGG
May 2013

APPROVED BY:

L. Baker Perry
Chairperson, Thesis Committee

Christopher A. Badurek
Member, Thesis Committee

Dorothy K. Hall
Member, Thesis Committee

Kathleen Schroeder
Chairperson, Department of Geography and Planning

Edelma D. Huntley
Dean, Cratis Williams Graduate School

Copyright by Johnathan W. Sugg 2013
All Rights Reserved

Abstract

SATELLITE PERSPECTIVES ON THE SPATIAL EXTENT OF NEW SNOWFALL IN THE SOUTHERN APPALACHIAN MOUNTAINS. (May 2013)

Johnathan W. Sugg
B.S., Appalachian State University
M.A., Appalachian State University

Chairperson: L. Baker Perry

The southern Appalachian Mountains (SAM) are a heavily forested mid-latitude mountain region and provide an ideal location for assessing the suitability of satellite-derived snow maps and explicitly linking atmospheric circulation to the spatial patterns of new snowfall. Although a variety of synoptic-scale circulation regimes contribute to mean annual snowfall (ranging from roughly 25 cm in the lowest valleys to over 250 cm at the highest elevations), atmospheric processes have largely been absent from previous efforts to quantify the spatial patterns of new snowfall.

In this thesis, the suitability of fractional snow cover (FSC) maps from the Moderate Resolution Imaging Spectroradiometer (MODIS) is examined and the spatial extent of snowfall is determined according to synoptic-scale circulation. Version 5 FSC and true color snow maps are analyzed after 122 snow events (e.g., Miller A/B cyclones, southeastward tracking clippers, and NW Flow snowfall) from October 2006 to April 2012 to provide a suitability analysis of MODIS products for use in the SAM. MODIS data are evaluated based on their suitability by snow year, climatological season, synoptic-scale circulation, and

between heavy and light snowfall events.

For each event, FSC distribution and total snow covered area are calculated and then compared with available in-situ observations from Poga Mt., North Carolina and from National Weather Service cooperative observer stations. Case studies are presented to discuss linkages of synoptic-scale circulation with resulting snow cover patterns in the context of other meteorological products. Results indicate the SAM presents unique meteorological, physical, and spectral characteristics that are ideal to evaluate the suitability of MODIS for measuring snow cover. Out of 122 observed snow events, 63 are considered suitable for analysis with the FSC maps. MODIS successfully mapped 89% of the heaviest snowfall events and less than 50% of the lighter events. The highest FSC values are observed after Miller A/B cyclones, southeastward tracking clippers, and on windward slopes following Northwest Flow snowfall events.

These findings indicate that MODIS data can be successfully used to link broader atmospheric circulation processes of snowfall with the spatial patterns of snow cover. The methods employed in this thesis are readily transferrable to other mid-latitude mountain regions with dense forest cover. In particular, these results will be useful for future studies seeking to incorporate remotely sensed data for understanding synoptic perspectives between individual events. The findings presented here are important for contributing to knowledge of future climate changes to snow cover in the SAM and in other mid-latitude mountain regions.

Acknowledgements

Many thanks are due to a number of individuals whose assistance was instrumental in the completion of this thesis. Foremost, Dr. L. Baker Perry provided valuable guidance in the formation of ideas, direction of research, and continued support for this research project. I thank Dr. Christopher A. Badurek for assistance and support with GIScience objectives and statistical analyses included in this research. Dr. Dorothy K. Hall provided much appreciated advice for using the MODIS data products and a source of encouragement for pursuing such a topic in the southern Appalachian Mountains. Dr. George A. Riggs provided further assistance using the MODIS data.

I am grateful for funding support from the ASU Office of Student Research and the Cratis D. Williams Graduate School for a Graduate Research Grant. I thank the ASU Department of Geography and Planning for assistance with travel funding.

I also acknowledge the following data sources: the National Aeronautics and Space Administration's REVERB ECHO Data Portal, the National Weather Service Cooperative Observer network, the NOAA Air Resources Laboratory (ARL), NOAA's Hydrometeorological Prediction Center, the State Climate Office of North Carolina, the University of Wisconsin-Madison Space Science and Engineering Center, and Dr. L Baker Perry for Poga Mt. snowfall data.

Lastly, I thank my family and friends for their love and support while pursuing my Master's degree.

Table of Contents

Abstract.....	iv
Acknowledgements.....	vi
List of Tables	ix
List of Figures.....	x
Chapter 1.....	1
Introduction.....	1
Literature Synthesis	4
The Importance of Snow	4
Remote Sensing of Snow.....	8
Remote Sensing of Snow in Mid-latitude Mountain Regions.....	20
Atmospheric Circulation and Snowfall Patterns	25
Snowfall in the Southern Appalachian Mountains	30
Research Design.....	41
Chapter 2.....	42
Study Area: Southern Appalachian Mountain Region	43
Snowfall Data and Event Identification.....	45
MODIS Data and Suitability Analysis	48
Image Processing and FSC Values from Snowfall Events.....	53
Surface Maps and Trajectory Analyses used in Case Studies.....	57
Chapter 3.....	61
Introduction.....	61
MODIS Suitability Analysis.....	62
Spatial Patterns of Snowfall.....	72
FSC Variability by Synoptic Class.....	72
Windward and Leeward Contrasts during NWFS.....	83
Case Studies of Notable Events	89
Miller A/B Cyclone with Upslope Flow after Event Maturation (MAB-u).....	90

Southeastward Tracking Clipper with Upslope Flow after Event Maturation (SE-U)....	95
Gulf Surface Wave or Weak Low (Non-U).....	99
Northeastward Tracking Low Passing to the North with NW Upslope Flow(NE-U)...	104
NW Upslope Flow in Absence of Frontal or Surface Features (U).....	108
Leeward Surface Cyclone with NW Upslope Flow (LC-U)	113
Upper Level Cutoff Low with NW Upslope Flow (CL-U).....	119
Chapter 4.....	124
Suitability of MODIS Snow Cover Products in Mid-latitude Mountain Environments	125
Fractional Snow Cover Variability in the SAM	127
Implications	128
Limitations.....	130
Future Work.....	132
List of Abbreviations and Acronyms.....	134
Bibliography	136
Appendix A.....	145
Appendix B.....	147
Biographical Information.....	149

List of Tables

Table 1.1. MODIS band combinations and bandwidths	17
Table 1.2. MODIS bands used in the snow cover products.....	18
Table 2.1. Synoptic classification scheme	47
Table 2.2. Summary of snow events.....	48
Table 3.1. Comparison of events by synoptic class	64
Table 3.2 Events where cloud cover $\geq 30\%$	65
Table 3.3. Distribution between heavy and light events.....	69
Table 3.4. Snow cover values between U and M*-U	77
Table 3.5. Differences in averages of meteorological data.....	83
Table 3.6. Snow cover between windward and leeward slopes.....	84
Table 3.7. Summary of case studies.....	89

List of Figures

Figure 1.1. Spectral reflectance of snow.....	10
Figure 1.2. Snow particle types	11
Figure 1.3. NOAA IMS map	13
Figure 1.4. MODIS true color and fractional snow cover	15
Figure 1.5. Terra and Aqua predicted passes.....	16
Figure 1.6. Spectral reflectance of cloud and snow	19
Figure 1.7. Visible reflectance of the snow	22
Figure 1.8. 500 hPa heights over the continental U.S.....	26
Figure 1.9. Blowing and drifting of low density snow	29
Figure 1.10. Typical synoptic pattern for Miller A/B events.....	33
Figure 1.11. Typical synoptic pattern for NWFS events	34
Figure 1.12. Distribution of NWS COOP observer stations.....	38
Figure 1.13. Blowing and drifting snow during a light NWFS event.....	39
Figure 2.1. Study area map	45
Figure 2.2. MODIS suitability schematic	50
Figure 2.3. True color snow map from 3 January 2008.....	51
Figure 2.4. True color snow map from 2 March 2010.....	51
Figure 2.5. Melting in the true color snow map.....	52
Figure 2.6. Classified FSC map for tile H11V05	53

Figure 2.7. Reclassified DEMs	55
Figure 2.8. ArcToolbox Model Builder example	56
Figure 2.9. NOAA HYSPLIT backwards air trajectory.	59
Figure 2.10. NOAA Surface analysis map from 19 December 2009	60
Figure 3.1. MODIS true color snow map on 13 April 2008.	63
Figure 3.2. FSC snow map from 15 December 2010	65
Figure 3.3. MODIS snow maps by climatological season.....	67
Figure 3.4. MODIS snow maps by snow year	68
Figure 3.5. MODIS products by synoptic class	70
Figure 3.6. Average percent cloud cover	73
Figure 3.7. Total snow covered pixels by synoptic class.....	74
Figure 3.8. Alberta Clipper true color snow map from 06 March 2012	76
Figure 3.9. Percent of snow covered area by synoptic class.....	78
Figure 3.10. Percent of total study area by synoptic class	80
Figure 3.11. Greatest snow extent by synoptic class	842
Figure 3.12. Total Snow Covered Pixels on Windward vs. Leeward Slopes	844
Figure 3.13. Average FSC during NWFS (U) events	88
Figure 3.14. FSC percent of the total study area during NWFS (U) events.	88
Figure 3.15. NOAA surface analysis from 19 December 2009.....	92
Figure 3.16. NOAA HYSPLIT backwards air trajectory	93
Figure 3.17. MODIS true color snow map from 22 December 2009	94
Figure 3.18. MODIS FSC map from 22 December 2009	94
Figure 3.19. NOAA surface analysis on 05 March 2012.....	96

Figure 3.20. NOAA HYSPLIT backwards air trajectory	97
Figure 3.21. MODIS true color image from 6 March 2012.....	98
Figure 3.22. MODIS FSC map from 6 March 2012.....	98
Figure 3.23. NOAA HYSPLIT backwards air trajectory	101
Figure 3.24. NOAA surface analysis	102
Figure 3.25. MODIS true color image from 10 February 2011.....	103
Figure 3.26. MODIS FSC map from 10 February 2011	103
Figure 3.27. NOAA HYSPLIT backwards air trajectory on 22 February 2009.....	106
Figure 3.28. NOAA surface analysis	107
Figure 3.29. MODIS true color image on 23 February 2009	107
Figure 3.30. MODIS FSC map on 23 February 2009.....	108
Figure 3.31. MODIS FSC map on 28 February 2008.....	110
Figure 3.32. NOAA surface map on 27 February 2008.....	111
Figure 3.33. NOAA HYSPLIT backwards air trajectory on 26 February 2008.....	112
Figure 3.34. MODIS true color image on 01 March 2008	113
Figure 3.35. NOAA HYSPLIT backwards air trajectory on 28 October 2008.	116
Figure 3.36. NOAA surface map on 28 October 2008	117
Figure 3.37. MODIS true color image on 29 October 2008.	118
Figure 3.38. MODIS FSC map on 29 October 2008	118
Figure 3.39. NOAA HYSPLIT backwards air trajectory on 29 November 2011	121
Figure 3.40. NOAA surface analysis on 30 November 2011	122
Figure 3.41. MODIS true color image on 01 December 2011	123
Figure 3.42. MODIS FSC map on 01 December 2011.....	123

Chapter 1

Introduction and Background

Introduction

Snow plays a crucial role in the Earth's hydrology and surface energy balance by moderating feedbacks that influence variations in the global climate system. Out of all the major land cover types, snow cover exhibits the largest seasonal variation in spatial extent and affects local to global climates through its radiative and thermal properties (Barry et al. 1985; Frei et al. 2012). In mountain regions, snowfall controls the amount of runoff throughout the melt season, affects local temperature through surface albedo feedbacks, and provides a significant resource for many populations (Barnett et al. 2005; Barry 2002; Pederson et al. 2011). Snowfall provides a major source of economic revenue through recreation and tourism development in these areas, but can also be a source of devastation during heavy events and avalanching (Elsasser and Bürki 2002; Fitzharris 1976; Millsaps and Groothuis 2003). Projections indicate that water resources will become increasingly scarce under future climate scenarios, a situation that is likely to be exacerbated in mountainous regions through enhanced warming, decreased snowfall, and earlier onset of the spring melt season (Barnett et al. 2005; IPCC AR4 Ch. 4 2007).

Assessing snow cover patterns in mountain regions remains a challenge for a variety of reasons. Topography (e.g., aspect, elevation, exposure, and slope) strongly influences snowfall accumulation and subsequent ablation processes, leading to pronounced spatial

variability of snow cover (Doesken and Judson 1997; Perry and Konrad 2006a). In-situ observations are typically limited to open areas at lower elevations and provide a coarse resolution of available snowfall data occurring on mountain tops and along high elevation ridges (Rasmussen et al. 2012). Broader synoptic circulation processes, occurring at sub-continental scales and playing out on the order of one day to one week, have largely been absent from previous studies seeking to quantify snow cover patterns in mountains (Keighton et al. 2009). In particular, it is necessary to determine how the spatial variability of snow is influenced by prevailing atmospheric conditions in mountains. Linking processes at the synoptic scale with the resulting snow covered area offers promising results for developing new forecasting techniques and improving understanding of snowfall variability (Sugg et al. 2012).

In the southern Appalachian Mountains (SAM), mean annual snowfall totals range from roughly 25 cm in the lowest valleys to over 250 cm at the highest elevations (Perry et al. 2010b). Enhanced monitoring and predictive capabilities of snow accumulation are needed because snow is particularly difficult to measure, especially when high winds result in blowing and drifting (Doesken and Judson 1997; Rasmussen et al. 2012). This characteristic is compounded by the National Weather Service (NWS) WSR-88D scanning precipitation radar performance where shallow orographic snowfall may not be detected due to beam blockage from the topography or overshooting (Keighton et al. 2009). In addition, upper air soundings are not typically located in mountain areas and thus, do not adequately convey the mesoscale atmospheric variability that exists in mountains. Integration of in-situ NWS cooperative observer (COOP) station observations with snow cover products from the Moderate Resolution Imaging Spectroradiometer (MODIS) has provided a relatively

successful method for improving modern snow mapping techniques since these sensor measurements provide a continuous spatial resolution of snow cover (Fuhrmann et al. 2010; Hall et al. 2010; Sugg et al. 2012).

Given future projections of global climate change, the expected frequency and intensity of snow events in the SAM are still largely unknown (IPCC AR4 Ch. 4 2007). For example, one hypothesis points to warmer temperatures influencing reduced snowfall totals at lower elevations but promoting an increase of certain event types at high elevations due to associated high water vapor content in the atmosphere (Perry 2006). Changing patterns of precipitation phase from snow to rain in mid-latitude mountains may subsequently affect future snowline elevations (Minder et al. 2011; Pavelsky et al. 2012). Related suggestions pinpoint amplified global circulation patterns as a major influence on increased seasonal snow cover variability at local scales (Cohen et al. 2010; Francis et al. 2009). For these reasons, validation of numerical forecast models is extremely difficult in mountainous terrain. Therefore, the integration of remotely sensed data along with COOP data offers some promise in improving snowfall monitoring and can then be used to validate numerical weather prediction (NWP) in mid-latitude mountain regions (Lackmann 2011).

Literature Synthesis

This section provides background on the importance of snow and significance to climate, remote sensing of the cryosphere including snow, and remote sensing of snow in mid-latitude, mountain regions using MODIS. Furthermore, this section outlines the relatively small body of work related to snowfall in the SAM, including seasonal climate normals, notable events, orographic snowfall, and synoptic influences on snowfall development. These topics are used to form a discussion on the influence of atmospheric circulation on snowfall patterns in the SAM. Lastly, the chapter concludes with specific objectives developed in the design of this research and highlights research questions.

The Importance of Snow

Snow is a critical natural resource with hydrologic and societal implications. Snow albedo, or reflected shortwave radiation, can influence local, regional, and hemispheric climate patterns by moderating surface energy balances through feedback mechanisms and can influence atmospheric circulation at a variety of scales (Doesken and Judson 1997; NSIDC 2012). Snow and ice cover have the largest effect on global surface albedo when compared to other cover types, especially in the high latitude regions (Frei et al. 2012). Inter-annual variability of snow cover extent has a significant influence upon the amount of radiation reaching the Earth's surface in these regions, and subsequent changes to diabatic processes can result in localized cooling or warming of surface temperatures (Cohen and Rind 1991; Robock 1980). Snow cover also acts as a thermal insulator, preventing sensible heat flux into the lower atmosphere and promoting a cooler surface environment. The high albedo, or reflectivity, of snow increases the amount of reflected energy leaving the surface.

Radiational cooling at the surface can promote a continued positive feedback mechanism, leading to negative temperature anomalies at local and regional scales (Cohen and Rind 1991).

In mountain regions, seasonal snowfall is a common occurrence and provides a valuable source of water for major population centers located downstream. More than one-sixth of the global population depends on runoff from glaciers and mountain snow packs for freshwater supply (Barnett et al. 2005). In the arid or semi-arid regions of the tropics, as much as 80% of the freshwater supply originates in mountain regions (Messerli et al. 2004). Many large cities in the Andes of Bolivia and Peru are located above 2,500 m and depend almost entirely on meltwater from snow and ice (Vuille et al. 2008). In the western United States, snowpack in the Rocky Mountains accounts for 75% of all the water in streams and rivers, and these estimates are likely much higher for other regions including the European Alps and the Himalayas. An estimated 625 million people are living in the mountains of developing countries and are highly susceptible to variations in future climate regimes (Messerli et al. 2004). Increased warming, changes to precipitation delivery as rain compared to snowfall, and growing populations have further aggravated the problem of available water resources and present a formidable challenge for sustainability.

General circulation models (GCMs) have been used in forecasting scenarios to indicate an increasing scarcity of water resources for populations that were already vulnerable (Christensen et al. 2004). Seasonal snowfall moderates the hydrologic cycle by storing water in the snowpack during winter that is gradually released by melting events throughout the spring and summer season. As warming has continued, melting events have occurred earlier in the spring and snowfall has become more variable throughout the winter, effectively

reducing the carrying capacity of a typical snow pack (Mote et al. 2005). These trends have been simulated in the Himalayan Hindu-Kush, North American Rockies, and the South American Andes, even though these regions exhibit considerable variability in precipitation delivery mechanisms (Barnett et al. 2005; Vuille et al. 2008). Demand for fresh water is typically highest during the summer and early autumn seasons, yet predicted intensity of melting events will exceed river storage capacities as winter runoff is immediately lost to the oceans earlier in the season (Barnett et al. 2005).

Mountain populations are increasingly vulnerable to hazards that result directly or indirectly from heavy snowfall events. On 7 March 2006, parts of Europe including Austria and southern Germany experienced particularly heavy snowfall of 100 cm or more over the course of several days. Many residents had to be evacuated, as building rooftops are more susceptible to collapse under the weight of the heavy snow (Pinto et al. 2007). Infrastructural damage is also common during heavy snow (Niziol 1987). Other hazards from snowfall that produce devastating effects in mountain regions include the susceptibility of snowmelt triggered landslides and snowmelt related flood risks (Graybeal and Leathers 2006; NWS 1998). Avalanches are perhaps the most significant hazard as they are especially destructive to human life and property, and are more prone to occur where the combination of heavy snow and wind loaded steep slopes is present (Birkeland and Mock 1996; Fitzharris 1976; Laternser and Schneebeli 2002). Case studies have been well documented and modeled, further characterizing the risk of deaths and property damages (Kawagoe et al. 2009).

Monitoring changes in seasonal snow is an important aspect of detecting climate change and can provide valuable information related to mitigating the future human impacts of snow in the near and long term (IPCC AR4 CH. 4 2007; Robinson and Frei 2000; Robinson 1993).

Several hypotheses exhibit concerns as to whether heavy snowfall events, with varying frequency, will become more intense as a continued result of global climate change (Cohen et al. 2010; Francis and Vavrus 2012). The role of Arctic amplification through increased warming episodes has been implicated as a determinant affecting the availability of moisture present for winter precipitation processes as well as destabilizing the lower troposphere (Francis et al., 2009). In addition, snow cover advance in the northern hemisphere autumn modulates the Siberian High, a blocking anticyclone that promotes the invasion of arctic air further south into the mid-latitudes. These conditions exhibit considerable influence on the synoptic-scale circulation in the northern hemisphere and can be used to produce a skillful winter forecast (Cohen et al. 2010; Orsolini and Kvamstø 2009; Seager et al. 2010). While processes are complex and attribution of climatic events due to anthropogenic causes is challenging, snow cover provides a major control on the dynamics of the atmosphere at multiple spatiotemporal scales (Cohen and Rind 1991).

Improved forecasting of future snowfall under climate change will offer benefits of monitoring conditions when hazards are more likely to occur in mountains, but also points the way towards extending economic benefits of winter economies through tourism opportunities. In North Carolina alone, the estimated total economic impact of winter tourism in the ski industry for 2003 was almost \$120 million, a value that is likely considerably higher today (Millsaps and Groothuis 2003). Climate change has also been documented as a major threat to tourism revenue in mountain regions on a global basis (Koenig and Abegg 1997; Messerli and Ives 1997; Scott et al. 2007). Improved forecasting techniques offer one solution for monitoring snowfall reliability, maximizing snow consistency through the use of artificial snowmaking, and increasing the longevity of the industry (Elsasser and Bürki 2002;

Steiger and Mayer 2008). For these reasons, monitoring snowfall and snow cover variation will become increasingly important at multiple scales as projected warming continues (IPCC AR4 CH. 4 2007).

Remote Sensing of Snow

While in-situ measurements of snow from automated weather stations (AWS) or from manual observations are particularly useful in making accurate measurements of snow depth, density, and other values like water equivalent, they are somewhat limiting due to high cost, low spatial coverage, and time (Rasmussen et al. 2012). Likewise, access to field sites in mountains can be especially difficult in the winter season. The development of remote sensing techniques in the satellite era have increased capabilities of acquiring large amounts of data at relatively short intervals (Robinson and Frei 2000). Thus, the scale of research has continued to evolve, allowing scientists to pursue questions related to broader geophysical patterns of the Earth's surface (Bishop et al. 2004).

The remote sensing of snow depends on the surface albedo, or the measurement of outgoing radiant energy flux divided by the incoming radiant energy flux at a specified wavelength (Warren 1982). Every feature on the Earth's surface carries a unique spectral reflectance curve that varies across wavelengths of the electromagnetic spectrum. The optical properties of snow are best defined by two features across the electromagnetic spectrum, with high reflectance values in visible wavelengths, and very low reflectance in the short-wave infrared wavelengths (Foster et al. 1987). Modern remote sensing techniques take advantage of this unique spectral combination by employing multiple algorithms onboard spaceborne

imaging radiometers and multispectral scanners, whereby a detection of higher pixel values in an image will indicate snow cover compared to other surface types (Hall et al. 2001).

The spectral reflectance of freshly deposited snow in the visible portions of the spectrum between 0.4 and 0.7 μm is very high, and exhibits a slow decrease as snow ages (Figure 1.1). The opposite effect is observed in the near-infrared, between 0.75 and 1.4 μm , when aging snow packs are marked by a considerable reduction in surface albedo (Hall et al. 2005; Wiscombe and Warren 1980). Visible albedo is affected very little by variations in grain size that occur as snow packs age or begin to melt since snow is still highly reflective to the naked eye. However, overall albedo is reduced by 25% or more when melting causes snow grains to grow and bond into larger clusters (Nolin and Liang 2000). Snow crystals offer little resemblance to their original size and shape over time and metamorphose through diurnal temperature ranges, humidity, and wind conditions (Hall et al. 2005) (Figure 1.2). Snow pack aging is also complicated by anthropogenic soot emissions, introduction of dust, or other outside matter which tend to reduce the surface albedo, making snow less detectable by sensors. Thin snow packs can be problematic for detection since reflectance values are influenced by the albedo of underlying surface cover types. The presence of cloud cover is also a major issue since cloud exhibits a similar reflectance curve to snow in the visible portion of the spectrum and because it prevents monitoring of the surface below the clouds (Ackerman et al. 1998; Platnick et al. 2003; Riggs and Hall 2002).

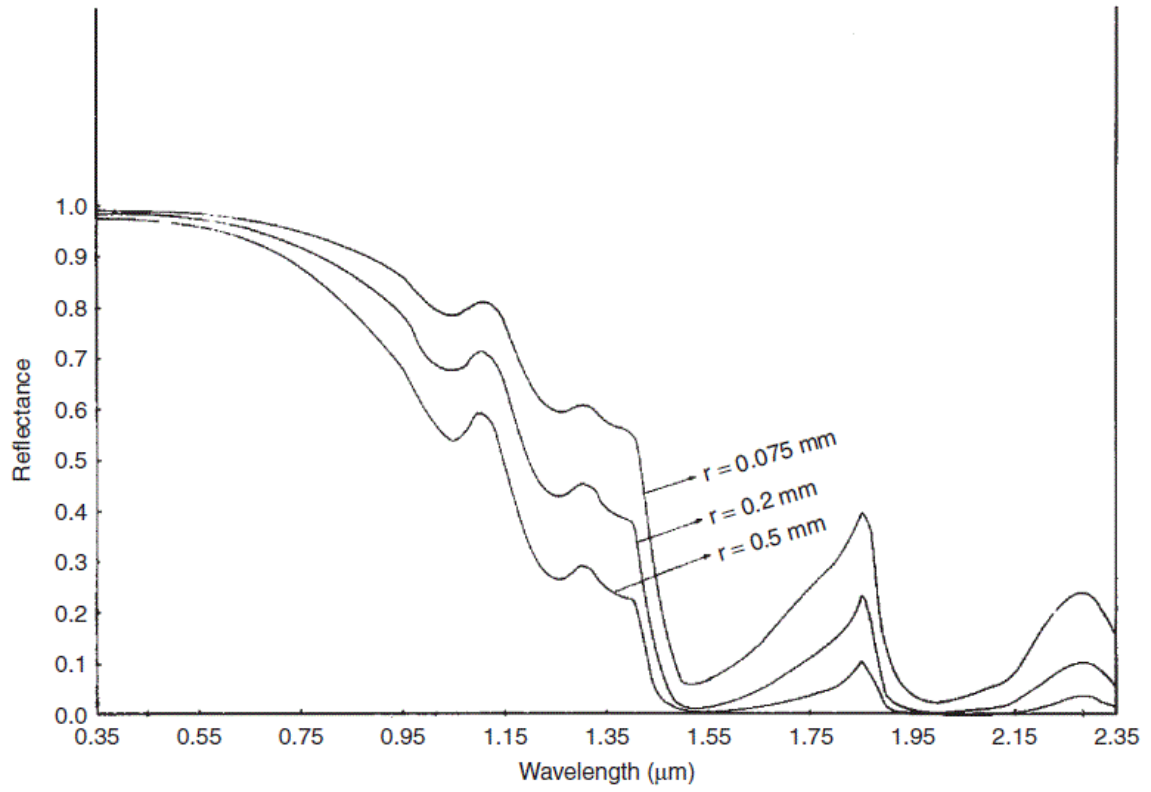


Figure 1.1. Spectral reflectance curves of various sized snow crystals. Reprinted with permission. (Choudhury and Chang 1979)

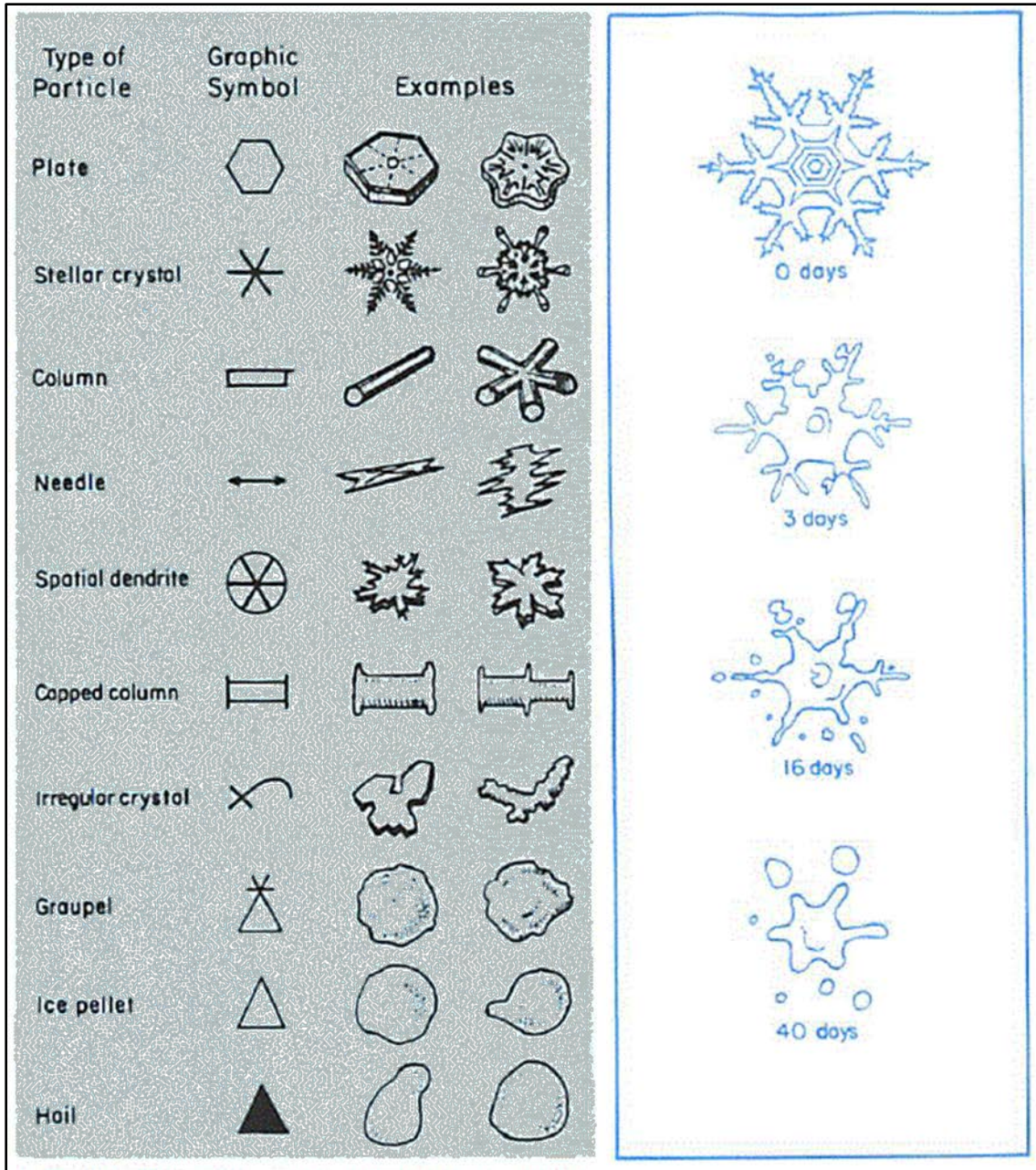


Figure 1.2. Snow particle types and temporal range of deformation. Reprinted with permission. (Doesken and Judson 1997)

The historical development of snow cover monitoring through remote sensing techniques represents a recent, yet important development for scientists to be able to improve hydrologic models and GCMs (Hall et al. 2005). Records of snow cover mapping extend back to the initial application of modern remote sensing to determine the extent of snow cover across the

northern hemisphere. This task was initiated by NOAA in 1966 using visible satellite imagery and has continued to provide one of the most consistent records of environmental data through satellite based remote sensing (Frei et al. 2012; Hall et al. 2005; Klein and Barnett 2003).

The beginning of the Landsat program in 1972, hosted by the National Aeronautics and Space Administration (NASA), allowed scientists to produce basin-wide snow cover maps from multispectral scanners at 80 m resolution using the MSS sensor (NASA 2012). While the Landsat program continues today with the TM and ETM+ sensors at 30 m resolution, it is largely unsuitable for monitoring snow cover in the SAM due to inadequate temporal resolution of the pass interval of the satellites roughly every 16 days. This point is especially relevant during the autumn and spring months when snow cover may change daily (Hall et al. 1995; Hall et al. 2005; Klein and Barnett 2003; Robinson 1993). The Landsat TM/ETM+ platform does provide a useful opportunity to ground truth performance in MODIS products since many 30 m pixels fit within one pixel at more moderate resolutions (Salomonson and Appel 2004). However, multiple studies have been conducted comparing Landsat data with other sensors in regions where snow packs are more seasonally consistent (Painter et al. 2009; Rittger et al. 2012).

Subsequent advances in technology have continued to improve the availability and resolution of snow cover data products. In 1997, the Interactive Multi-sensor Snow and Ice Mapping System (IMS) began to incorporate imagery from various sensors including the Advanced Very High Resolution Radiometer (AVHRR), the Geostationary Operational Environmental Satellite (GOES), and the Special Sensor Microwave Imager (SSM/I) to manually delineate snow and ice boundaries on a daily basis for the northern hemisphere

(Hall et al. 2005; NOAA 2013; Ramsay 1998). Under this system, imagery is incorporated with derived map products (e.g., AMSR-E and NCEP Models) and surface observations as an operational input into several NWS computer weather prediction models (NOAA 2013). This near perfect record of snow cover has allowed scientists to determine an annual net decrease in northern hemispheric snow cover since that time period (Frei et al. 2012; Robinson and Frei 2000). However, these products require analyst input, a direct shift away from an automated platform, and at 25 km resolution, present very coarse detail for scientists looking to focus on finer scales (Figure 1.3). This resolution essentially provides no value in mountain regions.

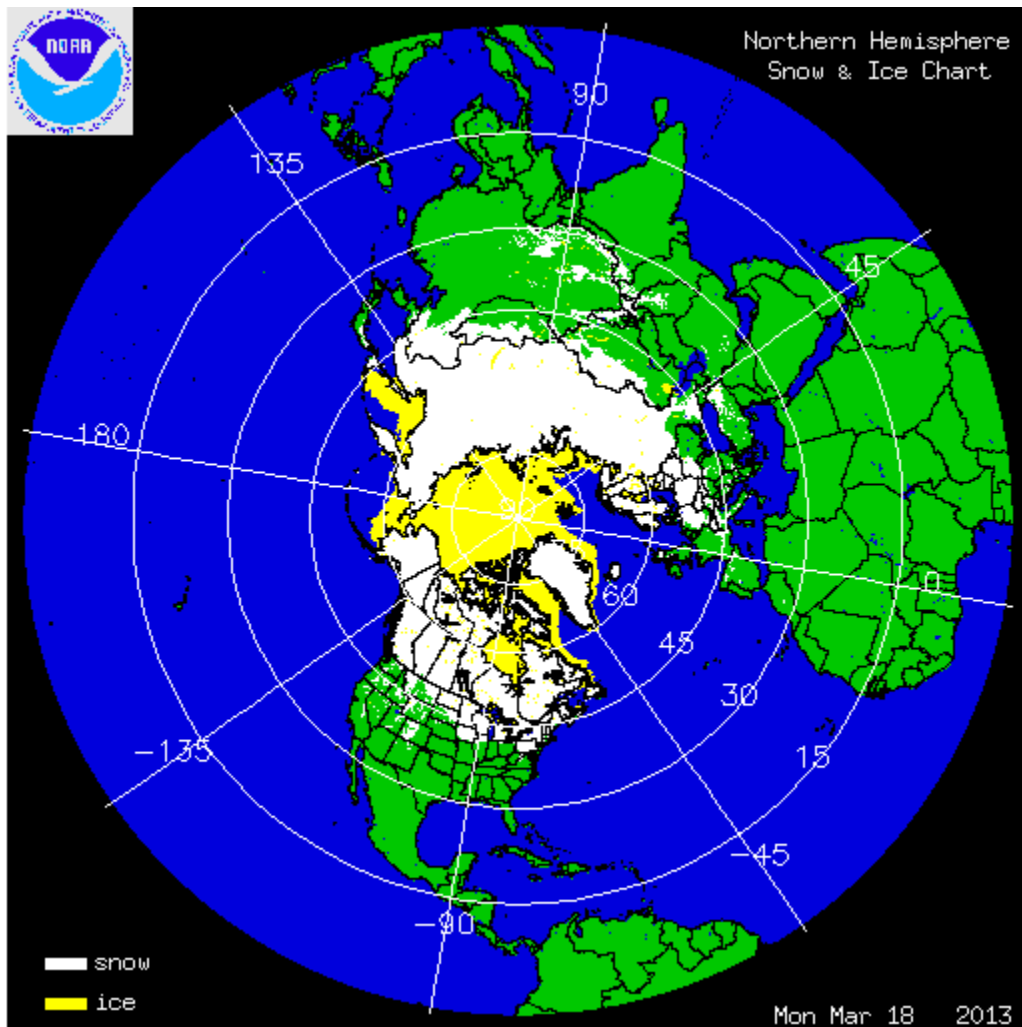


Figure 1.3. NOAA IMS snow and ice chart for the Northern Hemisphere. (NOAA 2013)

Since 1999, remotely sensed snow mapping data products have improved drastically with the development of MODIS. Launched in conjunction with the Earth Observing System on the Terra and Aqua satellites by NASA in 1999 and 2002, respectively, MODIS has since provided daily global snow cover maps at 500 m spatial resolution (Hall et al. 2002) (Figure 1.4). MODIS data have provided the ability to generate statistical coverage on a pixel by pixel basis for specifically analyzing snow cover. The original snow mapping algorithm employed on MODIS used criteria tests to satisfy snow cover classifications and in some cases, generate 250 m spatial resolution maps (Hall et al. 1995). Whereas previous remote sensing methods were adapted to perform on the Landsat TM platform, the snow mapping algorithm has proved to be more accurate in identifying snow pixels where snow coverage is greater than 60%. Thus, the move to specialized applications of MODIS imagery products represents a directional shift away from a more vegetation-based platform to observe snow at moderate scales. Snow mapping classification techniques provide more consistent results and are able to better capture the highly reflective properties of snow (Hall et al. 1995).

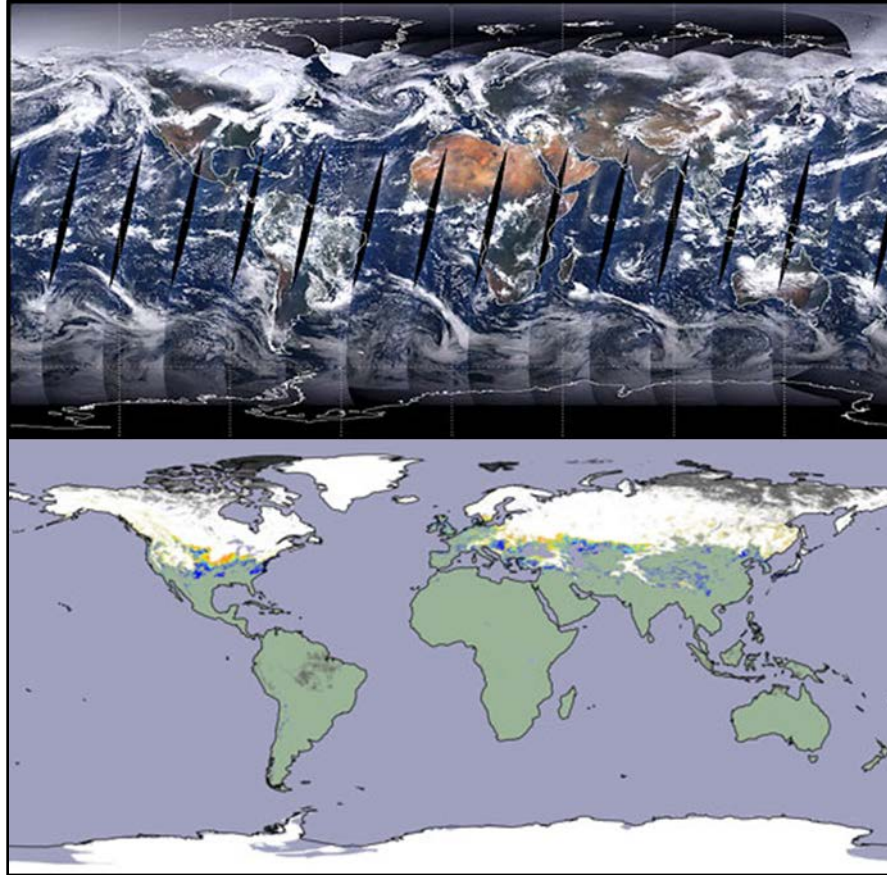


Figure 1.4. Example of the MODIS true color (upper) and global fractional snow cover maps (lower). (NASA 2013)

MODIS is an imaging radiometer that collects reflectance values from the surface using a tracking scan mirror across 36 discrete spectral bands of the electromagnetic spectrum. Terra provides a sun synchronous descending orbit, passing the equator around mid-morning, local time. Aqua provides a sun synchronous ascending orbit, though equator crossing occurs in the afternoon, local time (NASA 2012) (Figure 1.5). Sensing both the visible and thermal infrared parts of the spectrum, MODIS has a swath width on the order of $\pm 2,000$ km (Table 1.1, Table 1.2). These passes are suitable for global coverage on a daily to near-daily basis and doubles the opportunity to acquire suitable imagery when snow is detected (Hall et al. 1995).

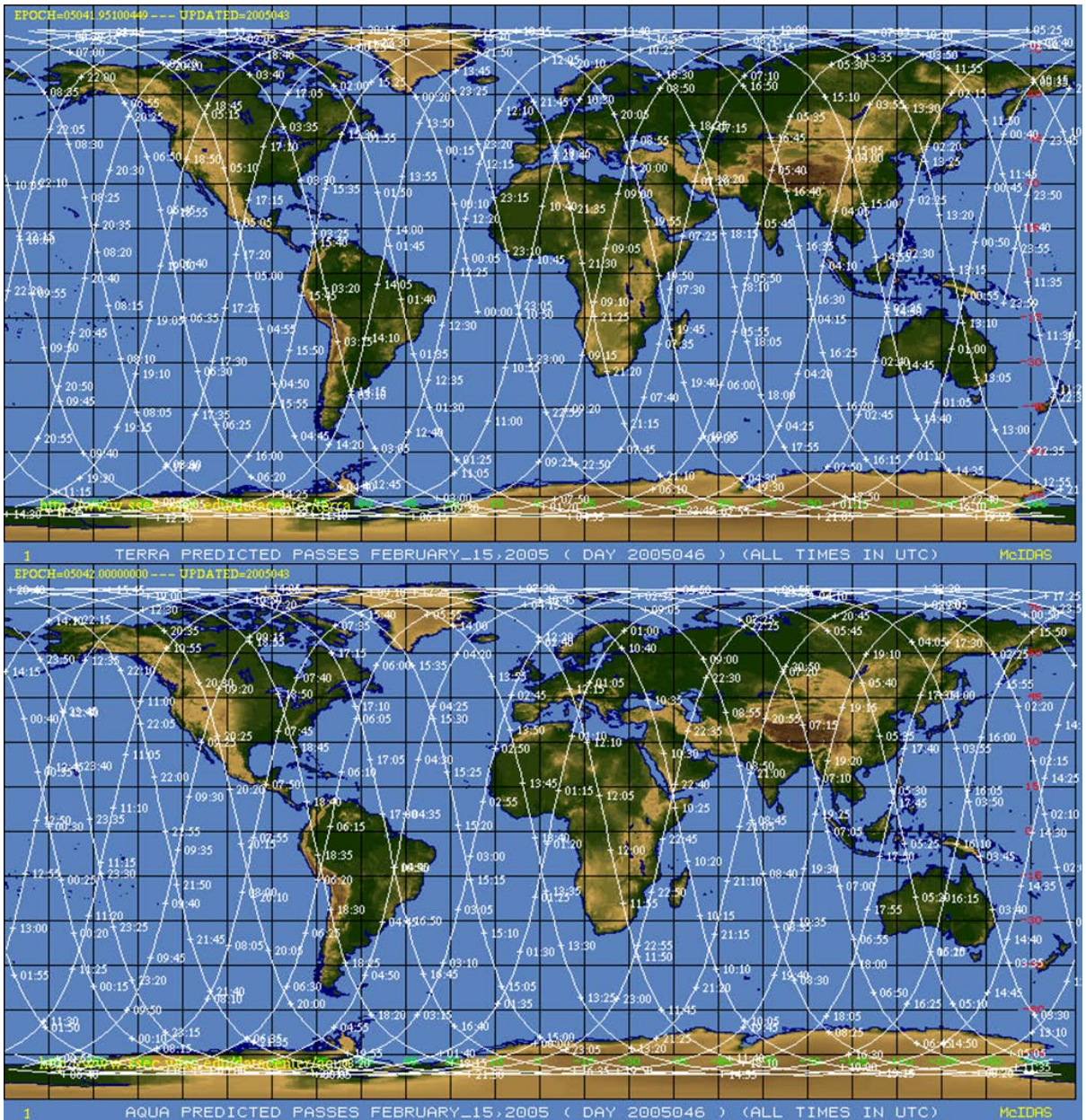


Figure 1.5. Terra (upper) and Aqua (lower) sample of predicted passes for a given day, 15 February 2005. (NSIDC 2013)

Table 1.1. Primary uses of the MODIS Band combinations and bandwidths. (NSIDC 2013)

Primary Use	Band	Bandwidth	Spectral Radiance
Land/Cloud/Aerosols Boundaries	1	620-670 nm	21.8 W
	2	841-876 nm	24.7 W
Land/Cloud/Aerosols Properties	3	459-479 nm	35.3 W
	4	545-565 nm	29.0 W
	5	1230-1250 nm	5.4 W
	6	1628-1652 nm	7.3 W
	7	2105-2155 nm	1.0 W
	8	405-420 nm	44.9 W
	9	438-448 nm	41.9 W
	10	483-493 nm	32.1 W
Ocean Color Phytoplankton Biogeochemistry	11	526-536 nm	27.9 W
	12	546-556 nm	21.0 W
	13	662-672 nm	9.5 W
	14	673-683 nm	8.7 W
	15	743-753 nm	10.2 W
	16	862-877 nm	6.2 W
Atmospheric Water Vapor	17	890-920 nm	10.0 W
	18	931-941 nm	3.6 W
	19	915-965 nm	15.0 W
Surface/Cloud Temperature	20	3.660-3.840 μm	0.45 W (300 K) ¹
	21	3.929-3.989 μm	2.38 W (335 K) ¹
	22	3.929-3.989 μm	0.67 W (300 K) ¹
	23	4.020-4.080 μm	0.79 W (300 K) ¹
Atmospheric Temperature	24	4.433-4.498 μm	0.17 W (250 K) ¹
	25	4.482-4.549 μm	0.59 W (275 K) ¹
Cirrus Clouds Water Vapor	26	1.360-1.390 μm	6.0 W
	27	6.535-6.895 μm	1.16 W (240 K) ¹
Cloud Properties	28	7.175-7.475 μm	2.18 W (250 K) ¹
	29	8.400-8.700 μm	9.58 W (300 K) ¹
Ozone	30	9.580-9.880 μm	3.69 W (250 K) ¹
Surface/Cloud Temperature	31	10.780-11.280 μm	9.55 W (300 K) ¹
	32	11.770-12.270 μm	8.94 W (300 K) ¹
	33	13.185-13.485 μm	4.52 W (260 K) ¹
Cloud Top Attitude	34	13.485-13.785 μm	3.76 W (250 K) ¹
	35	13.785-14.085 μm	3.11 W (240 K) ¹
	36	14.085-14.385 μm	2.08 W (220 K) ¹

The snow mapping algorithm takes advantage of the unique spectral combination of snow by using the Normalized Difference Snow Index (NDSI) and also incorporates elements of the Normalized Difference Vegetation Index, employed on Landsat, to account for land cover types where snowpack exists in dense forest cover (Hall et al. 2002; Klein et al. 1998). The NDSI is defined as the difference of reflectance observed in the visible band 4 and the short-wave infrared band 6 divided by the sum of the two reflectances where

$$NDSI = (b4-b6)/(b4+b6). \quad (1)$$

Like other band ratioing techniques, the NDSI reduces atmospheric influences on viewing geometry and is suitable for estimating the fractional snow cover (FSC) within a pixel. This process is critical for studying snow in more localized areas associated with small watersheds or mountainous terrain (Salomonson and Appel 2004).

Table 1.2. MODIS bands used to produce the MODIS snow cover products. Reprinted with permission. (Hall and Riggs 2007)

Band number	Bandwidth (μm)	Terra and/or Aqua
1	0.62–0.67	Terra & Aqua
2	0.841–0.876	Terra & Aqua
3	459–479	Terra & Aqua
4	0.545–0.565	Terra & Aqua
5	1230–1250	Terra & Aqua
6	1.628–1.672	Terra
7	2.105–2.155	Aqua
31	10.780–11.280	Terra & Aqua
32	11.770–12.270	Terra & Aqua

One major limitation of any multispectral system, as mentioned earlier, is the difficulty of cloud cover obscuring the surface. Efforts have been made to improve discrimination through the development of the MODIS cloud mask, since many atmospheric and surface processes require measurements that offer a clear view of the surface (Platnick et al. 2003). Cloud reflectance is often higher than that of land surfaces in visible portions of the spectrum, and in many cases, is nearly indiscernible from snow cover (Figure 1.6). This low contrast is especially noticeable when thin cirrus and low cumulus clouds are present (Ackerman et al. 1998).

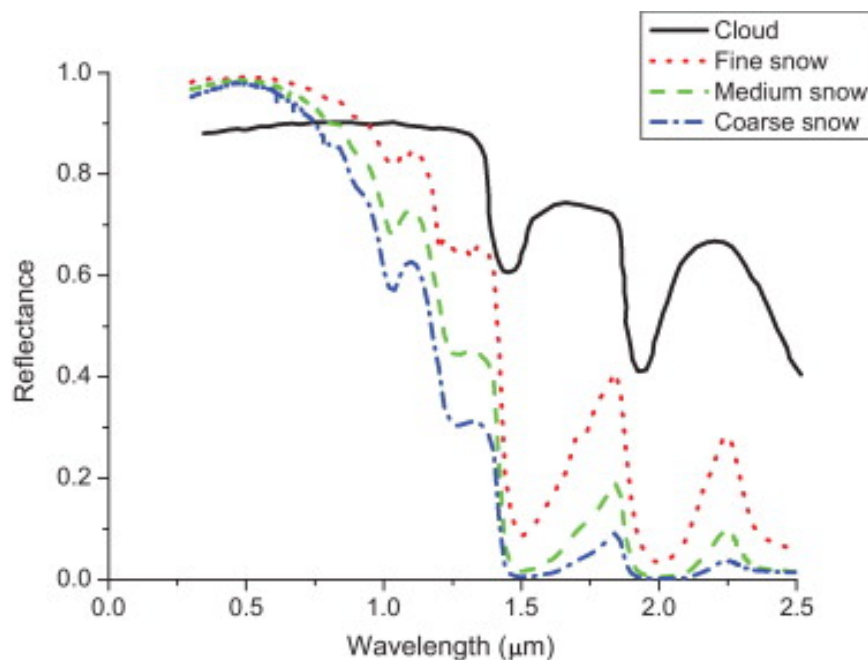


Figure 1.6. Spectral reflectance curves of cloud and snow. Reprinted from Tang et al. 2013, with permission from Elsevier.

A secondary problem occurs in the MODIS cloud mask itself, which is generally cloud conservative and often produces erroneous masking errors when snow is present on the ground (Klein and Barnett 2003). This amount of error is minimal from a quantitative perspective, but qualitatively, visual impacts of snow cover maps are negatively affected

when snow/cloud confusion occurs (Hall and Riggs 2007). Land with significant cloud-shadowing or thin, sparse snow cover along snow pack edges is most susceptible to this error. In these cases, between 0.001 and 2% error can remain after correction depending on the type and mix of clouds in the swath (Hall et al. 2001). MODIS products are most accurate in clear sky conditions where surface land cover types present the major obstacle to snow detection (Klein and Barnett 2003). In areas that are associated with significant cloud coverage during or immediately after snow events, only a minimal amount of days may be suitable for application of MODIS products to study snow cover (Hall et al. 2001).

MODIS represents a fully automated production environment with improved spectral discrimination of snow and other features. Though MODIS is limited by the presence of cloud cover blocking the surface and may not adequately capture ephemeral snow, the data are of significance for climate studies at moderate scales where quality control is necessary. MODIS snow maps are very accurate and represent the most modern application of remote sensing for monitoring snow cover (Hall et al. 1995; Hall et al. 2002; Hall et al. 2010). Over time, developments and characteristics of the snow mapping algorithm have been well documented and are kept current as products evolve (NASA 2012; Salomonson and Appel 2004).

Remote Sensing of Snow in Mid-latitude Mountain Regions

Snow monitoring has been a consistent priority for understanding variations in the global climate, but within the given studies, fewer have concentrated on snow monitoring in mountain regions with complex terrain and instead have been concerned with high latitude continental snow cover (Frei et al. 2012; Kelly et al. 2003). Mid-latitude mountain ranges

between 30 and 50 degrees present a unique opportunity for research since 26% of the global population resides within these areas and mountain snowfall is relevant from both climatic and societal perspectives (Diaz et al. 2003; Messerli et al. 2004). Detecting snow cover at moderate spatial scales in the mid-latitudes is challenging for several reasons. First, frequent thawing during the winter season is not uncommon, and variation in atmospheric circulation can produce extreme variations in temperature (Chang 2009; Watanabe and Nitta 1998). Accumulation and ablation processes are further complicated by the presence of heavily vegetated slopes and a multitude of land cover types. Extensive riming in the canopy makes snow more easily detectable whereas detecting snow cover beneath dense forest is more difficult (Sugg 2012) (Figure 1.7). Another complication is that riming may be present in the absence of snow, and cloud cover can preclude any view of the surface in multispectral imagery. These factors, in combination with the influence of topography on the spectral signature and high spatial variability of snow cover, present a major challenge for quantifying the amount of snow in the mid-latitude mountain ranges of the world (Colby 1991).

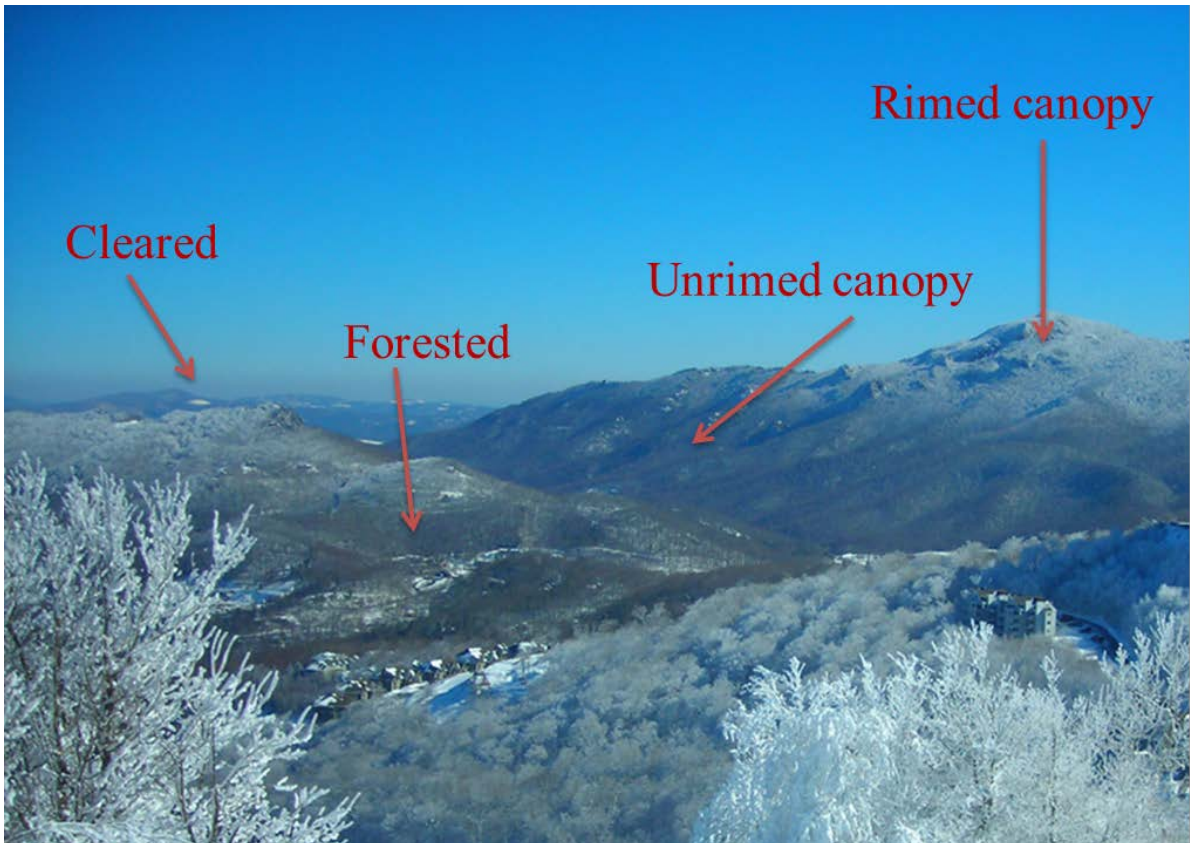


Figure 1.7. Visible reflectance of the snow in rimed canopies of the SAM compared to snow cover on the forest floor. Steep slopes with dense vegetation are also problematic for snow cover detection. Photo: Vicinity of Grandfather Mountain, North Carolina. J. Sugg.

One example from a mid-latitude mountain region using MODIS data is the Karasu Basin region in eastern Turkey. Accuracy assessments compared MODIS daily snow albedo performance with in-situ measurements from a limited network of AWS (Tekeli et al. 2006; Tekeli et al. 2005). The region is characterized by rugged topography with elevations ranging from 1,125 to 3,487 m and provided an ideal place for testing MODIS performance. In general, MODIS albedo values were within 10% of the field observations and indicated that better agreement was found at higher elevations where melting was less problematic for detecting the snow cover (Tekeli et al. 2006).

Daily snow cover maps were also compared against eight-day snow cover composites to calculate maximum snow extents given the extremely small number of weather stations. Major scale concerns occur when single ground measurements are used to provide a representative character of an area viewed by a satellite (Şorman et al. 2007). These scaling issues increased as the resolution of the satellite decreased and only exacerbated the effects of aspect, elevation, land use, and vegetation. Considerable variability may occur over short distances, and these effects may not be captured by one representative pixel value. Although MODIS tended to overestimate snow retrieval values, overall accuracy increased in this region. Similar studies are vital for improving snow mapping techniques in mountainous terrain to model snowmelt runoff and for improving forecasting capabilities (Şorman et al. 2007; Tekeli et al. 2006; Tekeli et al. 2005).

Likewise, the Sierra Nevada Mountains of eastern California served as a suitable location for testing MODIS products due to the range of topography, forest cover types, and seasonal snow cover found there (Dozier et al. 2008; Painter et al. 2009; Raleigh et al. 2013). One evaluation indicated that land surface temperature, snow grain radius, and vegetation fraction significantly reduced the accuracy of MODIS FSC measurements. Spectral mixing techniques using Landsat 30 m products were suggested as an alternative that maintained performance accuracy over multiple land cover classes and through a large topographical range (Rittger et al. 2012). However, recent updates to the snow mapping algorithm include the deletion of the temperature screen used in Version 5 of the FSC product to better capture snow surfaces in some scenarios of the Version 6 snow maps (Riggs and Hall 2012).

Previously, a portion of FSC values were blocked if they did not satisfy a series of tests related to surface temperature values of snow, a result that missed snow pixels under forest

cover (Rittger et al. 2012). The test area run over the Sierra Nevada Mountains displayed improvements in the accuracy of snow cover detection (Riggs and Hall 2012). The process of vetting various snow retrieval techniques is highlighted as a major priority in the Fourth Assessment Report of the Intergovernmental Panel on Climate Change, since uncertainties in snow extent from imprecise remote sensing retrievals limit a complete knowledge of snow albedo feedbacks in GCMs (IPCC AR4 CH. 4 2007; Rittger et al. 2012).

Accuracy assessments of the MODIS snow products were conducted for the 2000-01 snow season in the Upper Rio Grande River Basin of Colorado and New Mexico, as well as other portions of the Colorado Rockies (Hall and Riggs 2007; Klein and Barnett 2003). MODIS products were compared to the National Operational Hydrologic Remote Sensing Center (NOHRSC) snow maps and then evaluated against the network of Snowpack Telemetry (SNOTEL) station data. Over the entire snow season, MODIS and NOHRSC were marked by an overall agreement of 86%, though MODIS tended to overestimate the amount of snow cover at high elevations around the basin. SNOTEL snow depth data confirmed this tendency (Klein and Barnett 2003). MODIS consistently omits snow cover in marginal, low elevation areas where trace depths are a few centimeters or less, though this result has a minimal effect on overall accuracy when much deeper snow packs are also present. During one example, trace snow from a Colorado snow storm on 12 April 2005 was detected as cloud (Hall and Riggs 2007). Snow and cloud confusion is common, especially with ephemeral snow cover, though more studies using MODIS data are necessary to improve techniques for accurately mapping snow cover in mid-latitude mountain environments where these conditions are present.

Atmospheric Circulation and Snowfall Patterns

Although multi-scale atmospheric circulation processes exert considerable influence on the spatial patterns of snow cover and determine the location of windward and leeward slopes, few studies have explicitly linked atmospheric circulation and snowfall patterns. At global scales, the importance of hemispheric teleconnections and circulation indices are evident in the recent severe winters of 2009-10 and 2010-11 in the eastern U.S (Cohen et al. 2010). The negative phase of the Arctic Oscillation (AO) is associated with the introduction of cold polar air from extensive upper level troughing (500 hPa) (Figure 1.8). Record breaking snow cover extent and low temperatures observed across the U.S. during the period are attributed to the negative phase of the AO (Seager et al. 2010). Furthermore, the presence of the warm phase of ENSO (El Niño) provides an active northern hemisphere sub-tropical jet stream, promoting ideal conditions for snowfall in the southeast when low temperatures persist (Foster et al. 1983; Kelly et al. 2012). The extent to which these processes have influenced snow cover with specific regard to the SAM is more difficult to define. Persistent low-level NW flow was quite common during the season in addition to several major Gulf low systems that tracked northeast along the Atlantic coast, leading to positive snowfall anomalies in the mountains (Perry et al. 2010a).

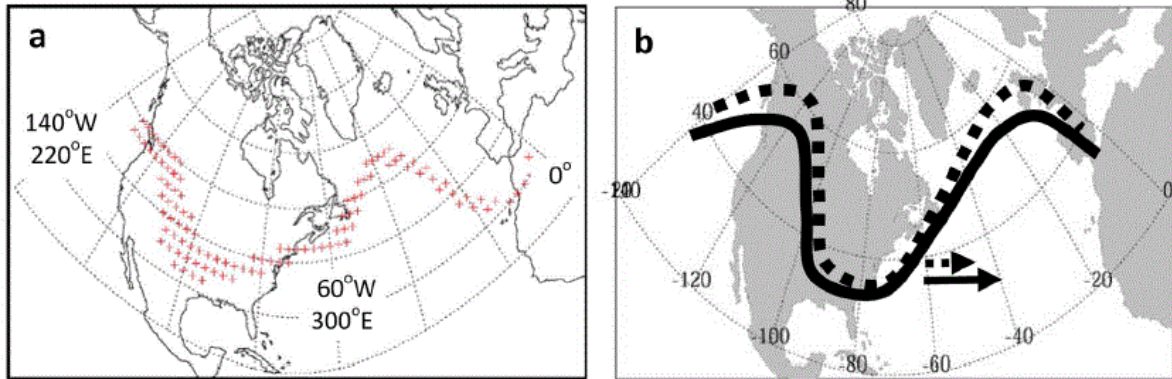


Figure 1.8. (a) Examples of selected ranges of 500 hPa heights over the continental U.S. (b) Ridge elongation in upper level heights leading to persistent high pressure outbreaks. Reprinted with permission. (Francis and Vavrus 2012)

Atmospheric circulation processes at the synoptic scale determine the amount of moisture transport available for snowfall development in the mountains. Associated antecedent upstream air trajectories are linked with the path of low level flow regimes and control the resulting snow cover patterns from orographic snowfall (Perry et al. 2007). This is especially the case when topography promotes the convective lifting required for orographic snowfall development in a conditionally unstable atmosphere (Zängl 2005). Moisture must be present in shallow layers along with low temperatures in order for snowfall to occur along windward slopes of a mountain barrier (Dore et al. 1992). Examples of synoptic influence on heavy orographic snowfall have been documented in the New Zealand Southern Alps, the northern Rockies, and in California's Sierra Nevada range (Birkeland and Mock 1996; Hooker and Fitzharris 1999; Neiman et al. 2008).

In the SAM, the presence of an upper level trough provides the necessary cold air from regions further north as well as embedded vorticity maxima. Upstream anticyclones allow low level wind shifting to occur as wraparound flow from the northwest (Lackmann 2011; Perry and Konrad 2006a). The resulting snow cover pattern is typically isolated to high

elevation windward slopes and ridges, though spillover effects from high winds and low density snow may increase accumulation in leeward areas (Minder et al. 2011). This snow cover pattern is contrasted with the resulting snow cover extent of Gulf or Atlantic Lows where lowland Piedmont regions may also receive significant accumulations from intensified cyclogenesis and available moisture associated with these systems (Kelly et al. 2012). Snow cover patterns are less recognizable under these synoptic conditions since the spatial coverage of snow tends to be continuous, though the degree of synoptic influence often controls the extent and persistence of snow cover (Sugg et al. 2012).

Most of the research on snowfall development in mountains has focused upon mesoscale atmospheric processes and sought to improve high resolution numerical models. For example, slight atmospheric instability in the upstream environment can significantly enhance precipitation totals on windward slopes when cloud liquid water content is highly concentrated (Minder et al. 2011). Mesoscale investigations reveal considerable variability in the upstream environment as a major factor in determining which slopes are favored for snowfall development. Significant ice accretion in the cloud environment can yield higher fall speed velocities when snowfall occurs as graupel (Perry et al. 2008). During these scenarios, leeward slopes tend to experience very little accumulation since moisture is precipitated out very quickly along windward slopes. Atmospheric instability, available low-level moisture, and sensible and latent heat fluxes also play a major role in the location of the snowline elevation on mountain slopes (Minder et al. 2011). While the snowline is not always present in the SAM due to variability of event types, it greatly controls the spatial extent of the snow cover. Mesoscale investigations have highlighted the role of these factors

in orographic snowfall development and yielded results related to the spatial extent of snow cover that will be useful to guide future remote sensing studies.

Results from field campaigns and high resolution modeling indicate there may be important links between multi-scale atmospheric processes and the spatial patterns of snow cover (Kingsmill et al. 2008; Zängl 2005). The presence of graupel or heavily rimed snow crystals can rapidly scavenge available low-level moisture and result in higher fall speeds, a process which leads to widespread accumulations on windward slopes and significantly less precipitation in leeward areas. High winds accompany many snowfall events in the SAM, and particularly during episodes of NW flow, low density unrimed snow particles are quite common. This combination likely shifts areas of significant accumulation further downwind as extensive blowing and drifting occur well beyond the windward slopes (Minder et al. 2011) (Figure 1.9). Similar observations in the SAM suggest that distinctive bands of snow showers in the form of horizontal convective rolls also play a role in transferring the observed accumulations farther downwind than is typically observed with orographic snowfall (Schultz et al. 2004).



Figure 1.9. Blowing and drifting of low density snow is common during events with significant wind.
Photo: J. Sugg.

Characterizing the spatial patterns of snowfall is an important step in understanding the influence of multi-scaled atmospheric circulation patterns. In the SAM, changes in the topographic distribution of aspect, elevation, and slope greatly affect the spatial patterns of snow cover over short distances. Only a few studies have tackled the problem of quantifying snow cover patterns in mountains using MODIS data (Rittger et al. 2012; Tekeli et al. 2005). Despite the limited exposure, they have increased future opportunities for research in this area and have shown some promise in defining the areal snow extent in mountains, especially for significant events where the snow cover is highly recognizable. Methods using MODIS FSC data offer the most potential for addressing the limitations of previous work where limited observational networks only provided a representation of snow measurements from a few high elevation sites. Success in future research relies upon the suitability of MODIS to

address these specific problems in mountain environments and in further characterizing the multi-scaled atmospheric influences discussed here.

Snowfall in the Southern Appalachian Mountains

The general southwest to northeast trend of the mountain ranges in the SAM produces distinct windward and leeward slopes under certain event types which are enhanced by the presence of rugged topography (Perry 2006; Sugg et al. 2012). Snowfall is quite common and the unique character of the elevational gradients between locations produces remarkable differences in snowfall climatologies (Perry et al. 2007). Higher elevation sites like Mt. Mitchell in North Carolina can average as much as 75 cm more accumulation from northwest flow snowfall (NWFS) than nearby Asheville, North Carolina (Perry et al. 2007). The current 30 year average annual snowfall for Boone, North Carolina (1,015 m), located in the region, is 102 cm. The most extreme climatological gradient, however, occurs in the Great Smoky Mountains, with 30 cm mean annual snowfall in low lying valley areas, and up to 254 cm at the highest elevations (Fuhrmann et al. 2010; Perry et al. 2010b).

While many events result in snow depths of a few centimeters or trace snow in low-lying valley locations (<1,000 m), some events may be extreme, resulting in snow depths of a meter or more on mountain ridges and peaks (>1,829 m). One such case is the 7 January 1998 snowmelt-related flood at Roan Mt. where snow depths had previously reached 1.2 m in some areas (Graybeal and Leathers 2006). After a week of melting in the snowpack, a 200 mm rain-on-snow event resulted in widespread flooding, seven deaths, and an estimated \$20,000,000 in property damages (NWS 1998).

Other major snowstorms and extended snowy periods have occurred during the past fifty years. Most notable is the February/March 1960 active storm track which was also characterized by periodic episodes of NWFS (Perry 2006). Between February and late March, record snowfall totals of up to 211 cm covered the SAM. In fact, March 1960 broke all snowfall records for most locations across North Carolina. In the mountains, snowfall was an almost daily occurrence, creating emergency situations requiring the Red Cross and National Guard to airlift food and supplies into the region (Hardie 1960; Perry 2006; Perry and Konrad 2006b). Maximum snow depth reported on the ground was 144 cm on 13-14 March in Boone, with snow drifts reportedly covering mature apple trees in some sections of Avery and Watauga Counties. Frequent synoptic-scale disturbance and persistent northwest flow related to a deep 500 mb trough across the eastern U.S. allowed low temperatures to persist, prolonging the snowpack through the end of March across major portions of the SAM, and extending well into May and June for some of the highest elevations (Perry 2006; Perry and Konrad 2006b).

A more recent and possibly more historic single event is the Superstorm of March 1993. Commonly referred to as the Blizzard of '93, the single storm impacts from this event are nearly unprecedented across the region. The storm developed along a stationary front in the Gulf of Mexico and deepened rapidly as it tracked northeastward. Snowfall developed in the western mountains by the afternoon of 13 March, and by the next morning, most valley locations had received 30-61 cm of snow. Mountain peaks and ridges observed much higher snow depths (Goodge and Hammer 1993; Perry 2006). By the event end, snow depths reached nearly two meters at the most isolated high elevations with depths around one meter commonly recorded throughout the rest of the region. Roads remained impassable and most

of the mountain counties imposed a state of emergency and martial law as temperatures plummeted behind a northwest wind shift (Goodge and Hammer 1993). December 2003 and the 2009-10 winter season also stand out in more recent memory as active snowy periods marked by heavy snowfall, active storm tracks, and persistent cold temperatures (Kelly et al. 2012; Perry et al. 2010a).

Limited attention has been given to synoptic systems affecting southeast snowstorms in part due to the relative paucity of events compared to other regions where snowfall is more prevalent. Thus, two general methodologies of examining synoptic-scale features have been present in climate research; the synoptic approach and the case-study approach (Mote et al. 1997). Synoptically, snow events in the SAM are characterized by multiple schemes in which upper level circulation patterns influence the path of the storm track and provide necessary low temperatures for snowfall development. Synoptic scheme detail varies by event type. The SAM is situated solidly in the mid-latitude range between 35 and 38 °N, and is susceptible to a number of conditions ideal for the development of major snowstorms.

Synoptic activity causing the largest snowfall totals across the SAM is attributed to Miller Type A and Miller Type B cyclones (Figure 1.10), followed by a number of other event types (Miller 1946; Perry and Konrad 2006a). These Gulf low systems also develop from the primary synoptic patterns related to major snow events across the entire eastern U.S. (Kocin and Uccellini 1990). During a Type A event, cyclogenesis occurs along a frontal boundary originating in the Gulf of Mexico that allows cold continental air masses to separate from moist tropical air. The subsequent surface low generally tracks northward across the eastern seaboard and can further intensify, producing heavy snowfall in the SAM.

A Miller Type B event is characterized by surface lows that extend north along the western side of the SAM and are succeeded by secondary surface-low development along the Atlantic that continues the pattern, often producing heavy snowfall and freezing rain along the southeastern slopes of the SAM (Miller 1946). During both of the Miller A/B cyclones, isentropic lift and cyclonic vorticity advection typically provide the synoptic forcing for snowfall development during the early stages of the event evolution, while upslope flow is common after event maturation. The importance of 500-hPa differential vorticity advection, as well as the complexity of topographic barriers, has been highlighted as a major component of synoptic-scale forecasting in heavy snowstorms across the southeastern U.S. (Mote et al. 1997).

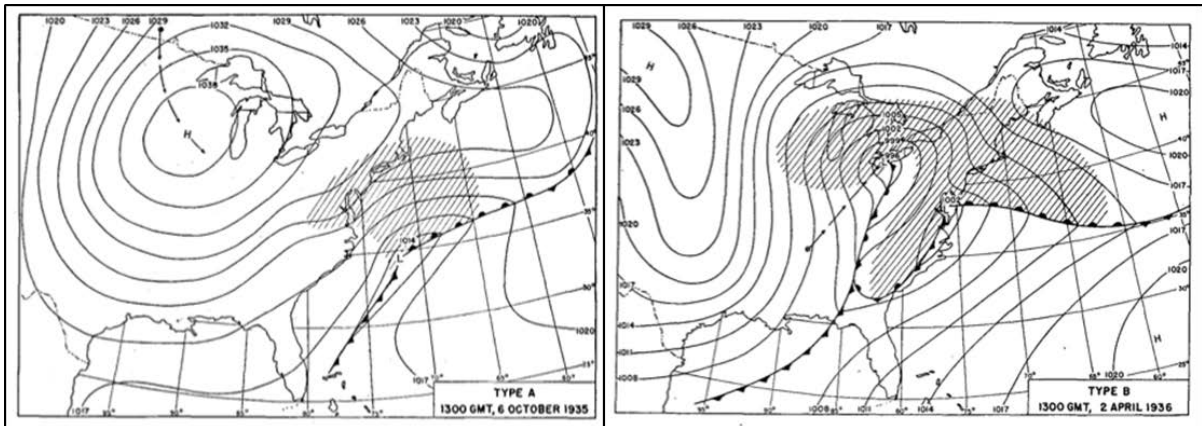


Figure 1.10. Typical synoptic pattern for Miller A (left) and Miller B (right) events. Reprinted with permission. (Miller 1946)

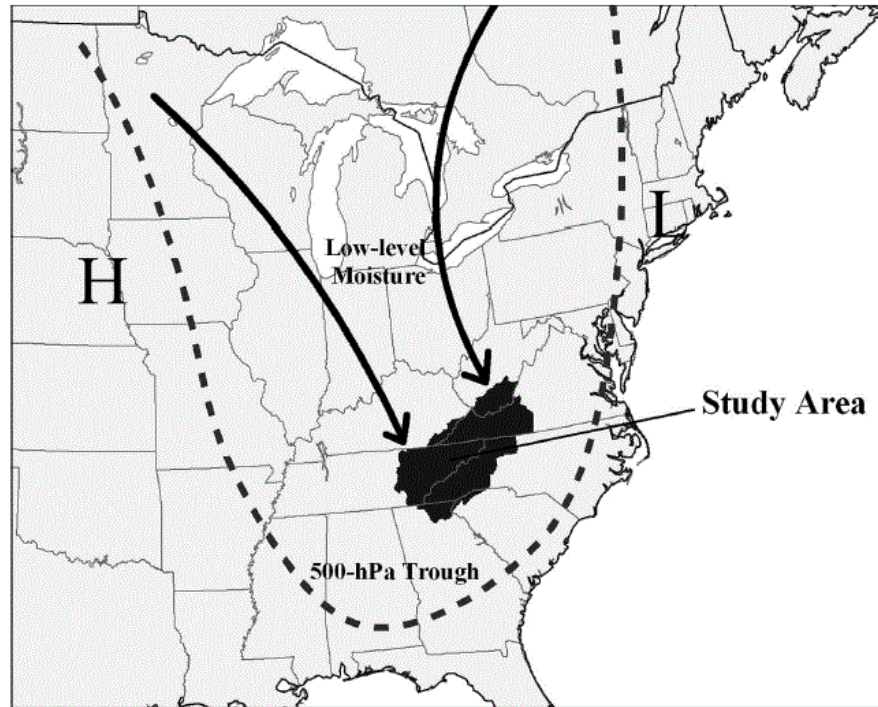


Figure 1.11. Typical synoptic pattern for NWFS events. Reprinted with permission. (Perry et al. 2007)

Other important synoptic patterns conducive to snowfall in the SAM include upper level cutoff lows, southeastward tracking clippers, and northeastward tracking Colorado lows (Perry et al. 2010b). During upper level cutoff systems, deep 500 hPa troughs can be separated from the dominate flow pattern. During these slow moving systems, temperatures below freezing in combination with vorticity maxima often produce heavy snowfall well into the valley bottoms. This pattern is contrasted with the southeastward-tracking Alberta clippers that are particularly fast moving and produce lower snowfall totals. Snowfall is also lower density (Perry et al. 2010b). The Gulf of Mexico and the Atlantic Ocean do not provide moisture in these systems as the dominant flow pattern comes from the northwest where air masses tend to be colder and drier. Finally, northeastward-tracking Colorado lows passing to the north of the region occasionally produce snowfall from isentropic lifting ahead of the frontal passage or as wraparound flow behind the system. Snow accumulations are typically

light due to lower level warm advection across southeast portions of the SAM (Perry et al. 2010b).

NWFS accounts for over 50% of annual snow events affecting the SAM and produces a distinct spatial pattern of snow cover favoring high elevation windward slopes. NWFS events occur as a result of upslope flow in absence of surface or frontal features, though it is important to note that upslope flow can also occur after the event maturation in association with most of the synoptic classes mentioned above. There are instances where only isentropic lifting and southerly flow are responsible for producing snowfall, and NWFS may not occur in these cases. Little is known about smaller scale topographic influences of variability in snow distribution from NWFS (Perry and Konrad 2006a; Perry et al. 2010b; Zängl 2005). Further assessing the synoptic classification of snow cover patterns using MODIS data is of interest for defining snow extents from multiple synoptic-scale circulation regimes. Case studies in the SAM and North Carolina piedmont have been previously conducted with relative success (Hall et al. 2010; Sugg et al. 2012).

While spatial variability of snow accumulation during NWFS events is difficult to capture from the sparse network of COOP station observations, recent simulations shed more light on the role of atmospheric, elevation, and topographic influences on variable snow covered area (Perry and Konrad 2006a; Miller 2012). These factors are important for predicting the antecedent processes of snowfall accumulation before MODIS data are analyzed. NW flow typically occurs from incoming shallow moist layers perpendicular to the major SW to NE axis of the SAM range (Figure 1.11). From a synoptic perspective, this flow pattern is often accompanied by upper level high pressure in the form of an upstream anticyclone. Surface level low pressure systems in the form of cyclones may supply available

wrap around moisture, though NW flow typically occurs in absence of synoptic-scale support (Perry et al. 2007). When a Great Lakes connection is present in low level flow patterns, shallow moisture is available for snow crystal formation as orographic lifting occurs along the North Carolina-Tennessee border. The majority of NWFS events resulting in light accumulations are a product of mid-level subsidence and limited moisture in the atmosphere. During these more common events, topography, vorticity maxima, and convection provide the necessary forcing for snowfall development (Miller 2012; Perry et al. 2007).

Multivariate regression models successfully predicted average annual NWFS, but relied heavily upon elevation as a determinant, providing a reduction in variability of spatial patterns between event types and underpredicting snowfall along lower elevation windward slopes (Perry and Konrad 2006a). In addition, backwards air trajectories were shown to be a significant determinant of the antecedent conditions leading to high regional variability of snow depths in the SAM between multiple events (Perry et al. 2007). While GIS techniques have been useful to derive relationships between topography and snowfall in the SAM, the availability of MODIS FSC data provides a unique opportunity to analyze snow cover from multiple event types on an individual basis across several gradients (e.g. elevation, slope, aspect) (Fuhrmann et al. 2010; Hall et al. 2010; Sugg et al. 2012).

Limitations for accurately measuring snowfall have not been thoroughly addressed. Consistent measurements of snow in the SAM are problematic since the network of COOP stations is sparse for high elevation areas. COOP stations are primarily situated in low lying open areas, and even then may only present a limited record of observational data (Perry and Konrad 2006a). Data are often collected by volunteers, contributing to inter-observational variability between stations. Likewise, only four COOP stations are located above 1,200 m in

the region, presenting serious limitations for making broader assessments about snowfall at high elevations (Perry et al. 2007) (Figure 1.12). In-situ observations of snow are critical, despite the coarse spatial coverage from COOP stations in mountains, since they provide ground based measurements of actual snow depth, new snowfall, and liquid water content (Rasmussen et al. 2012). These records are often the best available data in the SAM and provide a window of opportunity for assessing multiple research areas. The development of the Community Collaborative Rain, Hail, and Snow Network (CoCoRaHS) since 2006 has substantially increased the resolution of daily weather data collected by trained citizen weather volunteers, though it remains uncertain as to whether these data are useful for validating satellite imagery (CoCoRaHS 2012). These issues are of importance for addressing how well snow is measured and points the way towards developing other methods for quantifying the amount of snow on the ground (Rasmussen 2012).

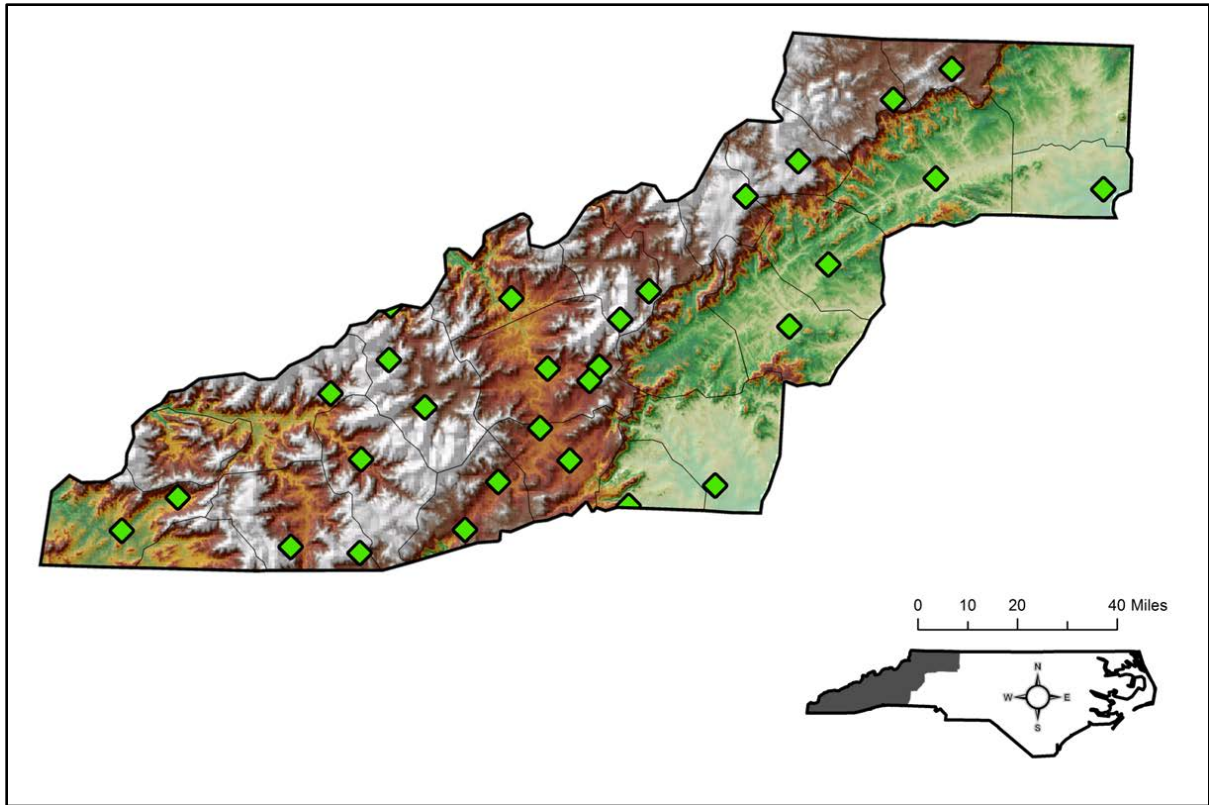


Figure 1.12. Distribution of NWS COOP observer stations across western North Carolina. Mountain locations are underrepresented.

Another limitation is that snow cover in the SAM is often ephemeral, a unique characteristic compared to other regions where a seasonal snowpack covers the ground for months out of the year. Existing on the order of hours to days as a result of environmental conditions, ephemeral snow can have significant economic consequences related to Department of Transportation snow removal operations, school or business closures, and tourism impacts in the ski industry (Fuhrmann et al. 2010; Hall et al. 2010; Millsaps and Groothuis 2003). In low lying parts of the SAM, many residents may not be used to dealing with snow outside of extreme events. Trace amounts of snow present serious challenges for accurate detection at moderate scales since coverage may not extend over an entire MODIS pixel (Figure 1.13). When ephemeral snow is present on the ground for only a few hours,

ground truthing must be conducted at the exact time of sensor overpass in order to capture snow coverage before melting occurs (Hall et al. 2010). This presents a major challenge for snow mapping at snow pack edges or where snowfall commonly melts between events (Hall and Riggs 2007). Despite the difficulty of mapping ephemeral snow, lower elevation locations (<1,000 m) present an excellent opportunity to evaluate the snow cover patterns from individual snowfall events in contrast to other areas.



Figure 1.13. Blowing and drifting snow during a light NWFS event. Flat Top Mountain, North Carolina. Photo: J. Sugg

Many elevations across the SAM experience snow accumulations that last between a few hours and a few days, depending on local conditions (Perry and Konrad 2006a). Even in higher elevation areas where precipitation commonly occurs as snowfall during the winter season, it is not uncommon for rapid melting to occur hours after event maturation. Only some MODIS imagery will be able to capture snow due to the paucity of snow cover.

However, the SAM is an ideal location to test MODIS products since the twice daily temporal resolution of the sensor increases the chances of capturing the snow cover between individual events (Hall et al. 2010).

Research Design

The objectives behind the design of this thesis are based on the following justification: (1) the SAM presents unique physical, spectral, and meteorological characteristics that are ideal to evaluate the suitability of MODIS in measuring snow cover in a mid-latitude mountain environment; and (2) little is known about the link between broader atmospheric circulation processes of snowfall and the spatial patterns of snow cover in mountain regions. Greater understanding of regional hydrology and the multi-scale topographic influences of snow will prompt new research questions to determine how snow plays a role in mixed-process flood, drought, or other event mechanisms that occur in the SAM. Further assessing the synoptic classification of snow cover patterns using MODIS data is of interest for defining snow extents from multiple synoptic-scale circulation regimes including Alberta Clippers, Miller A/B cyclones, and NWFS. Given the importance of linking synoptic and atmospheric processes with snow cover patterns between often ephemeral snow events, this thesis is guided by two major research questions.

- 1) How effective are MODIS products for mapping snow cover in a heavily forested, mid-latitude mountain environment?
- 2) How does the spatial extent of snowfall vary by synoptic-scale atmospheric circulation?

Chapter 2

Data and Methods

This chapter describes the data and methods used to inform the research questions in this thesis, beginning with a description of the study area. Particular attention is given to a discussion of the topography based on previous research that highlights the unique nature of synoptic events and resulting snow cover patterns. The chapter continues by highlighting the source of snowfall data used to classify the various snowfall events occurring over the six-year study period from October 2006 to April 2012. In addition, data sources for the MODIS FSC and true color snow maps are examined. Methods for determining the suitability of the MODIS products for analysis in this study are also included.

A major focus in this chapter surrounds the image processing techniques used to derive FSC values from multiple snowfall events. This discussion is continued by outlining the subsequent analysis comparing the FSC values and true color imagery performance in context with the atmospheric and environmental conditions from each synoptic class. In particular, surface maps and trajectory analyses are described in case studies of individual events. This thesis offers a new approach for analyzing the spatial patterns of snow in the SAM by developing a suitability analysis for using the MODIS products, and by using these techniques to link the atmospheric circulation processes with the resulting snow covered area.

Study Area: Southern Appalachian Mountain Region

The SAM region extends from northern Georgia to southern West Virginia and from the Cumberland Plateau in the west towards the Blue Ridge foothills on the eastern side of the North Carolina mountains (Figure 2.1). The area trends southwest to northeast along with the general orientation of topography and covers approximately 137,952 km². Over thirty peaks above 1,850 m are distributed across the region, the highest of which are located in the vicinity of the North Carolina and Tennessee mountains. Specifically, the highest elevations >1,850 m are situated within the Great Smoky Mountains and Unaka Mountains of North Carolina and Tennessee, and within the Balsam and Black Mountains of North Carolina. Relief can be significant in some cases, particularly in the Great Smoky Mountains, where elevations range from <500 to >2,000 m within the span of several kilometers (Perry and Konrad 2006a). The east coast's highest peak, Mt. Mitchell, is located in the region comprising part of the Black Mountain range, and rises 2,037 m asl, while nearby Asheville, NC is situated at 650 m. Other notable high peaks include Mt. LeConte (2,010 m) and Clingman's Dome (2,025 m) in the Great Smoky Mountains, Grandfather Mt. (1,818 m) and Beech Mt. (1,678 m) in the Blue Ridge of northwestern North Carolina, and Roan Mt. (1,916 m) along the North Carolina-Tennessee border.

Lower elevation sites below 1,500 m extend into adjacent areas including northern Georgia and the southwestern Virginia highlands into southern West Virginia (Perry and Konrad 2006a). To the west, the Tennessee Valley is an extensive low lying area, containing the city of Knoxville, Tennessee and extending east towards the North Carolina border. Other low lying areas include the Blue Ridge foothills and the New River Valley, extending from the east side of the Blue Ridge escarpment further north into southwestern Virginia (Perry

2006). Land cover types in the region are a mix of conifer and deciduous forest, with spruce fir communities existing at higher elevations. Extensive riming in the canopy is common during colder events in these areas.

Distinctive windward and leeward slopes are usually well defined depending on the synoptic pattern. Pronounced topographic relief in association with the general SW to NE axial range of the mountains results in ideal conditions for orographic lifting during periods of low-level northwest flow. COOP stations have provided the primary venue for deriving snow measurements on a limited number of the high peaks, including Mt. LeConte and Mt. Mitchell (Figure 2.1). Despite their limited spatial and temporal coverage, these stations provide a useful reference for high elevation snow cover, especially when sites like Boone, North Carolina (1,016 m) can provide a comparison of in-situ observations from valley locations. However, this level of analysis represents a rough estimation of processes occurring on the region wide scale. Mesoscale wind patterns, downslope flow, and spillover effects, in combination with topographic factors, contribute to the high spatial variability of the snow cover that may fluctuate over the span of a few kilometers and a few days.

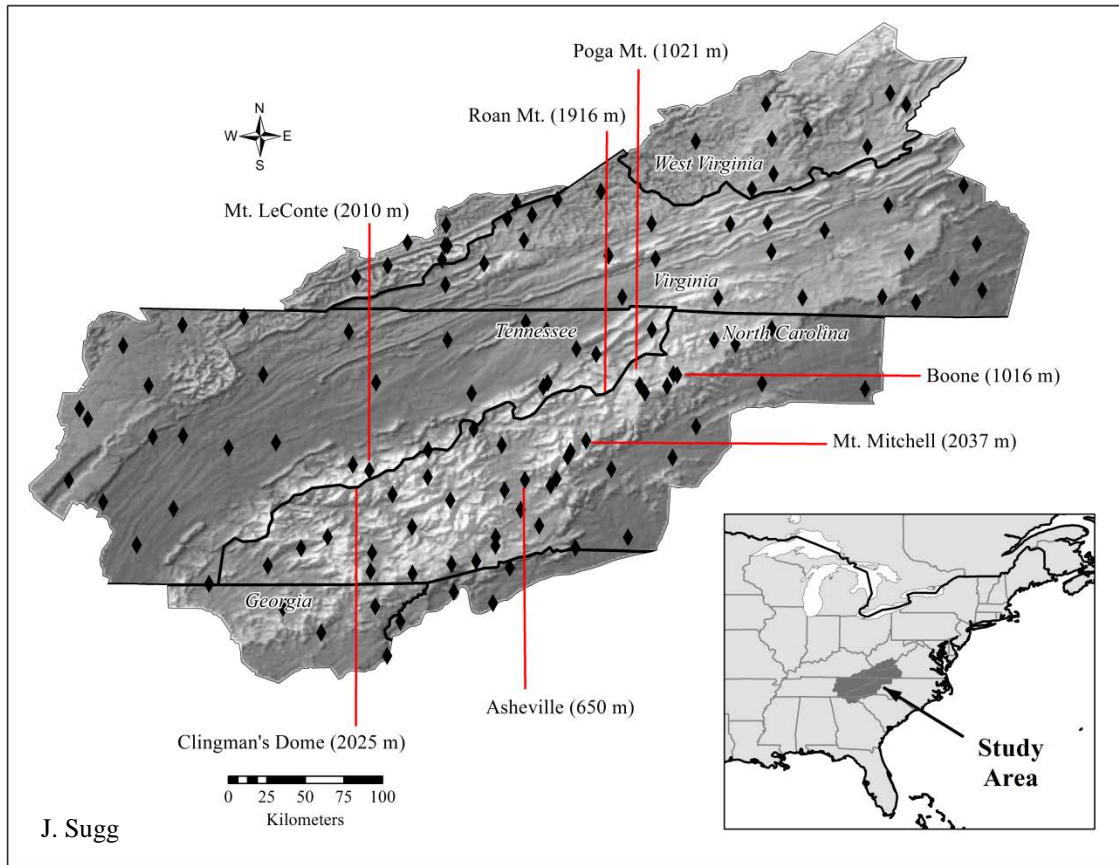


Figure 2.1. Study area map with locations of NWS COOP observer stations.

Snowfall Data and Event Identification

Snowfall data were obtained from a synoptic event classified database collected at Poga Mt., North Carolina (1,021 m) beginning in October 2006 through April 2012. The event data were collected by Dr. Baker Perry at Appalachian State University as part of an ongoing effort to characterize the multi-scale atmospheric processes associated with snowfall development in the SAM. Assignment of beginning, maturation, and ending hours during each snowfall event were used in conjunction with COOP station data to determine the appropriate time range of snow accumulation as a means of separation between individual events. COOP snowfall data from selected stations, primarily Mt. LeConte and Mt. Mitchell, were obtained from the NC State Climate Office Climate Retrieval and Observation Network

of the Southeast (CRONOS) Database to include analysis of snow events affecting the area when Poga Mt. received no snowfall (NC CRONOS 2012). Meteorological parameters collected in the snowfall data include new snowfall, snow water equivalent (SWE), snow-to-liquid ratio, density, relative humidity, wind direction, and synoptic classification scheme. Values are broken down by synoptic event class and are either calculated as an event total or averaged for the 2-hr period of heaviest snowfall. Temperature, relative humidity, and wind speed values are derived from one hour before and after event maturation (Table 2.2).

Individual snowfall events were classified by Perry et al. (2013) using a manual technique into the following eight synoptic classes: NE-U (northeastward tracking low passes to the north of the area), SE-U (southeastward tracking clipper that passes north or across the area), M*-U (combination of Miller or Gulf/Atlantic lows undergoing cyclogenesis across the area), CL-U (500 hpa cutoff low moves across the area, often slow), LC-U (lee cyclogenesis, surface low develops in the lee of the Appalachians), U (Upslope, NW flow in the absence of surface features), Non-U (other event types), and X-U (does not fit any synoptic class). It is important to note that any synoptic class may include a “U” postscript indicating the presence of upslope flow occurring at the event maturation hour. This classification system was derived from the scheme presented in Table 2.1, and developed into the classes listed above to provide an adequate number of events occurring within each class. One concern of this technique is that there is still considerable variability of meteorological parameters observed within each synoptic classification. However, these groupings provide the most adequate representation of each class that affects the region using averaged values of these parameters throughout the study period. From a remote sensing perspective, this technique is necessary to maximize the sample size of events from each

synoptic class, yet does not compromise the variability of meteorological parameters relative to each classification.

Table 2.1. Synoptic classification scheme used to derive the eight classes for snowfall events at Poga Mt., North Carolina.

Class	Description
NE-U	Northeastward tracking low passes to the north of the area
SE-U	Southeastward-tracking clipper passes north or across the area
M*-U	Miller A/B cyclones - displaying both A and/or B characteristics
CL-U	Cutoff Low - A 500 hPa cutoff low moves across the region (often slow & sometimes quasi-stationary)
LC-U	Lee Cyclogenesis - Surface low develops to the lee of the Appalachian Mountains
U	Upslope - NW upslope flow in the absence of synoptic-scale surface features
Non-U	Non-Upslope - includes Gulf surface waves, southwesterly low-level flow, and stationary fronts
X-U	Unclassified events

Table 2.2. Summary of snow events. Analysis is broken down by synoptic event class between 2006 and 2012. Values are averaged for the entire period. Temperature and wind speed values are derived from one hour before and after event maturation.

Synoptic Class	Percent of Events	Percent of Snowfall	Percent of SLE	Duration (Hrs)	Snowfall (cm)	Snow Liq. Equiv. (mm)	Snow-to-Liquid Ratio	Snow Density (kg m ⁻³)	Wind Speed (m s ⁻¹)	Wind Direction (Degrees)	Temperature (°C)	700 hPa Vertical Velocity (Pa s ⁻¹)
<i>NE-U</i>	16%	9%	9%	14	4.6	2.7	17	59	3.9	283	-2.4	0.30
<i>SE-U</i>	11%	17%	14%	20	11.7	6.3	19	54	3.5	276	-2.9	0.32
<i>M*-U</i>	16%	30%	23%	27	13.0	7.2	18	55	4.4	285	-4.5	0.23
<i>CL-U</i>	3%	2%	3%	13	5.1	3.9	13	76	2.1	281	-0.7	0.71
<i>LC-U</i>	6%	4%	5%	12	4.6	4.2	11	89	3.7	299	-4.3	0.53
<i>U</i>	25%	14%	12%	14	4.1	2.3	18	56	3.6	294	-5.1	0.37
<i>Non-U</i>	13%	15%	26%	17	8.4	9.7	9	115	2.7	122	-3.7	-0.20
<i>X-U</i>	11%	9%	9%	14	6.1	4.1	15	67	2.7	284	-2.7	0.30

MODIS Data and Suitability Analysis

A major component of this thesis involves an analysis of the MODIS snow products, primarily FSC, to determine the suitability for analyzing snow cover patterns within the SAM region. One hypothesis is that the SAM exhibits unique meteorological, physical, and spectral characteristics that make the region an ideal location for testing the MODIS snow products. These methods are developed on the basis of the unique environmental conditions when using MODIS imagery and should be applicable to future research in mid-latitude mountainous environments characterized by significant spatial and temporal variability of snow cover (Figure 2.2).

True color MODIS snow maps from both the Terra and Aqua platforms (Hall and Riggs 2013) were screened corresponding to the individual event maturation hour, defined as the period of heaviest snowfall (Figure 2.3). This process was undertaken using the MODIS

Today website, hosted by the Space Science and Engineering Center (SSEC) at the University of Wisconsin-Madison (UW-Madison SSEC 2012). While inherently subjective, this method provided a means to qualitatively examine the imagery at first glance. Individual snow events were deemed unsuitable for further analysis using the MODIS snow maps due to two main criteria:

- 1) If cloud obscured >50% of the snow surface in the study area, the image was discarded (Figure 2.4). In a few cases, greater than 50% cloud cover obscured non-snow covered areas, so the snow cover was still detected. Thus, these events were considered suitable for analysis using the MODIS snow maps. There is currently no method for retrieving snow pixel values beneath dense cloud cover on an individual event basis. For this reason, the suitability analysis developed in this study refers to clear sky conditions.

- 2) The true color images were previewed for up to five days after event end during the winter season (DJF) to minimize blocking of the surface and maximize retrieval of snow pixels. One to two days was considered the maximum time window for previewing the imagery during the fall (SON) and spring (MAM) months. This sample process relied upon the presence of low temperatures ($<0\text{ }^{\circ}\text{C}$) to preserve the snow cover over the course of several days. In the case of warm periods ($\geq 0\text{ }^{\circ}\text{C}$) where melting from the canopy or from the entire surface resulted in minimum snow retrieval values, the images were considered unsuitable for analysis (Figure 2.5). Events that were not suitable for analysis were documented based on the level of cloud cover or if too much time had passed after ablation occurred in the snowpack.

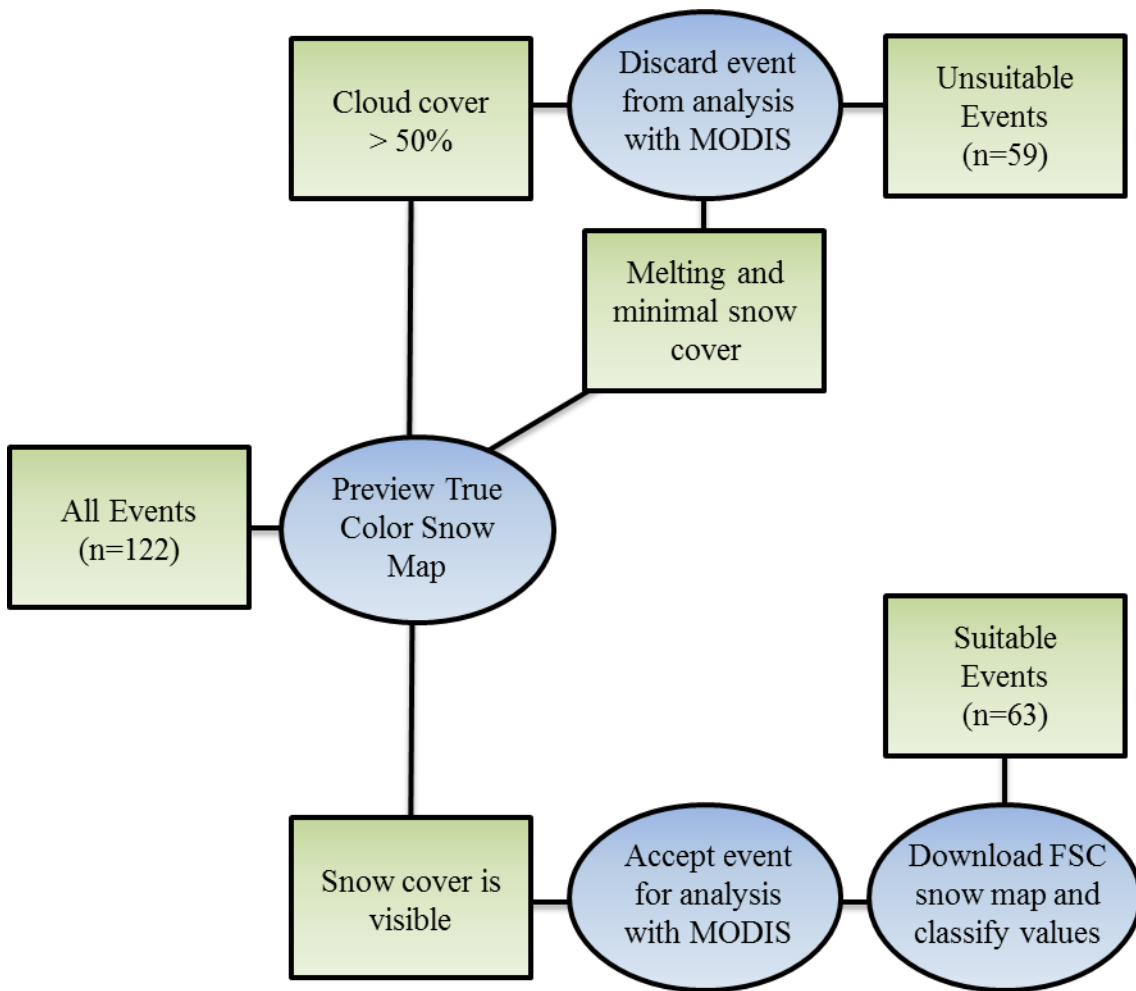


Figure 2.2. Schematic of methods for determining MODIS suitability used in this analysis.

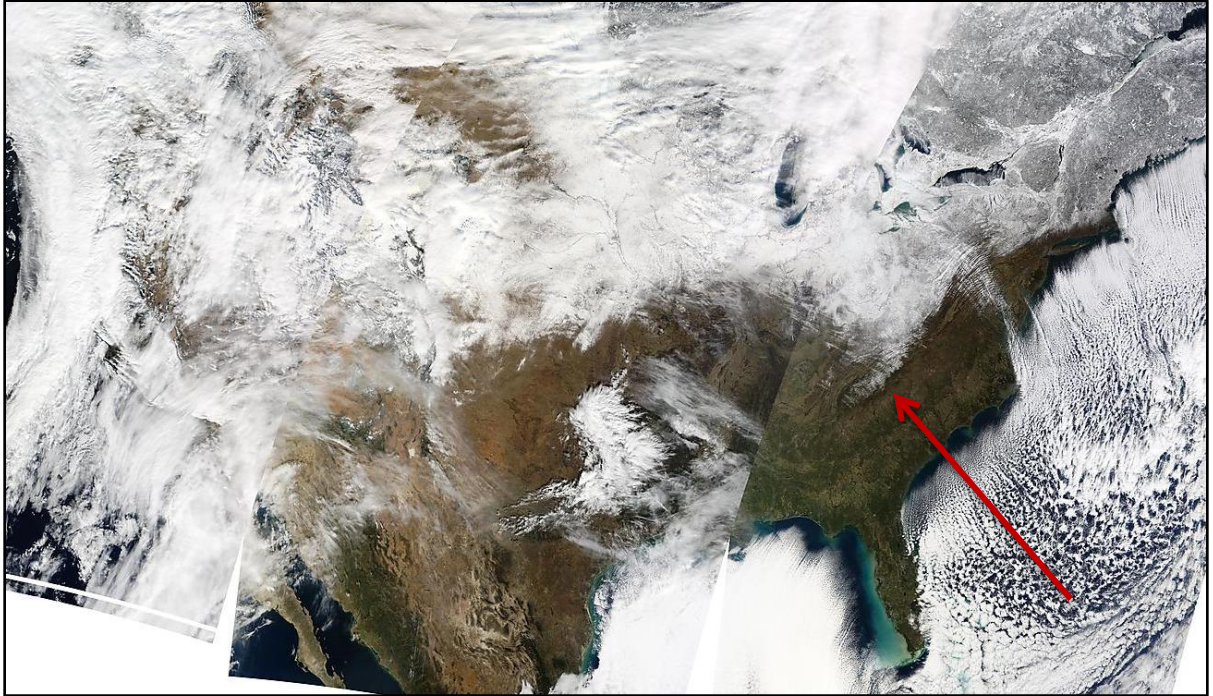


Figure 2.3. True color snow map from 3 January 2008. Snow cover is visible across much of the continental U.S., and is highlighted for the SAM region.

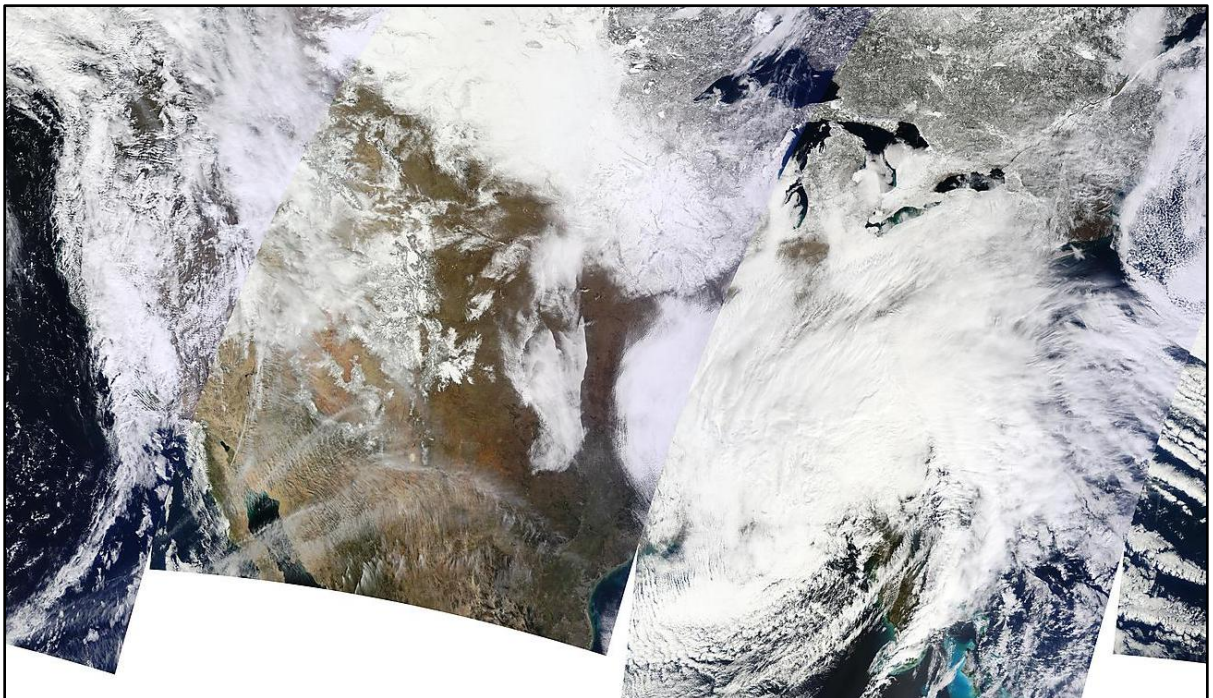


Figure 2.4. True color snow map from 2 March 2010. Extensive cloud cover blocking the surface prevents the sensor from viewing the snow covered area.



Figure 2.5. Progression of melting observed in the true color snow map. Focus is on the SAM region of western North Carolina and eastern Tennessee. Reflectance values of visible snow are diminished after one day.

Suitable snow events included in this study were quantified as a percentage of the total snow events occurring during the study period. In addition, the percentage of events unsuitable for analysis was quantified as a function of cloud cover and where melting was prevalent. This method provides an analysis of the reasons for which a snow event may be mapped using the MODIS products. Further analyses break down the distribution of events suitable vs. non-suitable for mapping as a function of synoptic class. No previous studies have determined which synoptic classification yields the most ideal situation for snow mapping.

MODIS FSC data used in this study provided a measurement of percent snow covered area within individual pixels across the SAM (Riggs et al. 2006). The FSC snow maps were obtained at 500 m resolution in HDF format from NASA's Earth Observing System Data and Information System (EOSDIS), Reverb ECHO data tool (EOSDIS 2009). Image acquisition dates were recorded along with the specific platform when downloading the FSC maps in order to determine the amount of time that passed from event maturation hour to suitable

image acquisition. This analysis used Version 5 of both the MOD10A1 (Terra) and MYD10A1 (Aqua) daily snow product to map FSC, which includes a tile of data gridded to a sinusoidal projection at approximately 1200 x 1200 km in area (Riggs et al. 2006). Pixel values range from 0-255 where 0-100 indicates the percent of snow in the cell, and values 101-255 indicate various combinations of cloud, water, and lake ice. The entire SAM study area falls within one tile, labeled horizontal number 11 and vertical number 5 (H11V05), minimizing the number of tiles needed for download between individual snow events (Figure 2.6).

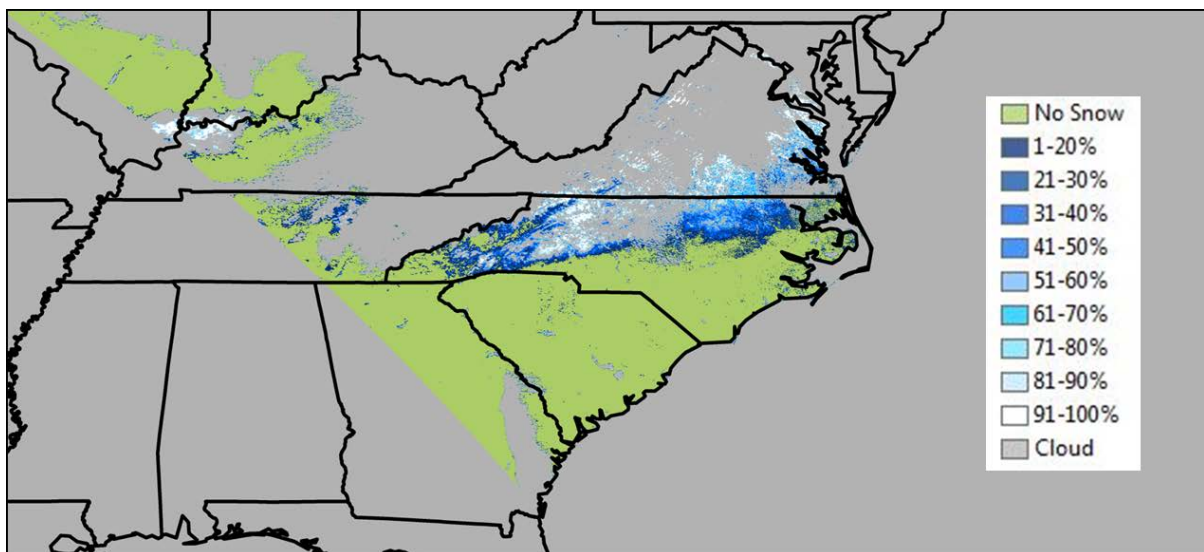


Figure 2.6. Classified FSC map for tile H11V05. Swath width extends over the entire SAM study area.

Image Processing and FSC Values from Snowfall Events

Analyses of the snowfall events by synoptic class were conducted on a region wide basis over the entire study area. Particularly with the M*-U event type, snow extents tend to be much more widespread, so analysis was tailored to reflect the overall extent of snow cover across the study area. This category includes MA (Miller A), MAB (Miller B), MBN (Miller B to the north), and MBS (Miller B to the south) systems. Other synoptic classifications that

were analyzed include the NE-U, SE-U, CL-U, LC-U, Non-U, and X-U event types. Total cloud cover was measured by raw pixel values, by calculating percentage, and comparing synoptic classes to further assess the amount of surface blocking occurring during the study period. Events were quantified by raw pixel counts of snow cover within the entire study area and also as a percent function of only the snow covered area, excluding values of No Snow and Cloud. FSC pixel values were aggregated into snow cover classes and averaged between all events. This process produced an average snow cover extent by FSC class that was compared to the other synoptic classes. All snowfall events were further separated by top and bottom quartiles of FSC extent to gain a perspective of maximum and minimum accumulations for heavier and lighter events.

In addition, analyses of FSC values were split between windward and leeward slopes for Upslope (U) events. This process provided a more thorough investigation of FSC performance compared to the analysis conducted for other synoptic classes on a region wide basis. The FSC maps were ingested in a GIS environment with a 90 m digital elevation model (DEM) and clipped to the study area boundary using ESRI's ArcGIS 10. Additional coarser resolution DEMs at 1, 10, and 20 km were derived using the Spatial Analyst toolbox extensions to provide a multi-scaled level of analysis for the (U) events. These scales most commonly represent the various physical processes occurring during orographic snowfall development, and were incorporated to analyze FSC in this context. For each DEM, two aspect files of windward and leeward slopes were created using “ $\text{aspect} \geq 225 \ \& \ \text{aspect} \leq 45$ ” in Raster Calculator. This formula produced the windward NW slopes as a “1, 0” binary which were then reclassified into a new file using a “0, 1” binary to create the leeward SE slopes (Figure 2.7).

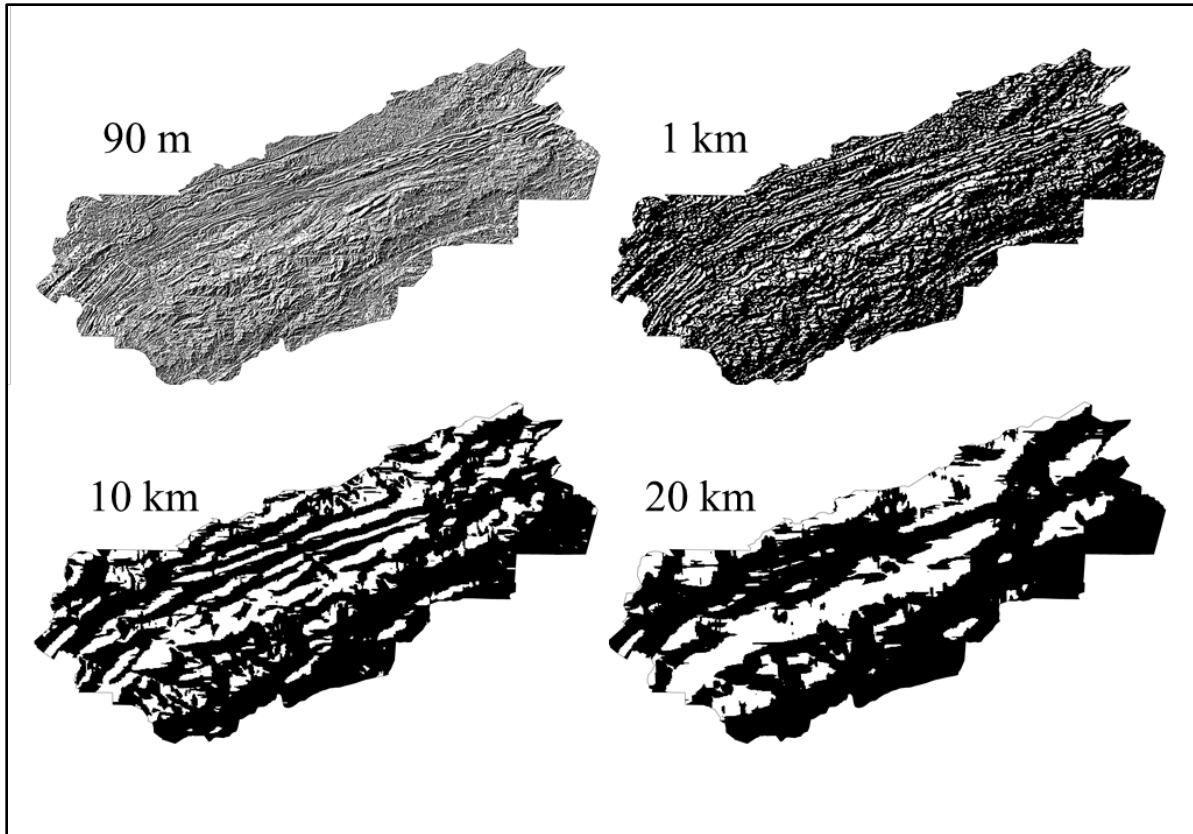


Figure 2.7. Reclassified DEMs at multiple resolutions represent windward and leeward aspects. White values indicate northwest aspects while leeward aspects are displayed in black.

FSC pixel values were parsed into separate raster files by windward and leeward slopes using the formulas “FSC * windward” and “FSC * leeward” in Raster Calculator (Figure 2.8). Histograms of FSC values on windward and leeward slopes of each event were classified using raster attribute tables where zero values are equal to “No Snow”, values 1-100 are equal to 1-100% FSC, and values 101 – 250 are equal to Cloud or Water. At-satellite reflectance values in band 4 and band 6 are used in combination with threshold criteria tests to determine the percent snow cover within each pixel (Hall et al. 2001). FSC pixel values were aggregated into classes based on the following scale, common in previous work using MODIS data: 1-20%, 21-30%, 31-40%, 41-50%, 51-60%, 61-70%, 71-80%, 81-90%, and 91-100% (Fuhrmann et al. 2010; Hall et al. 2010).

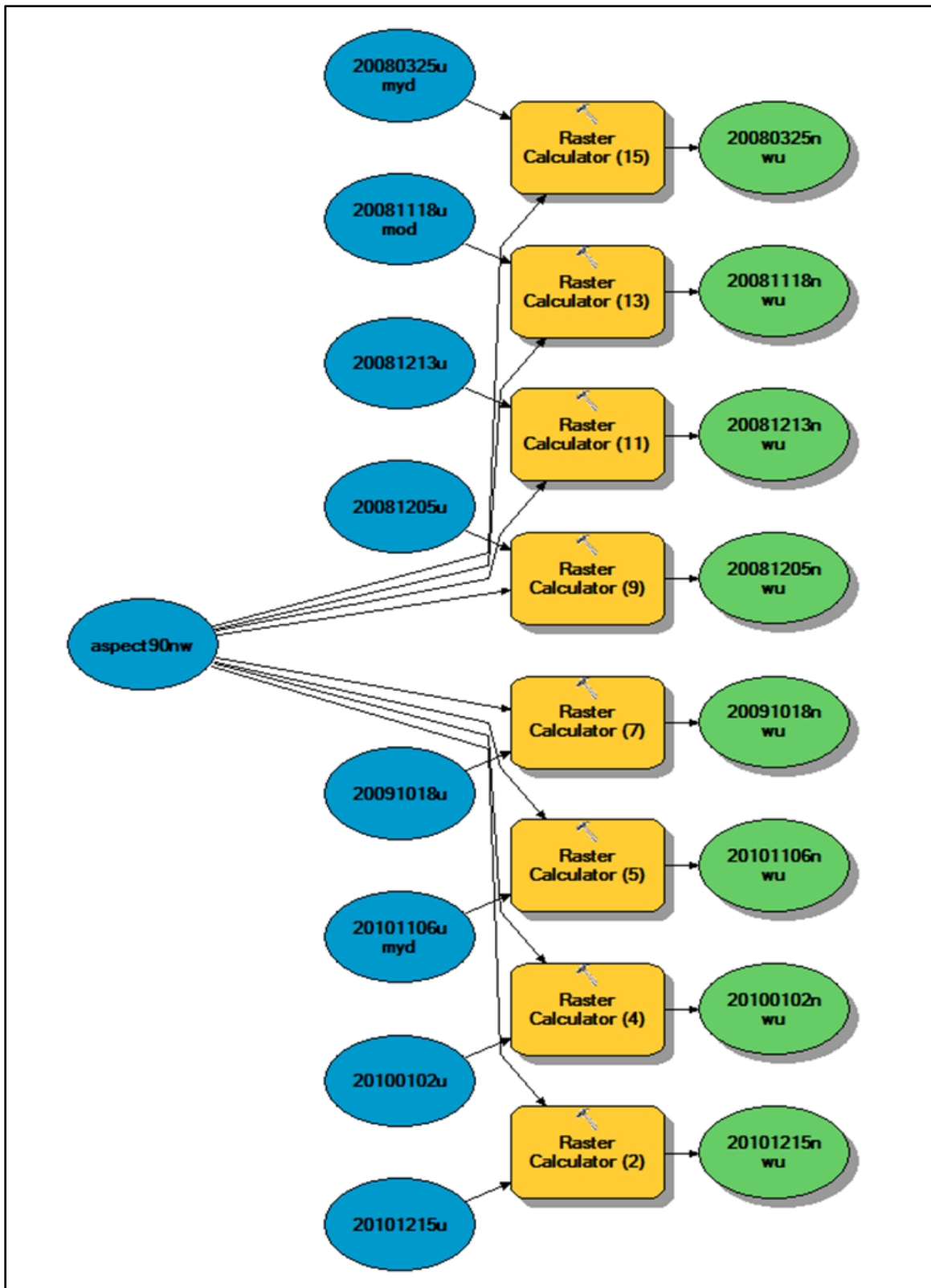


Figure 2.8. ArcToolbox Model Builder example used to reclassify FSC values for windward and leeward slopes. FSC for windward and leeward slopes was calculated for each of the 16 upslope (U) events using Raster Calculator.

Total cloud cover in each FSC image was quantified using pixel values to derive an analysis of NWFS events where the snow cover was most visible. FSC histograms were compared against the entire study area, incorporating “0” values of No Snow. The histograms were also compared by classes as a sole proportion of only the snow covered area, excluding the No Snow and Cloud bins. This technique minimizes the diminished returns of FSC performance during many NWFS events where accumulations are isolated to the highest peaks and may only occur within a few MODIS pixels across the entire study area. For each event, average differences of FSC between classes were calculated from windward and leeward snow extents.

Surface Maps and Trajectory Analyses used in Case Studies

The National Oceanic and Atmospheric Administration’s (NOAA) Hybrid Single Particle Lagrangian Integrated Trajectory (HYSPLIT) Model (Draxler and Rolph 2011) was used to provide 72-hour backward air trajectories from event maturation. Poga Mt., North Carolina (36.25 N, 81.91 W) was used as the trajectory ending location due to the incorporation of synoptic event classified data from that same location used in this study (Figure 2.9). Trajectories were derived at the 850 hPa level, roughly 1500 m, due to the importance of this height in determining interactions in the lower troposphere between shallow low level flow and the topography encountered along various aspects and slopes. In many cases, low level flow may occur completely below the mountain tops before topographic forcing occurs. Event backwards trajectories have been useful in determining air mass origin and are important components to determine the prevailing synoptic flow direction and height of air parcels leading to multiple snowfall events (Kelly et al. 2012; Perry et al. 2007).

U.S. Analysis Radar Composites and surface maps from NOAA's Hydrometeorological Prediction Center (HPC) were obtained from the Surface Analysis Archive from closest to each event maturation hour (NOAA 2012). Surface charts provided a view of prevailing low level synoptic flow patterns for each event (Figure 2.10). From these charts, analysis was conducted based on comparison of FSC performance in the MODIS product to determine likely synoptic conditions that lead to the various snowfall events across different regions within the SAM. These techniques have been incorporated on a case study basis from notable events within each synoptic class to further understand variations of snowfall between individual events. Likewise, this analysis is the best way to further develop the linkages between atmospheric circulation and resulting snow cover patterns in the SAM.

NOAA HYSPLIT MODEL
 Backward trajectory ending at 0100 UTC 13 Feb 10
 GDAS Meteorological Data

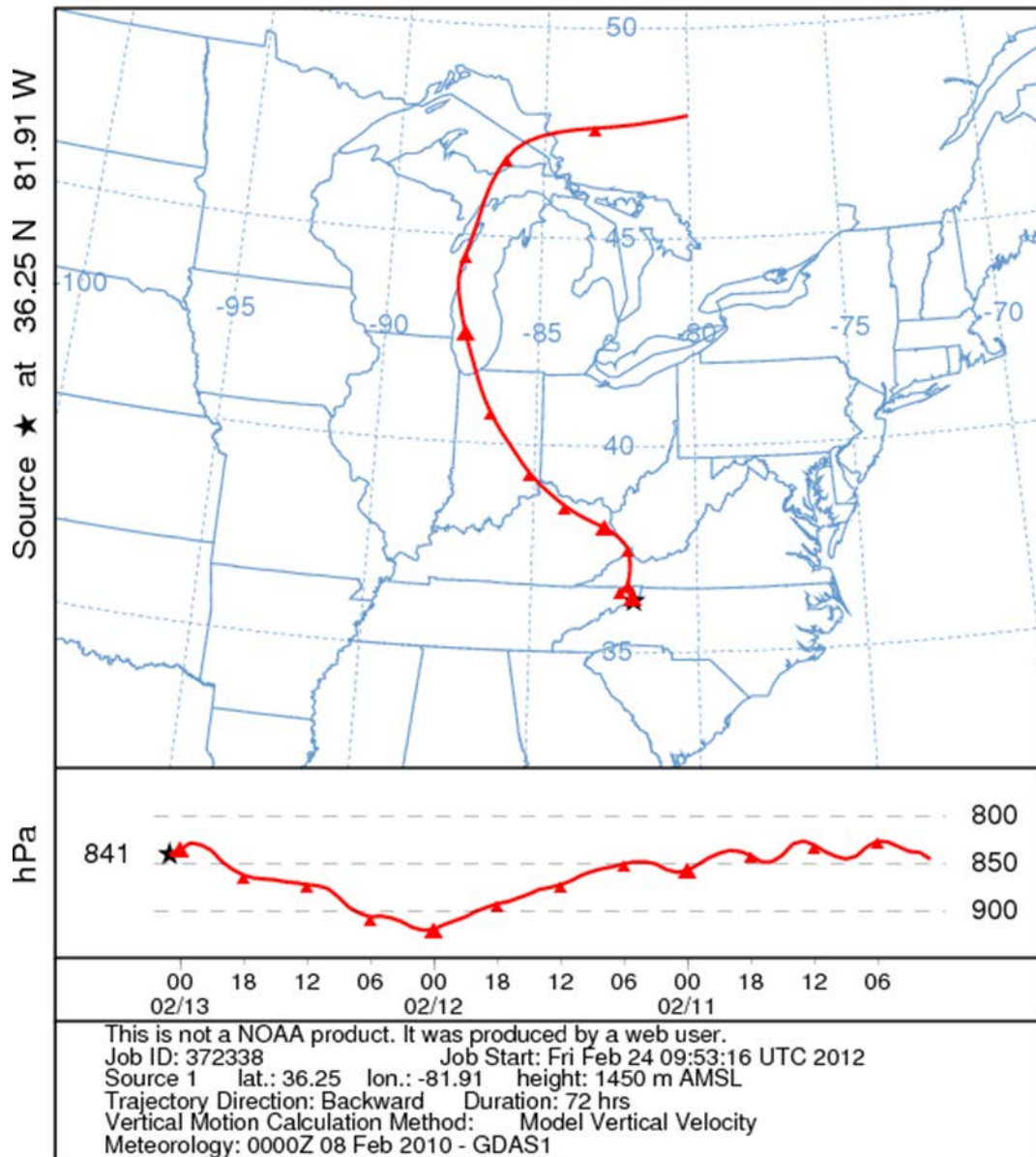


Figure 2.9. NOAA HYSPLIT backwards air trajectory.

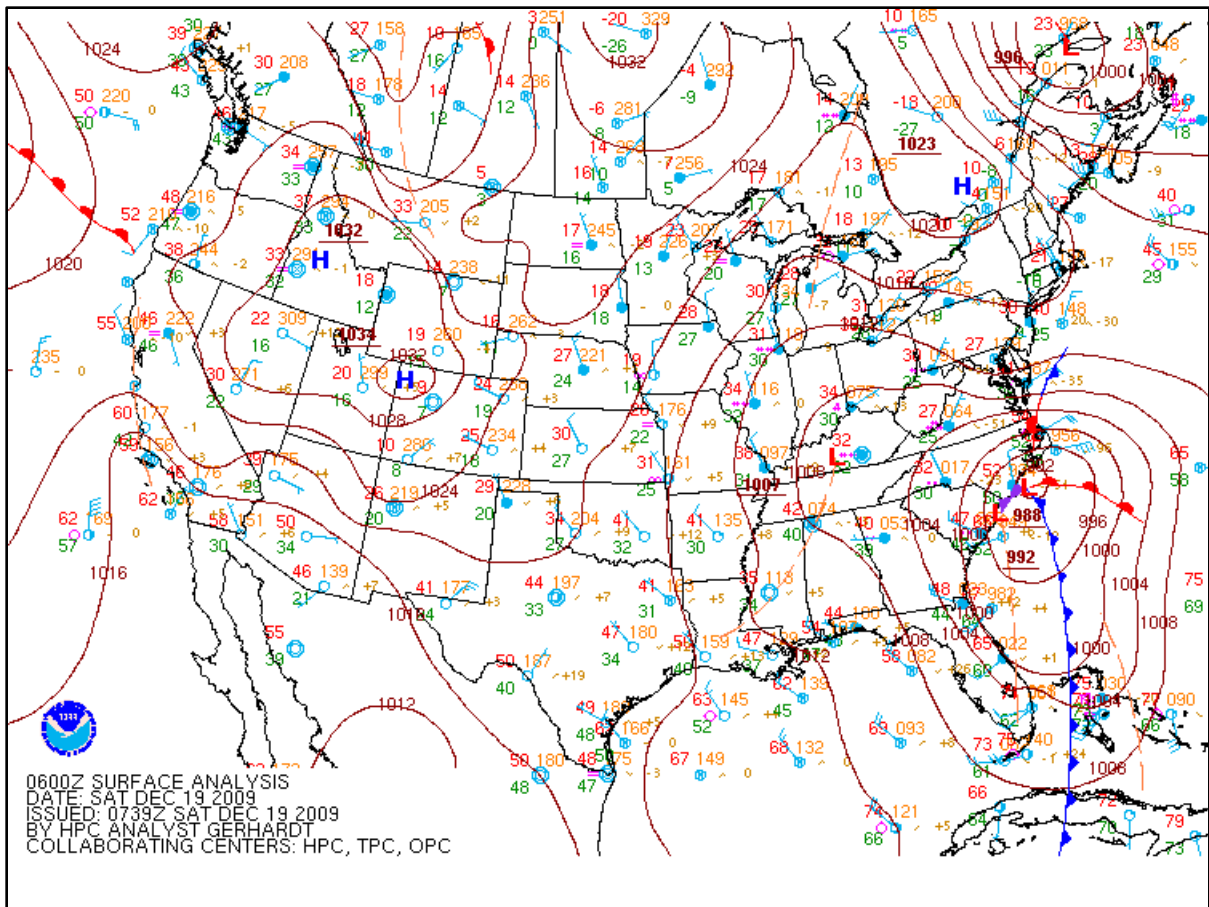


Figure 2.10. NOAA Surface analysis map taken from event maturation on 19 December 2009. Low level pressure patterns and cold/warm sectors are displayed.

Chapter 3

Results and Discussion

Introduction

The purpose of this thesis is to 1) evaluate the suitability of MODIS products in a heavily forested mid-latitude mountain region, and to 2) quantify the associated snow cover patterns resulting from different synoptic-scale circulation patterns. This chapter begins with a discussion of the suitability of MODIS in capturing the 122 snowfall events, and evaluates the image suitability by synoptic class, season, and year. The second section focuses on the spatial patterns of snowfall, including the FSC data by event type and windward-leeward contrasts for NWFS events. The third section addresses the variability of FSC through individual case studies from each event class. For this section, the snow cover pattern is analyzed through a discussion of the surface conditions, antecedent event trajectory, FSC map, true color product, and land cover effects. Event types within the study period displayed highly variable snow cover patterns in the MODIS data, and lead to interesting projections about future applications in similar studies.

MODIS Suitability Analysis

MODIS true color snow maps for 122 snow events from 2006-12 were screened based on two factors using the MODIS Today website. First, suitability for inclusion in this analysis was dependent on the amount of cloud cover in the snow maps. Second, rapid ablation also prevents adequate detection of the snow. During 59 snow events, MODIS data did not satisfy the criteria used to determine whether the imagery could be sufficiently analyzed. Cloud cover presents the primary obstacle for adequately detecting the snow. Of the 59, persistent cloud cover and blocking of the surface precluded 44 of the synoptic events from analysis with the FSC maps. Upslope (U) events in absence of surface or frontal features were the most common class where snow could not be measured due to cloud cover, as evidenced by the heavy bands of cloud occurring along windward slopes (Figure 3.1). New snowfall during these events is not possible to detect when cloud cover persists for days.

In addition to cloudy conditions, the FSC maps are further complicated by snowmelt before satellite overpass. Rapid snowmelt prevented further use of the snow maps for 10 events out of the 59 that were not analyzed. In-situ observations indicated the presence of higher temperatures (>0 °C) that would likely promote ablation in the snow pack, particularly on SE through SW slopes. As the true color snow maps are chronologically previewed, the snowpack rapidly disappears for these events. MODIS data were unavailable for the 5 remaining unsuitable synoptic events. The full list of classified events is presented in

Appendices (A, B). The remainder of results generated under this suitability analysis refers to clear sky conditions, as mentioned earlier.

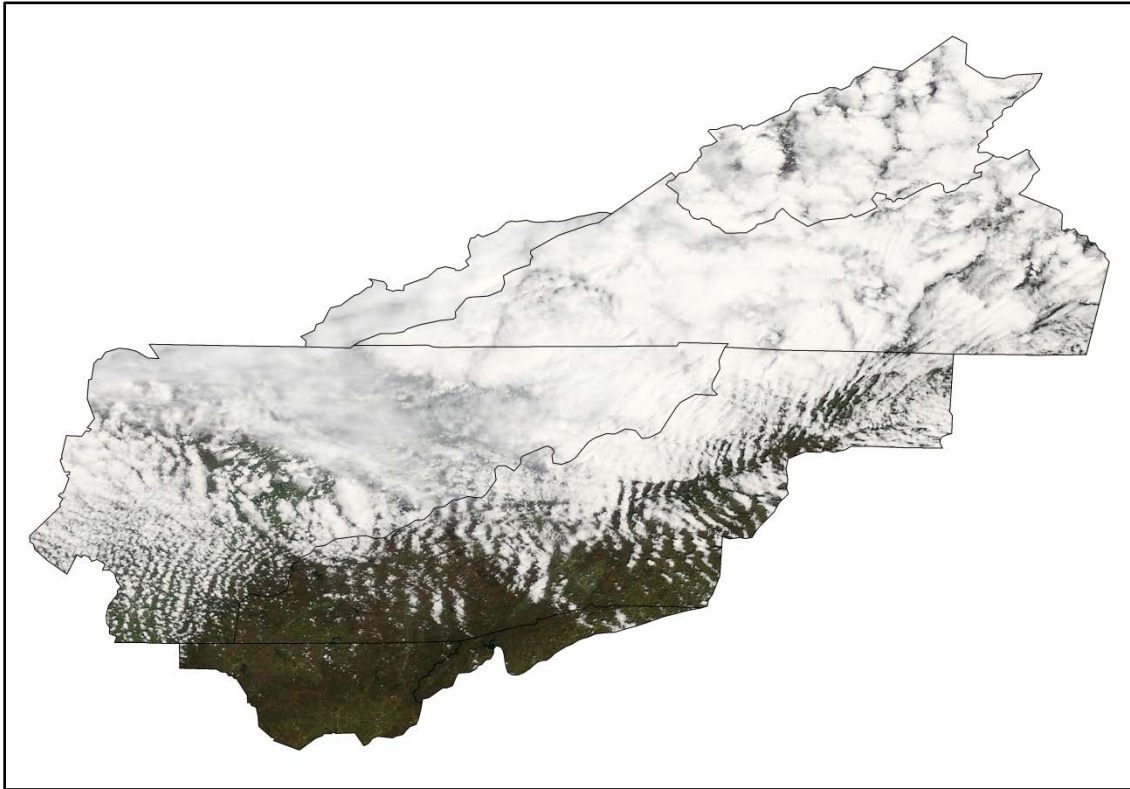


Figure 3.1. MODIS true color snow map displaying heavy cloud cover associated with Upslope (U) event on 13 April 2008, tile H11V05.

There were 63 events identified as having a suitable FSC map based on initial interpretation of conditions in the true color snow map. Miller A/B cyclones with NWFS occurring at event maturation (M*-U) were the most common event type suitable for mapping and represented 29% of the events. NW upslope flow in the absence of surface cyclone or frontal features (U) occurred 16 times (25%) among the suitable events as the second most common type (Table 3.1). There were 8 events (13%) where MODIS data were deemed suitable for analysis and displayed greater than 50% cloud cover. These are still included in the analysis since cloud solely obscured peripheral areas outside of the high

elevation ranges of the SAM (Figure 3.2). These cases were otherwise rare, and the snow surface was mostly if not entirely visible.

Cloud blocking does present a major limitation when considering the number of events which were marked by 30-50% cloud and still accepted below the 50% threshold for this analysis. FSC performance is reduced by the amount of cloud covered pixels in the snow maps, and in these cases snow cover is likely more continuous across the study area. Classes where snow cover was likely more continuous, though obstructed by $\geq 30\%$ cloud cover in some of the events, include the U, NE-U, SE-U, and M*-U classes (Table 3.2). No method was incorporated to adjust for these effects, and FSC values are analyzed despite this limitation of the 50% cloud threshold value. Thus, this technique presents a highly conservative estimate of the FSC in each event. There were 29 (46%) of the 63 images that exhibited clear skies with less than 10% total cloud cover. Snow cover patterns are highly visible during these events. The remaining 26 events (41%) exhibited some variation between these conditions.

Table 3.1. Comparison of events suitable for analysis by synoptic class. Total events n=122.

Synoptic Class	Suitable n=63	Unsuitable n=59	% Suitable
M*-U	18	7	72%
U	16	15	51%
SE-U	10	3	76%
NE-U	8	12	40%
LC-U	4	4	50%
X-U	4	11	26%
Non-U	2	4	33%
CL-U	1	3	25%

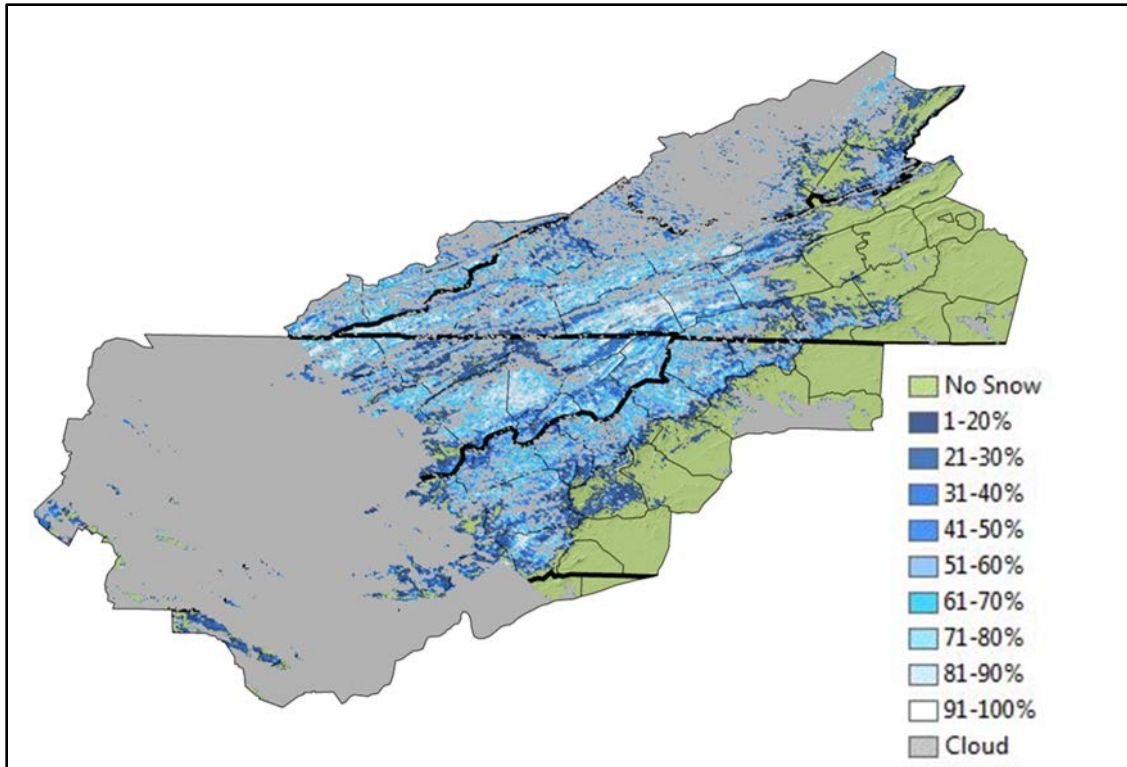


Figure 3.2. FSC snow map from 15 December 2010, tile H11V05. Cloud cover occupies greater than 50% of the total study area but is located in peripheral areas. The major portion of snow cover is still visible along the main axis of the SAM.

Table 3.2 Number of events where cloud cover $\geq 30\%$ in the snow maps that were still accepted in the analysis and are expected to reduce FSC values.

Synoptic Class	Cloud $\geq 30\%$	Suitable n=63	% Suitable
M*-U	10	18	35%
U	3	16	15%
SE-U	3	10	23%
NE-U	2	8	20%
LC-U	0	4	0%
X-U	0	4	0%
Non-U	0	2	0%

Of the 63 total events, the time lag thresholds for evaluating the imagery resulted in 10 FSC maps being collected on the same day as the event maturation hour. There were 45 FSC

maps acquired 1 to 2 days after the event end as a result of >50% cloud cover blocking the snow covered surface. The 1 and 2 day time lags used as the maximum threshold during the fall (SON) and spring (MAM) months were necessary for parsing the analysis by specific season. For the remaining events, 8 FSC maps were collected between 3-5 days after event maturation, which presented the maximum time allowance for suitable image acquisition used in this analysis. Only 1 snowfall event was captured in the imagery at 5 days after event maturation, which served as the maximum time lag threshold during the winter season (DJF). This event on 4 December 2010 was incorporated on the basis of low temperatures that preserved the snowfall pattern well after the event end, allowing a suitable image to be captured on 9 December 2010.

MODIS data were also analyzed according to climatological season throughout the study period (Figure 3.3). There were 16 events that occurred during the fall months. Of these, there were 8 events, representing 13% of the total, that were suitable for further study and analyzed using the MODIS data. There were 11 snowfall events (17%) that were suitable for analysis using MODIS during the spring months and 26 events occurring during the spring months overall. These results are contrasted with the majority of events (80) that occurred during the winter months, and 44 of these (70%) provided suitable conditions for using the MODIS snow maps. The winter months by far provide the best opportunity for assessing the snow cover not only due to the greater sample size of events, but also because of the extension of the timeframe for evaluating the quality of the snow maps. This ranking is closely followed by the spring months and finally the fall months when the snow cover is highly ephemeral due to the higher sun angle, higher temperatures, longer days, and higher ground temperatures.

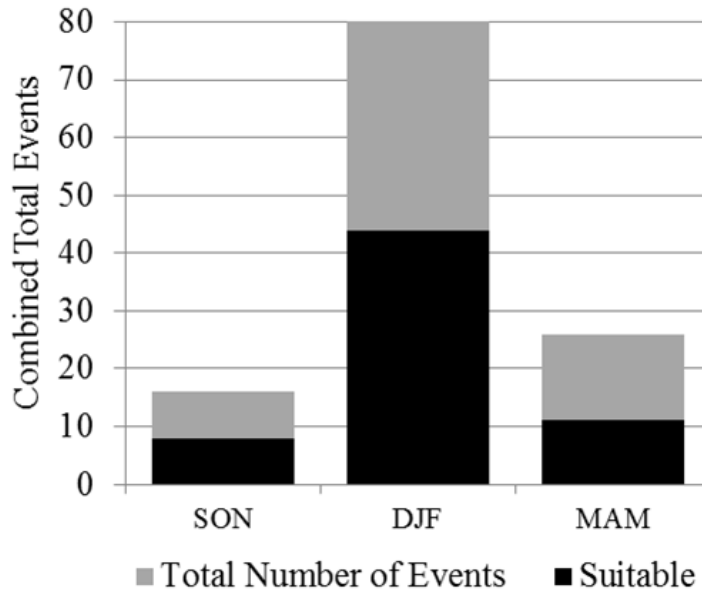


Figure 3.3. Analysis of snowfall events using the MODIS snow maps by climatological season.

Snow season from year to year showed little variation in the number of events that were included in the analysis (Figure 3.4). There were 10 events suitable for mapping during the 2006-07 snow season, followed by 11 suitable events during the 2007-08 season. Likewise, the 2008-09 snow year was characterized by 10 snowfall events that could be mapped using the MODIS data, and 11 occurred throughout the 2009-10 season. The final 2 snow years within the study period followed the same pattern since 13 events were suitable for mapping during the 2010-11 season, and only 8 occurred during the final 2011-12 season. Evaluating the number of total events occurring during individual snow years may provide useful comparisons in context with atmospheric circulation indices like the AO or ENSO. However, results fluctuated very little when solely quantifying the amount of images used in this analysis.

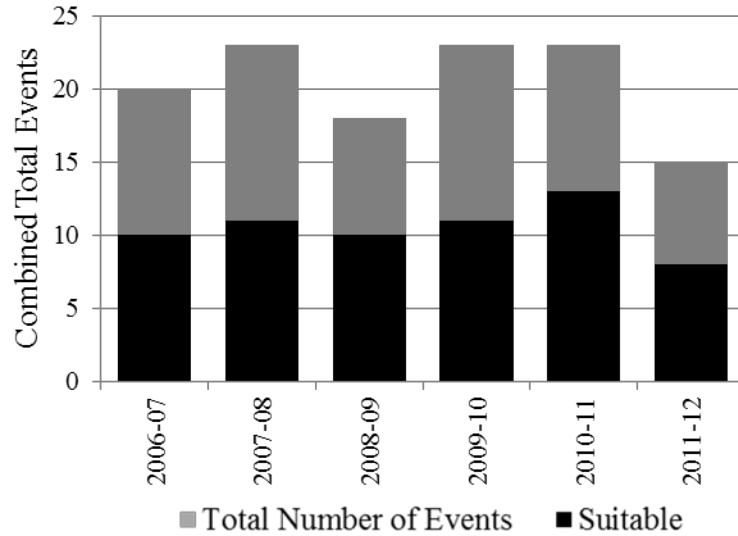


Figure 3.4. Analysis of snowfall events using the MODIS snow maps by snow year.

Heavy and light events occurring at Poga Mt. during the time period were examined according to MODIS image suitability (Table 3.3). Snowfall events where only trace snow was recorded were excluded from the upper and lower quartiles to determine how well the MODIS snow maps captured events that were marked by observable accumulation. No MODIS products were collected to examine trace events (n=10) since the snow surface was completely undetectable. The heavy events with higher snowfall totals provided a better opportunity to use the snow maps and 25 presented adequate conditions for detecting the snow cover. There were 3 events where conditions were unsuitable in the imagery for inclusion in this study. In the bottom quartile of light accumulation events, only 12 events were suitable for mapping, leaving 16 events where the snow maps were unacceptable for this study. Overall, the heavy events were much better suited to the likelihood of obtaining a suitable image, whereas in the light events, the availability of suitable MODIS snow maps was much more unpredictable. MODIS successfully mapped 89% of the heavy events compared to only 43% of the light events, a result that is fairly remarkable and worth further

investigation. One explanation may be the persistence and strength of the high pressure behind these storm systems, producing clear skies within 1-2 days. However, this result may be strictly related to the higher snowfall totals associated with the heavier events in general.

Table 3.3. Distribution of events suitable for mapping between heavy and light events. Success rates for mapping the suitable events are denoted as a percentage.

	Top Quartile	Bottom Quartile
Suitable	25	12
Unsuitable	3	16
% of events	89%	43%

Results indicate that assessing the suitability of the MODIS snow maps for further analysis is a necessary step to determine the amount and quality of available imagery. The snow cover in the SAM is often ephemeral and the FSC values are affected by variations in cloud and land cover type, thereby necessitating specific imagery requirements. For half of the synoptic classes, the amount of suitable events was either equal to or greater than the amount of images that were unsuitable and not included in this study. The upper level cutoff lows (CL-U) are excluded from further discussion due to the small sample size (n=1) (Figure 3.5).

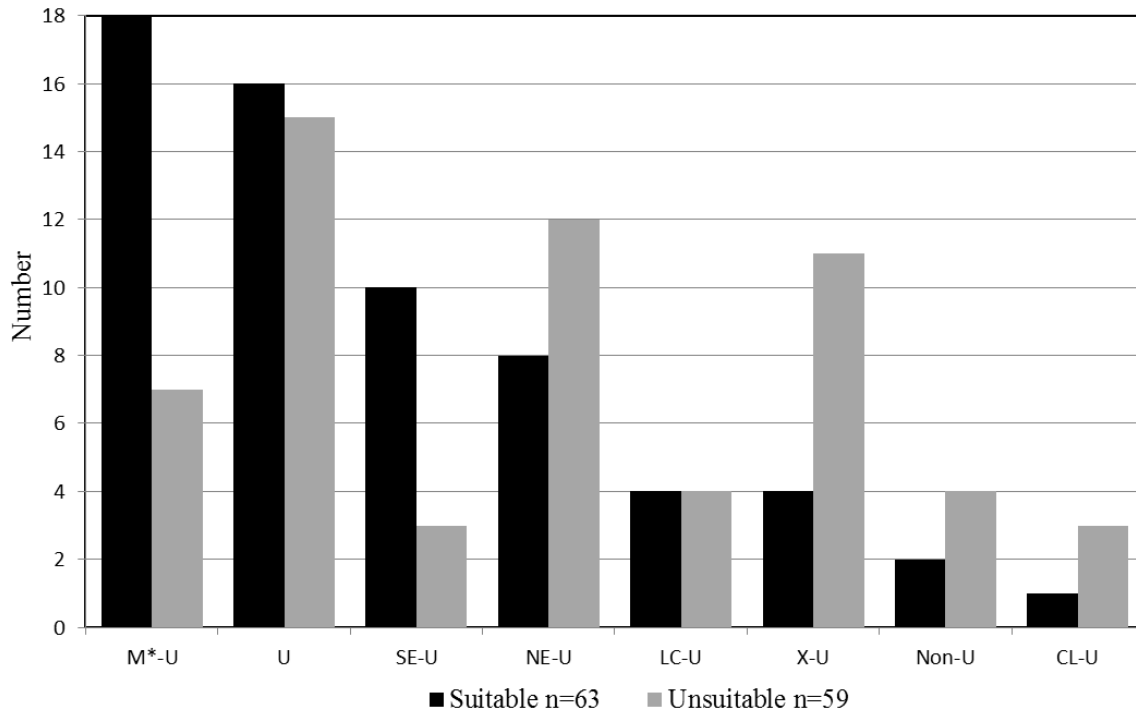


Figure 3.5. Number of snowfall events that are suitable for analysis using the MODIS products by synoptic class. For total number of events between 2006 and 2012, n=122. Suitable events follow a decreasing pattern.

Quantified assessments of the suitable events during the study period lead to projections that MODIS is best suited for mapping Miller A/B cyclones with upslope flow (M*-U), NWFS (U), and Southeastward tracking clipper systems (SE-U). Seemingly, these synoptic classes are also the most commonly occurring events in the SAM. Another explanation for the Miller and clipper systems is that snowfall tends to be heavier, spatially continuous, and more persistent during cold periods with low temperatures. Within each class, the heavy events are more likely to provide an opportunity to acquire suitable MODIS snow maps due to the higher accumulation totals. Documentation of the best image acquisition date after maturation hour provides additional data about the ability of MODIS to capture the snow cover. Results from the time lag analysis of best image acquisition date point the way towards future research which should seek to use MODIS data from 1-2 days after event

maturation. While this period provides the most ideal timeframe for gathering accurately representative snow maps, 3-5 days after event maturation are also acceptable during cold periods with low temperatures.

The final result of the suitability assessment is that 51% of the total snowfall events in the study period were considered suitable for snow cover detection. This technique required manually previewing 244 total true color snow maps from Aqua and Terra, however sample sizes of FSC maps for each snowfall event were quite limited at less than 20 for each event class. Future research should continue to quantify the percentage of events that are suitable for analysis using the FSC maps and make assumptions about the ideal snowfall events using larger sample sizes. No other study has used a similar method, so it is difficult to compare the performance in this assessment with others. However, a 51% success rate for the total snowfall events substantially improves the analysis of events using MODIS data under clear sky conditions when considering the difficulty of mapping snow cover in mid-latitude mountain regions with heavy forest cover. These results are promising for future applications of snow mapping using MODIS products based on the six-year study period and readily transferrable to other mountain regions.

Spatial Patterns of Snowfall

FSC Variability by Synoptic Class

FSC values were analyzed over the entire study area for all the synoptic classes. No variations between slope, aspect, or elevation were used to compare snow cover extents when examining the total change of snow cover over the entire region. Average percent cloud cover was initially quantified from each FSC map as a method to determine events where some of the snow cover was undetectable. There are several instances within the Miller A/B cyclones (M*-U) and southeastward tracking clippers (SE-U) where cloud cover occupied greater than 50% of the study area, though the snow surface is still detectable along the central portion of the region. These events experienced the greatest amount of cloud cover during the study period, and were closely followed by NWFS (U) and northeastward tracking lows (NE-U). When averaged as a percent of each class, cloud cover never occupied more than 40% of the entire study area. The snow cover is expected to be more continuous than measured in the snow maps for these cases (Figure 3.6).

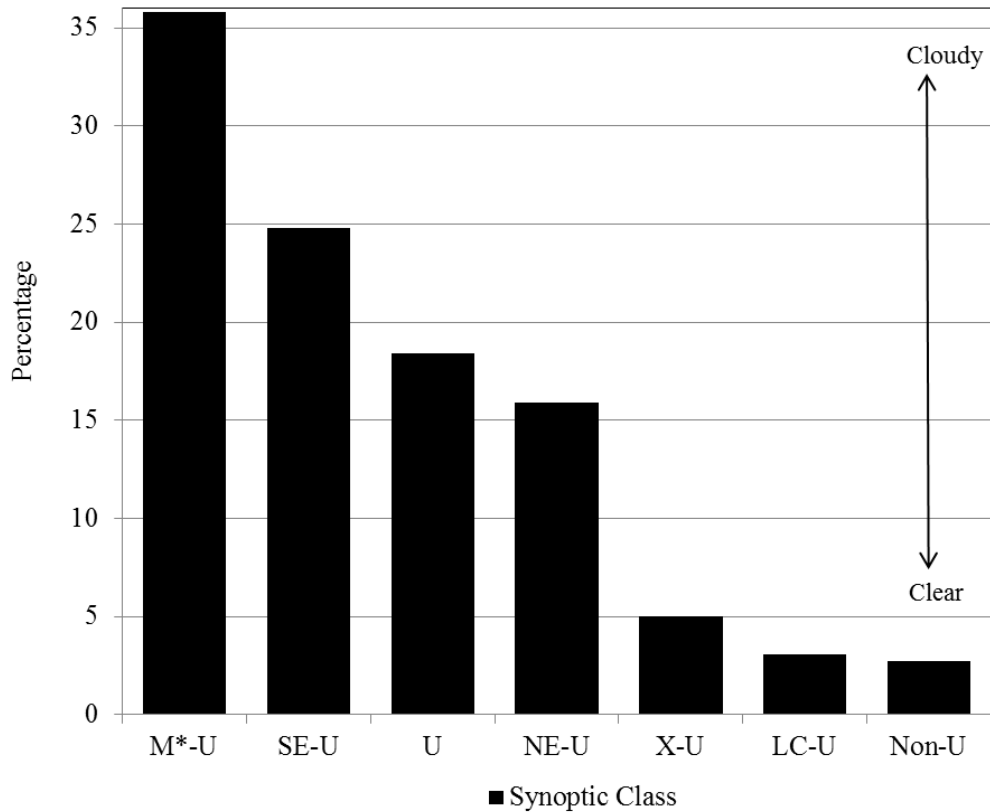


Figure 3.6. Average percent of cloud cover blocking the study area by synoptic class for the snowfall events that were included in the analysis using MODIS. Miller systems were marked by the most cloud cover, and non-upslope events were the most clear.

Snowfall events from each class were measured by raw total pixel counts of snow cover between 1 and 100% and converted to km^2 over the study area (Figure 3.7). Leeward surface cyclones (LC-U) and NWFS (U) experienced minimum snow covered pixel counts between 20,000 and 40,000 ($5,000 - 10,000 \text{ km}^2$). The raw snow covered pixel counts in these events are expected based on the prevailing atmospheric and synoptic conditions associated with their development. Lee cyclones typically track towards the Atlantic coast and snow accumulations may occur mostly outside of the study area. NW upslope flow in absence of surface features, discussed below, results in isolated snow cover at the highest elevations even though the sample size of these events at 16 was close to the maximum.

Northeastward tracking lows (NE-U), southwest low-level flow, and weak surface waves (Non-U) comprised the median values between 40,000 and 50,000 (10,000 – 12,500 km²) of snow covered raw pixel counts. Northeastward tracking lows (n=8) are frequently subjected to a rapid temperature fall behind a cold frontal passage which would promote more widespread snow accumulation and the Non-U events (n=2) tend to promote snowfall development along the NE to SW axis of the SAM, extending not much further beyond the study area boundary.

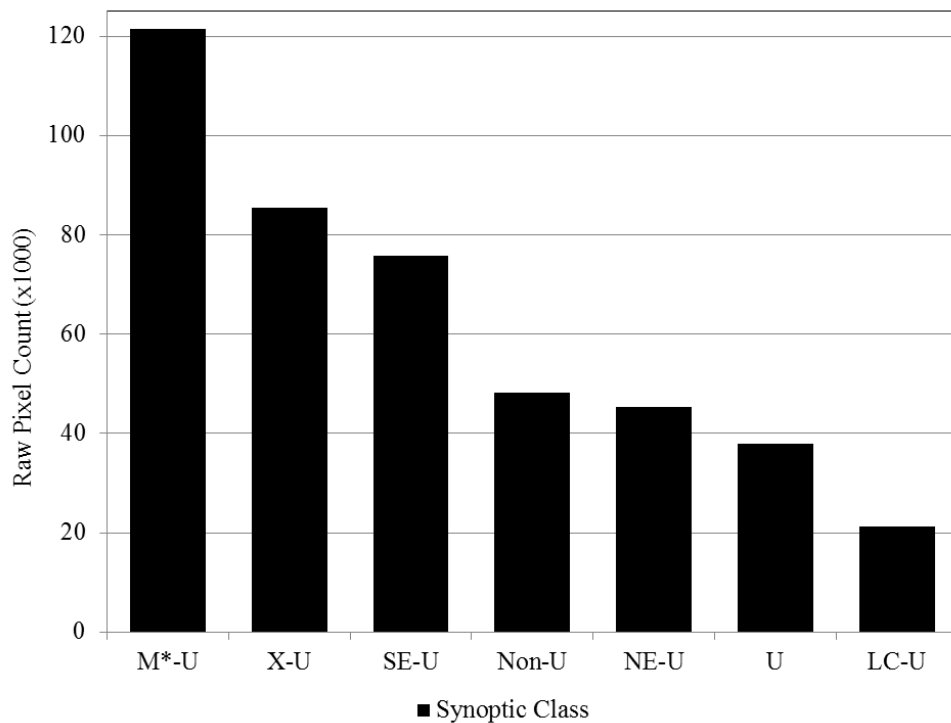


Figure 3.7. Total snow covered pixel counts by synoptic class. Miller systems produce the most snow covered area followed by decreasing values across the other synoptic classes. Lee cyclones with upslope flow produce the most minimal snow extents.

The maximum snow covered pixel counts occurred during the Miller A/B cyclones with upslope flow (M*-U) at over 120,000 (30,000 km²), unclassified events (X-U) at over 80,000 (20,000 km²), and during southeastward tracking clipper systems at over 70,000 (17,500

km²) (Figure 3.7). However, the confidence of snow cover extent for the unclassified events is particularly low due to a small sample size (n=4). The maximum snow cover extent occurring after the Miller A/B cyclones is to be expected based on the strong synoptic-scale forcing that commonly occur with these events. Snow cover values are also likely quite low due to the average cloud cover occurring within these classes. One hypothesis for the Miller A/B cyclones is that snow cover maxima also extend well beyond the study area boundary. This finding is in line with other studies that found the heaviest snowfall in the Great Smoky Mountains National Park occurred in association with the Miller A cyclones (Perry et al. 2010b). Therefore, heavy snowfall is also associated with the greatest spatial extent of snow cover.

The variability of snow cover within the clipper systems is remarkable given that some of the events occur well below the minimum extents of other event types, yet maximums also range beyond the top pixel counts within other systems. This characteristic highlights the sensitivity of the development of these systems in association with the preceding synoptic conditions. For example, a trough of low pressure extending well to the south of the region is required for many of these systems to develop, yet the passage of the clipper may also only affect isolated northern areas. Many of the southeastward tracking clippers are very fast moving, possibly limiting the amount of snow covered area from reduced snowfall totals.

The analysis of snow covered area is promising for analyzing the spatial patterns after the occurrence of future events where snow cover is highly variable across the region. This trait is particularly evident in events like the 05 March 2012 Alberta Clipper when portions of Ashe and Watauga Counties in northwestern North Carolina experienced sporadic and intermittent heavy bands of snowfall (Figure 3.8). The arrow in Figure 3.8 indicates a linear

pattern of snow associated with an intense convective band that resulted in spillover effects. Accumulations were otherwise light to non-existent across the remainder of the region and became more difficult to detect after significant melting occurred before the MODIS image was acquired.

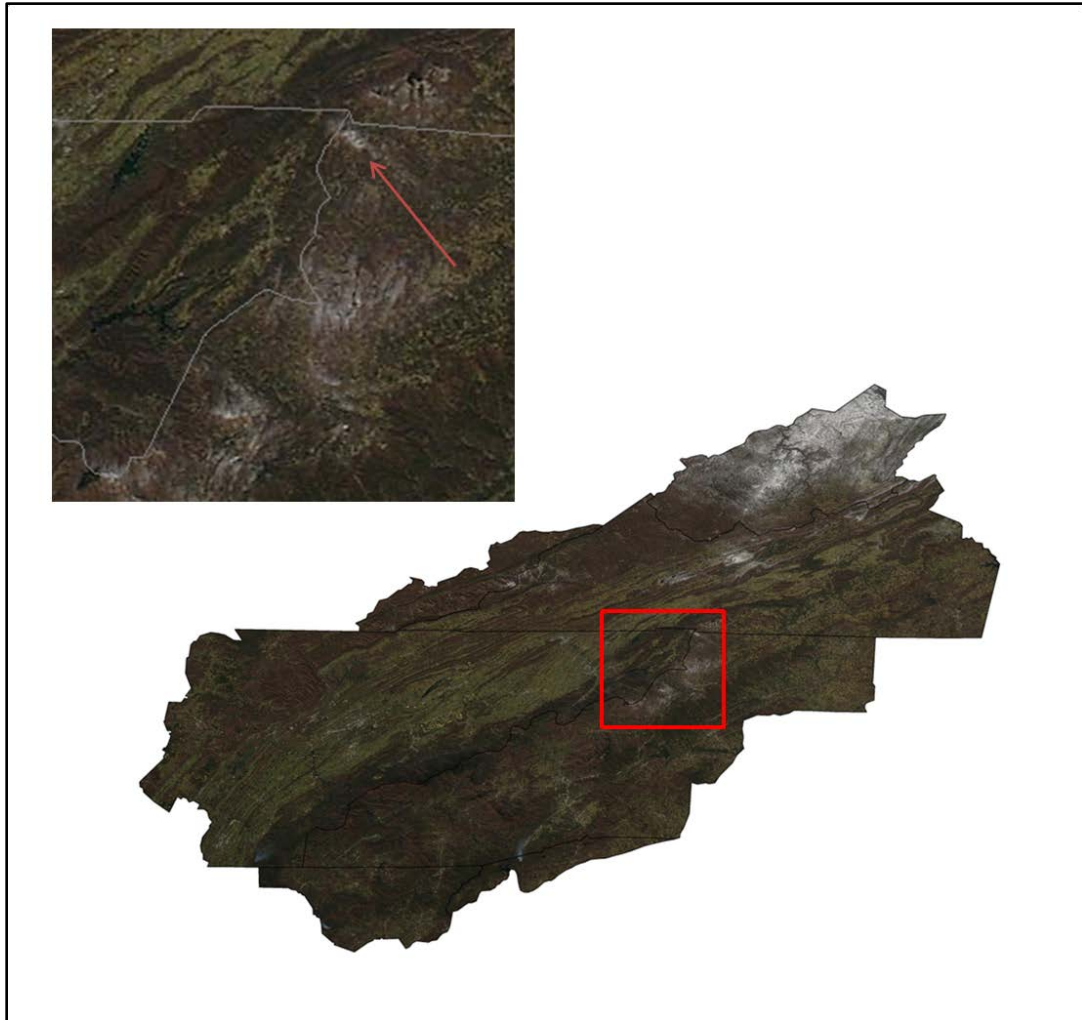


Figure 3.8. Intermittent and sporadic snow cover in the MODIS true color snow map from 06 March 2012, tile H11V05. The Alberta Clipper event was marked by significant melting after event end, resulting in some loss of snow cover in the image.

Statistical analyses were performed on the raw pixel count data to determine the relationships between snow cover among each synoptic class. As a general rule, sample sizes

between events were small, so non-parametric tests were applied. Pixel count data were tested for normality ($\alpha = 0.05$) using the Shapiro Wilks test. For data that were not normally distributed, including the M*-U and U event classes, differences of means were tested ($\alpha = 0.05$) using the Mann-Whitney U two-sample rank sums test. This analysis found that there is a significant difference between snow extent in the Miller A/B cyclones and the NWFS events (Table 3.4).

Table 3.4. Snow cover values between U (n=16) and M*-U (n=18) events. Measurements are denoted in raw pixel counts with >0% FSC and in km².

(U) Northwest Flow Snowfall		(M*-U) Miller A/B Cyclones	
Pixel #	Km²	Pixel #	Km²
105	26	16296	4074
1210	303	43018	10755
2068	517	44555	11139
5201	1300	45648	11412
8985	2246	47167	11792
9453	2363	61028	15257
12475	3119	71050	17763
24629	6157	86718	21680
36178	9045	92127	23032
36400	9100	125965	31491
47309	11827	136415	34104
64074	16019	141914	35479
64311	16078	146963	36741
64528	16132	166110	41528
72682	18171	180486	45122
155777	38944	197826	49457
-	-	214168	53542
-	-	369378	92345

FSC analysis as a percent of snow covered area exhibited similar characteristics among all classes (Figure 3.9). The 1-20% FSC class contained the most variability between event

types and also provided the maximum percent of area snow cover. The Miller A/B cyclones (M*-U) experienced the lowest area coverage below 40% in this class and lee cyclones presented the highest coverage within the class near 70%. One possibility for the low performance of snow cover among all classes is that land cover effects of dense vegetation reduce FSC on mountain slopes. The remainder of the FSC classes from 21-100% experienced a gradual decline in percent of snow covered area coverage as FSC increased among all classes. Above 80%, FSC is practically nonexistent, comprising less than 5% of the total snow covered area. Variability is minimized between event types when the snow cover is solely examined without regard to the total study area.

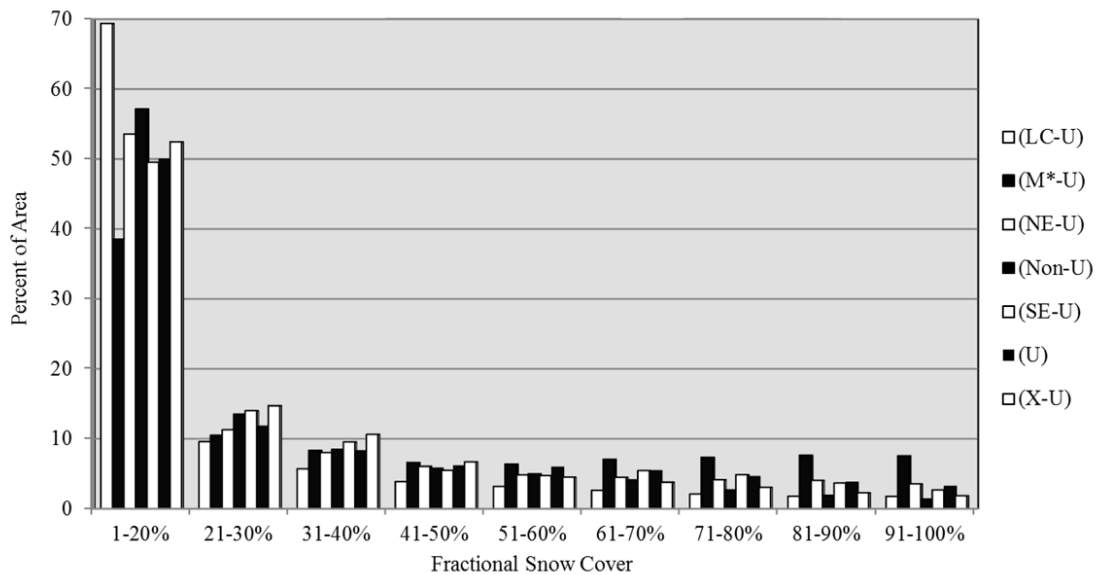


Figure 3.9. Fractional snow cover percent of snow covered area by synoptic class.

Variability between event types is more easily characterized when the FSC data are measured as a percent of the total study area, including values of No Snow and Cloud cover (Figure 3.10). The M*-U events result in the highest percentage of snow covered area across

nearly all of the FSC classes. The 21-30% FSC bin is the exception since the unclassified (X-U) events contain slightly more snow cover. Most notable among the M*-U events is the leveling off (21-60%) and eventual increase (61-100%) in FSC area among each class. The SE-U and X-U events experience the next highest amounts of snow cover among all the FSC classes, with a maximum occurring in the 1-20% bin at over 6% of study area snow cover. Lee cyclones (LC-U) provide nearly non-existent coverage in all FSC classes where the snow cover is between 0 and 3% of the entire study area. The median values of percent of area snow cover in each FSC class come from northeastward tracking lows (NE-U), NWFS (U), and non-upslope (Non-U) events.

The general pattern of maximum snow cover in the 1-20% bin followed by a leveling off of values across the remaining FSC bins is prevalent among all event types except the Miller cyclones (M*-U), which tended to increase. Vegetated mountain slopes are marked by reduced FSC even though snowfall is expected to be continuous during events with widespread coverage. Given the nature of accumulation associated with the Miller cyclones, these higher FSC values may be influenced by the location of open areas such as fields and pastures in the low elevations producing near 100% FSC. This pattern is not prevalent during other classes where accumulations are limited to the high elevations.

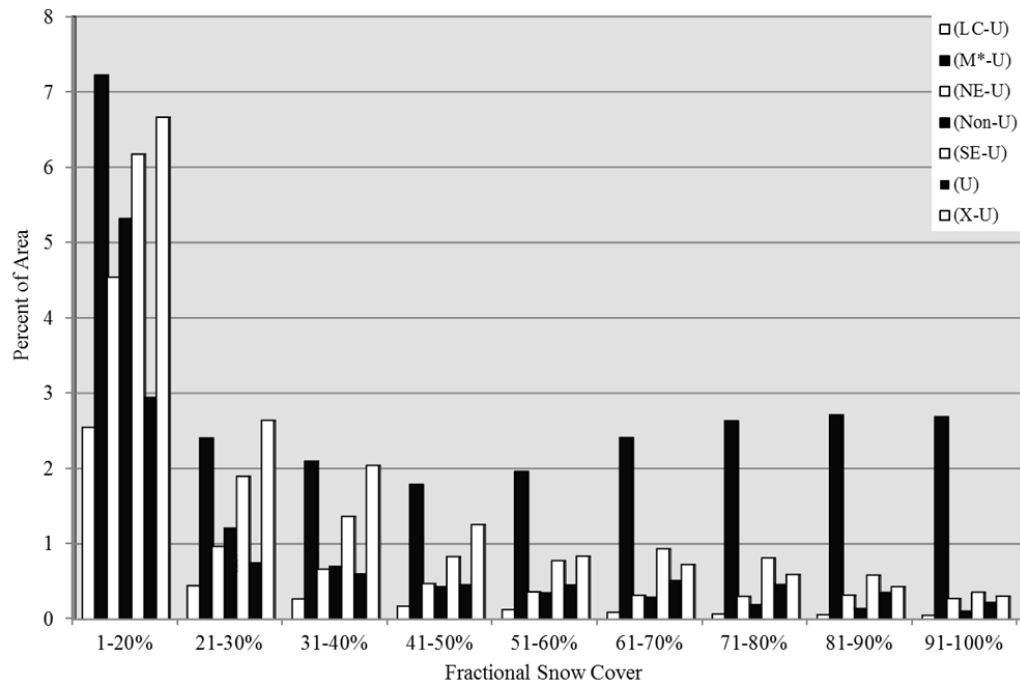


Figure 3.10. Fractional snow cover percent of total study area by synoptic class.

Upper and lower quartiles of snow covered pixel counts were determined for each synoptic class where the sample size of events was greater than or equal to four. These events are also represented in the true color snow maps (Figure 3.11). CL-U and Non-U event classes were not included in this analysis due to small sample sizes. The average snow cover for each quartile was compared to in-situ observations of meteorological data for each event from Poga Mt., North Carolina (Table 3.5). Snowfall, SWE, temperature, relative humidity, wind speed, and wind direction were averaged for both heavy and light events to provide a comparison of local conditions at this site. Snow extent in km^2 is indicated as a positive difference between every synoptic class. The Miller A/B cyclones (M*-U) experienced the greatest positive difference of snow cover between the heavy and light events, followed by southeastward tracking clippers (SE-U), and Unclassified (X-U) event types. Northeastward

tracking lows (NE-U) and Lee cyclones (LC-U) showed the smallest differences in snow cover between heavy and light events.

For each class, there is a positive difference in averaged snowfall totals from Poga Mt. between the upper and lower quartiles, suggesting the previously discussed result that the heaviest events also produce the most widespread snow cover. Consistent with this finding are the temperature values that follow a similar pattern. The majority of classes observe lower temperatures during the heavy events when compared to the lighter events. During four of the event classes, averaged temperature values from the upper quartiles of snow extent were lower by 4-8 degrees (C), a characteristic that would likely preserve more snow at or below the freezing level in upper quartile events. While it is extremely difficult to assess point data values and snow cover in an entire area, this result suggests the presence of a relationship worth testing further.



LC- U 14 February 2008



X-U 04 December 2010



NE-U 12 December 2010



U 15 December 2010



SE-U 07 January 2011



M*-U 11 January 2011



Non-U 10 February 2011



CL-U 29 November 2011

Figure 3.11. True color snow maps with the greatest snow extent by synoptic class. Images are arranged chronologically, tile H11V05.

Table 3.5. Differences in averages of meteorological data from upper and lower quartiles of snow extent. For heavy and light events, meteorological data were averaged and then summed to provide the difference for each synoptic class. SLE = snow liquid equivalent. Temperature and humidity were derived from one hour before and after event maturation.

Synoptic Class	Snow Extent Km ²	Snow cm	SLE mm	Temp. C	Relative Humidity
(M*-U) Miller Cyclones	50771	5.1	0.5	0.3	-9.1
(U) Northwest Flow Snow Events	21795	1.0	0.0	-7.3	-0.4
(SE-U) Southeastward Tracking Clippers	30546	6.2	0.1	-5.9	8.2
(NE-U) Northeastward Tracking Lows	23504	7.1	0.2	-4.2	-7.2
(LC-U) Leeward Surface Cyclone	10686	2.0	0.1	-7.9	-12.8
(X-U) Unclassified	34739	16.5	1.1	2.8	7.2

Windward and Leeward Contrasts during NWFS

FSC values between windward and leeward slopes for the 16 NWFS (U) events varied based on the individual event. Periods of weak NW flow or little available moisture may be responsible for events where only trace snow was observed at windward locations. In every event, however, windward slopes were characterized by a greater amount of raw pixel values of snow cover when compared to the leeward slopes. This factor was evident during periods of low accumulation and events that observed higher snowfall totals, as well (Figure 3.12). The SAM region is covered by 551,809 pixels in each raster where FSC resolution is 500 m. Thus, total area of the snow cover was calculated for each event as a portion of the 137,952 km² study area. Examples of minimum extents can be seen from 25 March 2008 where 642 pixels were classified as snow covered (160 km²) on the windward slopes while only 552 pixels contained snow (138 km²) on the leeward slopes (Table 3.6). A maximum extent occurred on 15 December, 2010 when MODIS detected over 88,000 pixels of snow cover (22,000 km²) on windward slopes and over 69,000 pixels of snow cover (17,250 km²) on leeward slopes.

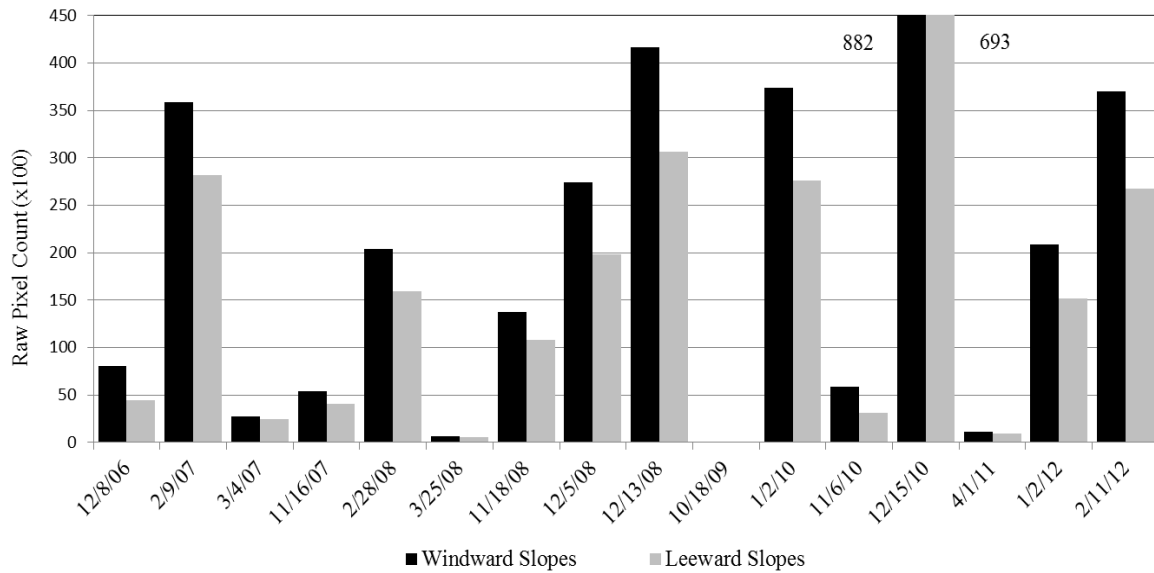


Figure 3.12. Total snow covered pixels on windward vs. leeward slopes. Data are plotted for the 16 NWFS (U) events that were suitable for analysis with the MODIS snow maps. For every event, snow cover is greater on windward slopes than leeward slopes.

Table 3.6. Snow cover (km²) between windward and leeward slopes for the 16 NWFS (U) events.

Date	Windward Slopes	Leeward Slopes	Percent Difference
12/8/06	2004	1106	58
2/9/07	8978	7043	24
3/4/07	686	609	12
11/16/07	1357	1003	30
2/28/08	5104	3980	25
3/25/08	161	142	13
11/18/08	3445	2708	24
12/5/08	6850	4957	32
12/13/08	10420	7655	31
10/18/09	18	8	78
1/2/10	9347	6895	30
11/6/10	1472	769	63
12/15/10	22054	17326	24
4/1/11	279	234	18
1/2/12	5227	3799	32
2/11/12	9253	6691	32

On average, windward slopes in the 90 m analysis contained 5,400 more snow covered pixels than were detected on leeward slopes, comprising an area of almost 1,350 km², though

for heavy events the difference rose upwards of 4,728 km². In the 10 km analysis, the windward slopes contained 619 more snow covered pixels than were detected on the leeward slopes. This area difference equated to near 155 km² of additional snow cover on the windward slopes. The 20 km analysis performed similar to the 10 km, and the average difference between windward and leeward slopes was 941 pixels, or roughly 235 km².

Differences between the aspects for the 10 and 20 km DEMs were less than 10 pixels in each FSC category and are influenced by the discrepancy between MODIS cell resolution and DEM resolution when performing operations in Raster Calculator. However, these resolutions provide a better representation of the NW and SE slopes occurring along the divide of the SAM, as opposed to the 90 m representation of the aspects, which does not capture the topography of the windward slopes as well. Though elevation was not included in this analysis, comparisons of raw pixel values highlight the isolation of snow cover occurring at high elevations. Compared to other event types where snowfall development is largely due to synoptic support, spatial patterns of snow cover are a reflection of atmospheric processes during upslope flow.

FSC classification analysis was initially conducted as a sole function of the snow covered area and later modified to compare classes over the entire study area including No Snow and Cloud values. Windward and leeward slopes performed similarly when viewing FSC in absence of No Snow or Cloud values. On both windward and leeward slopes, 1-20% FSC characterized an average 50% of the snow covered area (Figure 3.13). FSC values between 21-30% made up roughly 11% of the snow cover, and all subsequent FSC classes comprised less than 10% of the snow cover, respectively. A maximum of values in the 1-

20% FSC class likely indicates a probability of lower accumulation totals associated with NWFS occurring during the time period.

These results were consistent among the 90 m, 10, and 20 km analyses since FSC was evaluated only as a percentage of the snow covered area and FSC proportions remained the same at different resolutions. The total snow cover did vary when comparing the raw pixel counts. Examining the FSC as a percentage of the snow covered area also resulted in some leeward slopes containing more snow covered area compared to the windward slopes. This was particularly the case in the 21-30%, 41-50%, and 81-90% FSC classes, so this method may not be considered as useful for identifying the spatial patterns of NWFS.

When FSC was analyzed as a percent of the total study area, however, windward slopes performed better in every class compared to lower values on leeward slopes (Figure 3.14). In the 90 m analysis, averaged 1-20% FSC values from all events comprised 1.6% of the entire study area on windward slopes and 1.2% on the leeward slopes. Remaining FSC classes on both windward and leeward sides of the divide comprised 0.1-0.4% of the total study area. The 10 km analysis revealed a similar pattern where the highest amount of snow cover occurred in the 1-20% class and accounted for 1% of the total study on windward slopes and almost .08% on the leeward slopes. The remaining FSC classes on both windward and leeward slopes contained snow that made up 0.2% and below of the study area. The only difference in the 20 km analysis of FSC performance across the total study area is that the 1-20% class was marked by reduced snow cover at 1.1% on the windward slopes and 0.7% on the leeward slopes. Across all of the represented aspects during NWFS events, values of No Snow comprise the vast majority of the study area since previous snow packs have already

melted, effectively reducing the percent coverage of the snow across the total study area and isolating the high elevation, windward slopes.

Several factors may be influencing the stronger windward FSC performance presented in both analyses of snow covered area and total study area. Foremost is the fact that there are often times when windward cloud cover is quite common and leeward SE slopes are clear. As downsloping and warming of air parcels occur, moisture can dissipate to promote clear skies downwind of the accumulation area. Under cloud, FSC along windward slopes may be underestimated, indicating a more conservative measurement of the snow. Second, higher melting rates among SE slopes due to sun angle and warmer air may explain the reduction in FSC among the leeward slopes. Many portions of windward slopes, especially on north aspects, may never experience direct sunlight during the winter season. Finally, spillover effects may enhance accumulation totals on leeward slopes, suggesting that more complex relationships are of interest for defining the results from the snow maps. When the growth range of snow particles in the cloud microphysical environment is limited by particularly dry air and low temperatures, unrimed dendrites are subject to slower fall speeds and deposition further downwind (Dore et al. 1992). This factor would actually suggest some of the events where blowing is a more important factor for measurement of snow on the leeward side.

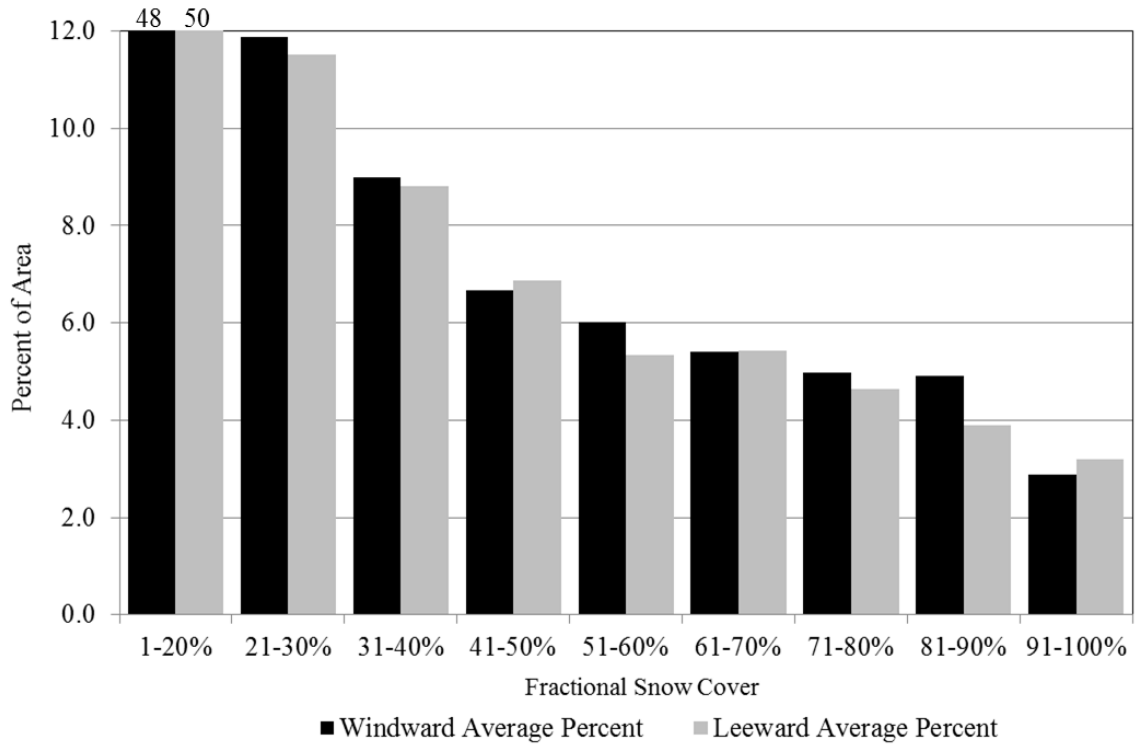


Figure 3.13. Average FSC of the percent snow covered area for the 16 NWFS (U) events. Some windward percentages constitute a greater portion of the snow cover than on leeward aspects.

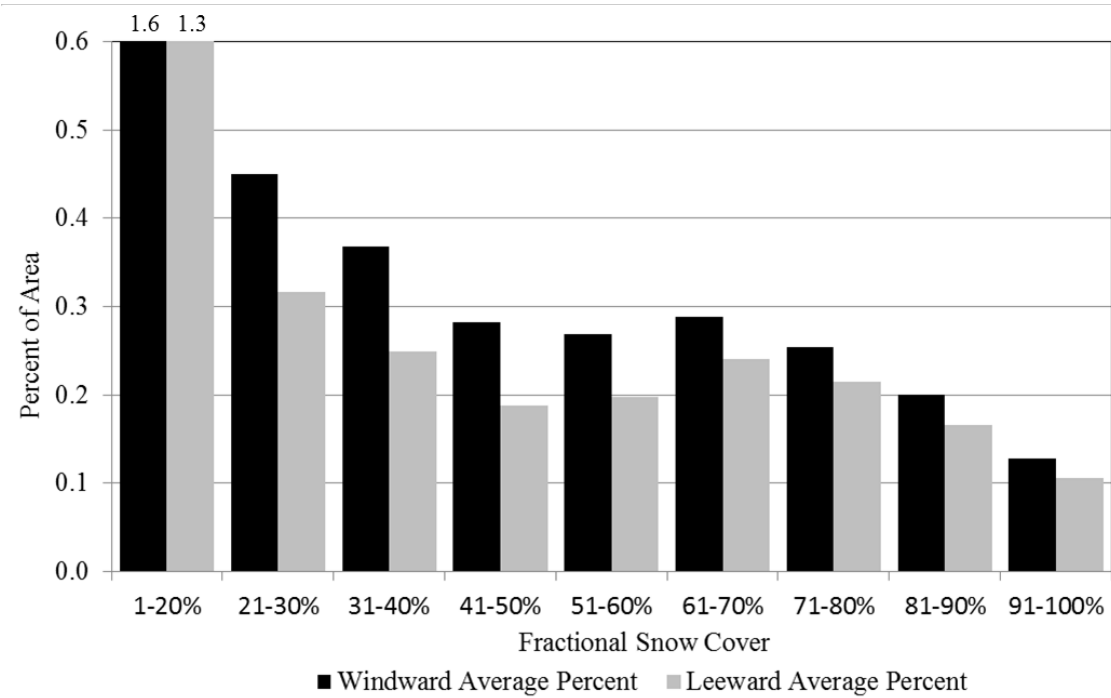


Figure 3.14. Average FSC percent of the total study area between windward and leeward aspects for the 16 NWFS (U) events.

Case Studies of Notable Events

Examining specific events within the period on a case study basis allows for an additional qualitative evaluation of the snow cover patterns using a synoptic perspective. HYSPLIT backwards air trajectories and HPC surface maps are incorporated for each snowfall event to determine the antecedent atmospheric circulation prior to event maturation. Snowfall event characteristics are incorporated from the manually classified event database at Poga Mt., North Carolina, as well as from COOP observer stations (Table 3.7). These data are combined with the MODIS FSC and true color products to form a discussion of how the synoptic or atmospheric processes may have shaped the spatial patterns of snowfall. In some cases, antecedent snow cover from a previous event or land cover issues affected the spatial patterns observed in the MODIS products. Unclassified events are excluded from the case studies, which are presented in order by average snow cover extent from greatest to least.

Table 3.7. Summary of case studies. Meteorological data were recorded at Poga Mt., North Carolina.

Event Maturation	Synoptic Class	Snow Extent Km ²	Snow cm	SLE mm	Temp. C	Relative Humidity
12/19/2009	MAB-u	49,457	38.9	1.9	-3.7	94.4
3/5/2012	SE-U	10,060	9.1	0.34	-3.5	90.1
2/10/2011	GU	15,024	2.54	0.07	-6	91.5
2/22/2009	NE-U	9,227	4.1	0.05	-4.7	87.7
2/27/2008	U	9,100	21.1	0.39	-7.2	91.4
10/28/2008	LC-U	1,536	5.6	0.22	-3	95
11/29/2011	CL-U	1,858	9.4	0.32	-1.3	92.9

Miller A/B Cyclone with Upslope Flow after Event Maturation (MAB-u)

The Miller A/B Cyclone occurring on 18 December 2009 dropped widespread accumulations of a foot or more across the study area that were more pronounced at higher elevations. Snow cover also extended across many valley locations and well into the Piedmont region. Surface analysis for the event maturation hour at 0000 UTC 19 December 2009 displays a low pressure system off the coast of North Carolina which supplied available moisture for snowfall to be widespread when combined with low temperatures across the study area (Figure 3.15). The backwards air trajectory ending at event maturation indicates NW flow occurring until 1200 UTC on 18 December, until the flow direction changed to the east, most likely from winds associated with the Miller cyclones off the North Carolina coast. The parcel rose from 900 to 841 hPa in the few hours before event maturation and promoted higher snowfall amounts associated with high elevation areas (Figure 3.16). Boone, NC recorded 37.6 cm, Poga Mt. 38.9 cm, Mt. Mitchell 71.1 cm, and further west, Mt. LeConte 72.4 cm, accumulation totals much higher across all locations when compared with other classes.

The true color snow map from the previous two days 20 –21 December before event end showed complete cloud obscuration of the surface since skies had not cleared and was deemed unsuitable for detecting snow. However, on 22 December, view of the surface is visible through gaps in heavy patches of cloud cover (Figure 3.17). This image offered the best view of the surface since the following days were marked by another incoming event and thus, more cloud cover. Boone recorded a daily average air temperature of 1.9 °C, so conditions warmed enough by this time to produce some melting at lower elevations, whereas Mt. Mitchell daily average air temperature was -7.2 °C. Snow reflectance is visibly

widespread across the entire study area, although the southwestern portion of the region appears snow free.

A snow shadow is present on the leeward (eastern) side of the escarpment over a smaller area of the foothills where accumulation totals may not have been as high compared to other areas. However, in-situ observations and discussion from the NWS winter storm assessment indicate that snow cover was continuous near 100% FSC across the region of the snow shadow (Lee and Moore 2009). NW flow during the event may have led to some downsloping effects prompting lower FSC values, though unlikely given the nature of the event. Forest cover is particularly dense along this portion of the escarpment, and melting in the canopy may have prevented MODIS from detecting as much snow cover across the steep slopes. FSC values in this area are particularly low at <20%, though the gradient of snow cover increases rapidly over short distances in all directions to near 100%.

The majority of pixels mapped as snow in the FSC product fell between 91-100% FSC and covered roughly 12,000 km² of the study area (Figure 3.18). In the 81-90% FSC bin, MODIS detected pixels covering almost 8,000 km² of the study area. MODIS detected the same amount of coverage in the 1-20% FSC bin along snow margins and in lower valley locations. Between 21-80% FSC, MODIS detected much lower values in each bin covering nearly 4,000 km² of the study area. Thick, patchy cloud cover obscured much of the snow covered area that may have fallen within this middle range of values. Over the entire study area, persistent low temperatures for days following event end preserved a widespread amount of snow cover across the region. Overall, the spatial pattern of snowfall from the Miller A/B event is much less idealized or recognizable when compared to other classes, though synoptic perspectives of the snowfall pattern are still evident in the snow cover maps.

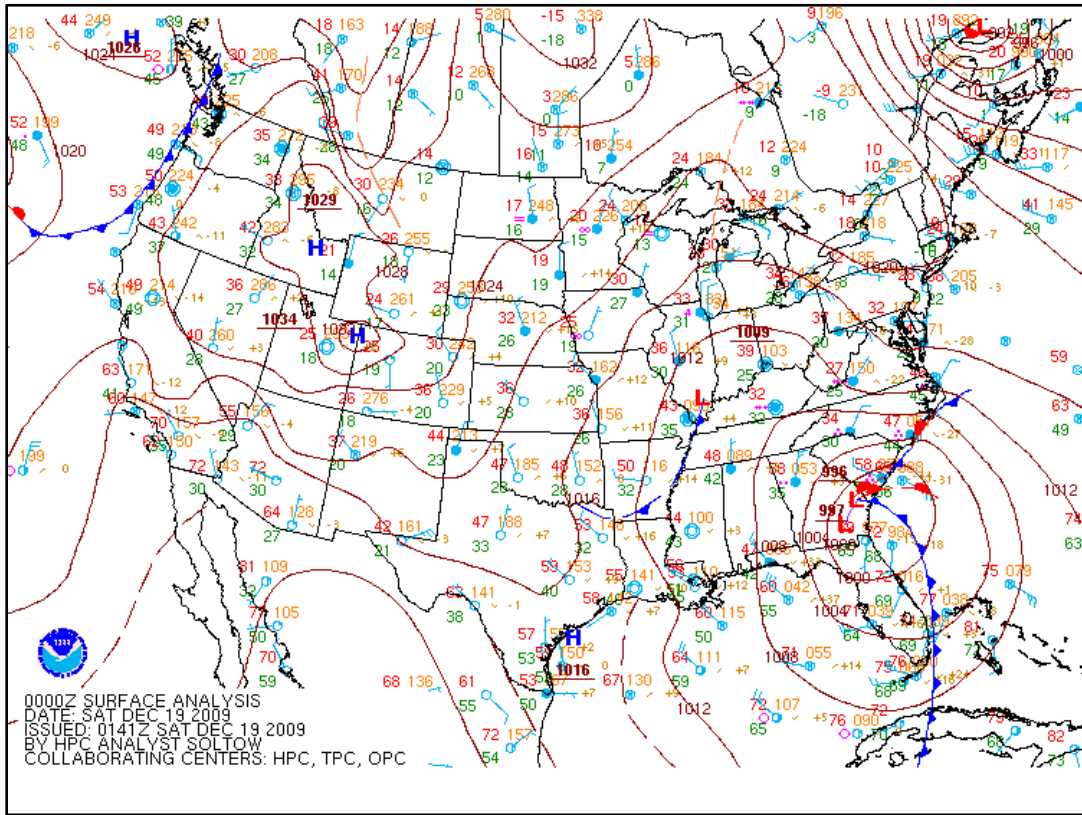


Figure 3.15. NOAA surface analysis from 19 December 2009 near event maturation hour. Large surface level low pressure system tracking up the coast of North Carolina contributed towards higher snowfall totals across the SAM.

NOAA HYSPLIT MODEL
 Backward trajectory ending at 0000 UTC 19 Dec 09
 GDAS Meteorological Data

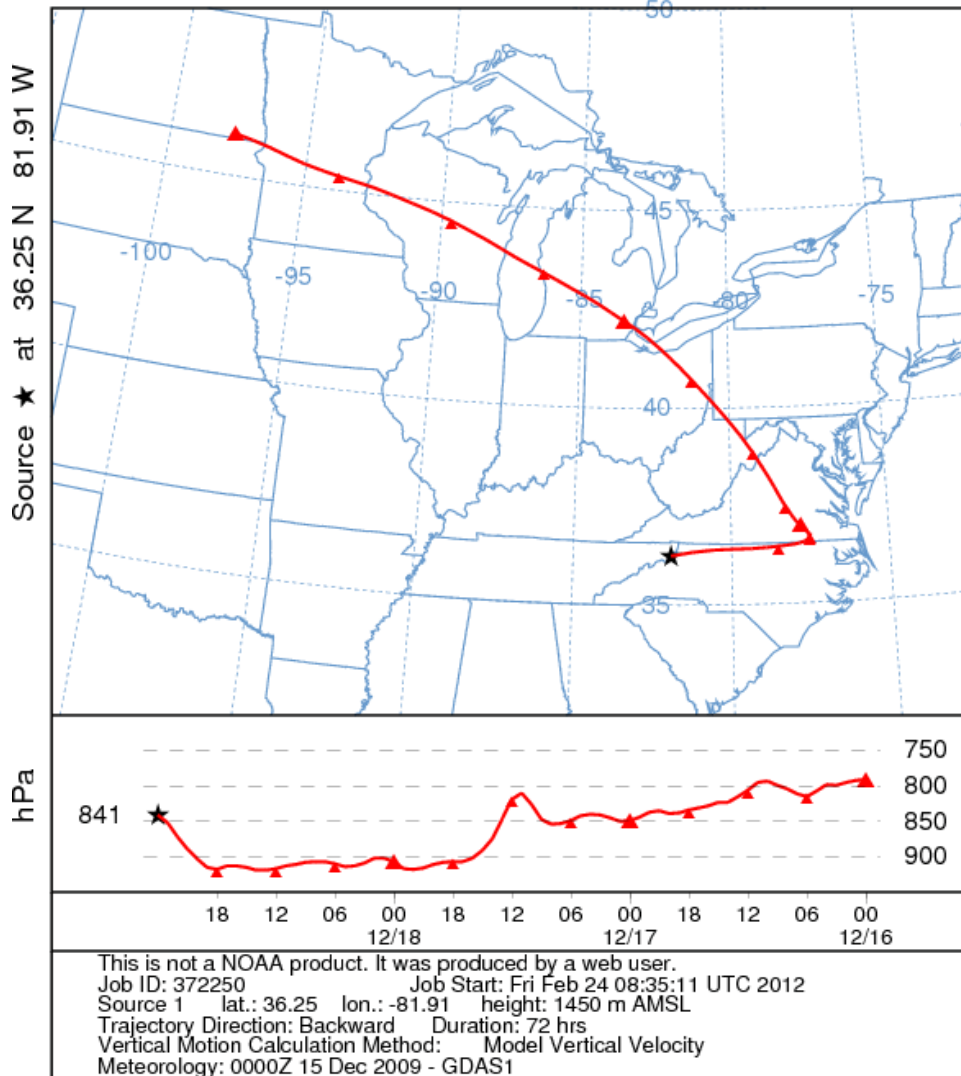


Figure 3.16. NOAA HYSPLIT backwards air trajectory for air parcels ending at Poga Mt., North Carolina. Descending motion, possibly related to the presence of upstream high pressure, occurs in the lead up to event maturation. Air begins to rise as it combines with wraparound flow from the Miller system before reaching Poga Mt.

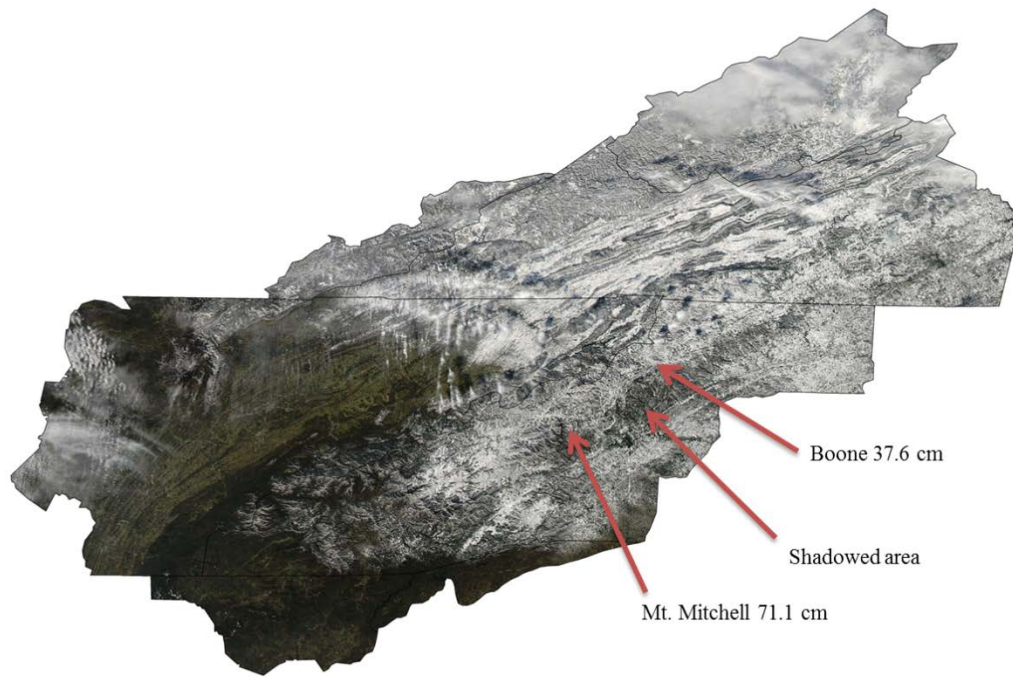


Figure 3.17. MODIS Aqua true color snow map from 22 December 2009 collected three days after event maturation for the MABu system, tile H11V05. Snow is visible through light cloud cover, and the majority of the surface is in clear view. Snow cover is widespread across the SAM and becomes more continuous into portions of Virginia and southern West Virginia.

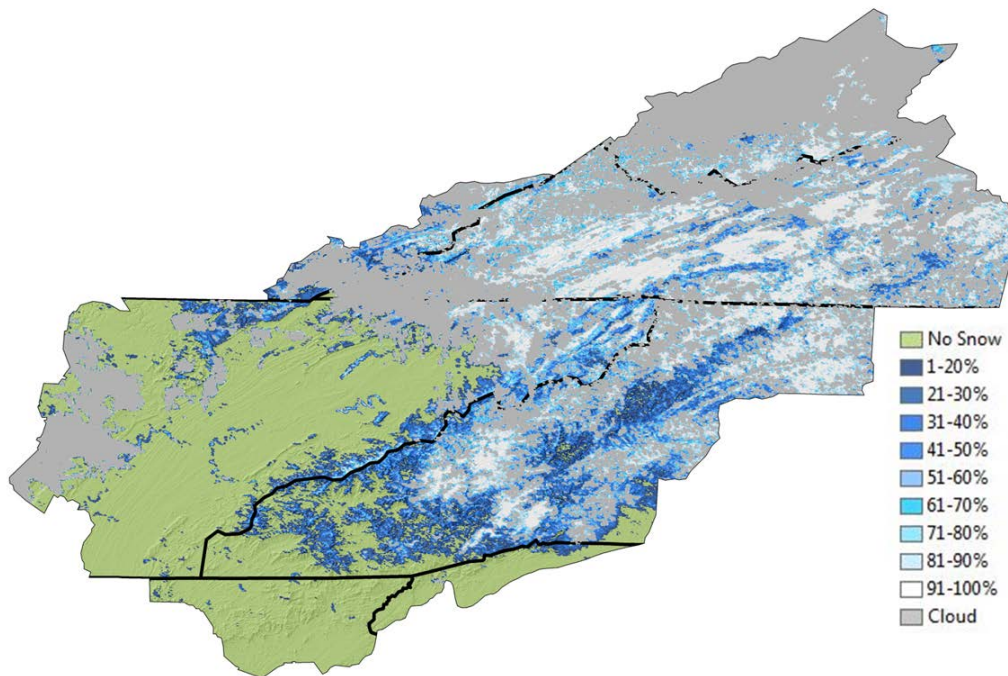


Figure 3.18. MODIS Aqua FSC map from 22 December 2009, tile H11V05. Cloud blocks some portions of the surface, but snow cover is assumed to be near 100% due to the widespread nature of accumulation from the MABu system. Darker values below 30% can be seen along the Blue Ridge escarpment and in the southwest mountains.

Southeastward Tracking Clipper with Upslope Flow after Event Maturation (SE-U)

Total accumulations from this Alberta Clipper event are isolated to a few high elevation areas of northwestern North Carolina and are mostly located in southern West Virginia. The surface analysis for the event maturation hour on 5 March 2012 at 1400 UTC displays northwesterly flow into the region that is enhanced by elevation or temperature, depending on local conditions at the surface (Figure 3.19). The HYSPLIT backwards trajectory shows the air parcel originating over portions of eastern Montana and descending to the surface along the trajectory course through the central U.S. In the final 6 hours before event maturation, the parcel rose from 950 to 849 hPa, providing the lift necessary for snowfall development intermittently across portions of the region (Figure 3.20). During this fast moving event, Boone, NC recorded 7.6 cm, Poga Mt. 9.1 cm, Mt. Mitchell 25.4 cm, and most other accumulation totals tended to favor areas further north. Western North Carolina and eastern Tennessee experienced trace amounts of accumulation.

The true color product from the day of event maturation showed cloud obscuration of the surface since skies had not cleared and was deemed unsuitable for detecting snow. However, the surface is visible over the majority of the study area on the following day and the snow cover is practically non-existent (Figure 3.21). Boone recorded a daily average air temperature of 1.7 °C, so conditions warmed to produce melting at lower elevations, whereas Mt. Mitchell daily average air temperature was -5.0 °C, and the snow cover is still preserved in certain areas.

The FSC product from 6 March 2012 is used to compare performance with the true color image (Figure 3.22). The majority of pixels mapped as snow by MODIS fell within 1-20% FSC and covered less than 6,000 km² of the study area. This event favored isolated areas

where conditions were ideal for snowfall. Most of the FSC is noticeable in southern West Virginia, though some isolated snow cover exists at higher elevations of northwestern North Carolina. Snow cover is especially visible in the higher elevation areas of Elk Knob and Snake Mt. in Watauga County, North Carolina and in the northern portion of Ashe County. A linear pattern of snow cover may be a result of convective bands of cloud cover. This event produced virtually no FSC higher than 50%. MODIS identified cloud cover in the northern reaches of the study area which is difficult to distinguish in the true color product. In this case, trace amounts of snow were undetectable when melt onset occurred after event end.

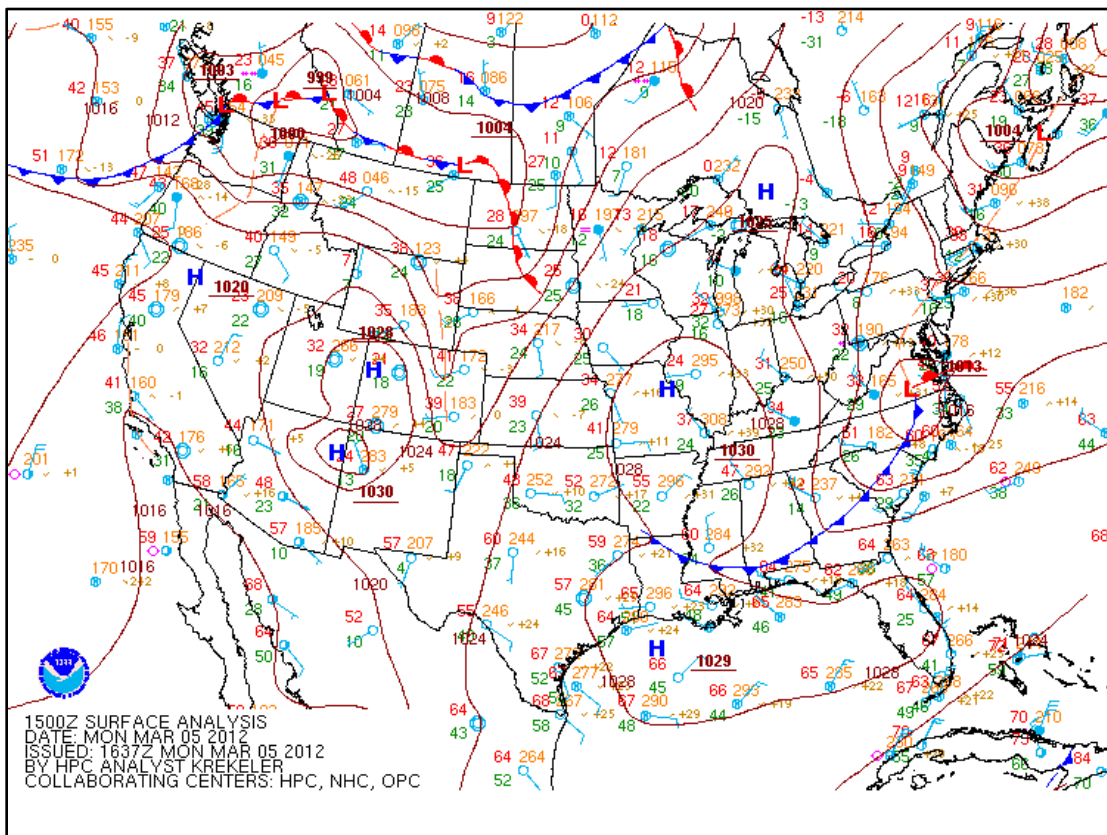


Figure 3.19. NOAA surface analysis near event maturation hour during the 05 March, 2012 Alberta Clipper event. The southeastward tracking clippers are marked by a cold frontal passage from the northwest over the SAM.

NOAA HYSPLIT MODEL
 Backward trajectory ending at 1400 UTC 05 Mar 12
 GDAS Meteorological Data

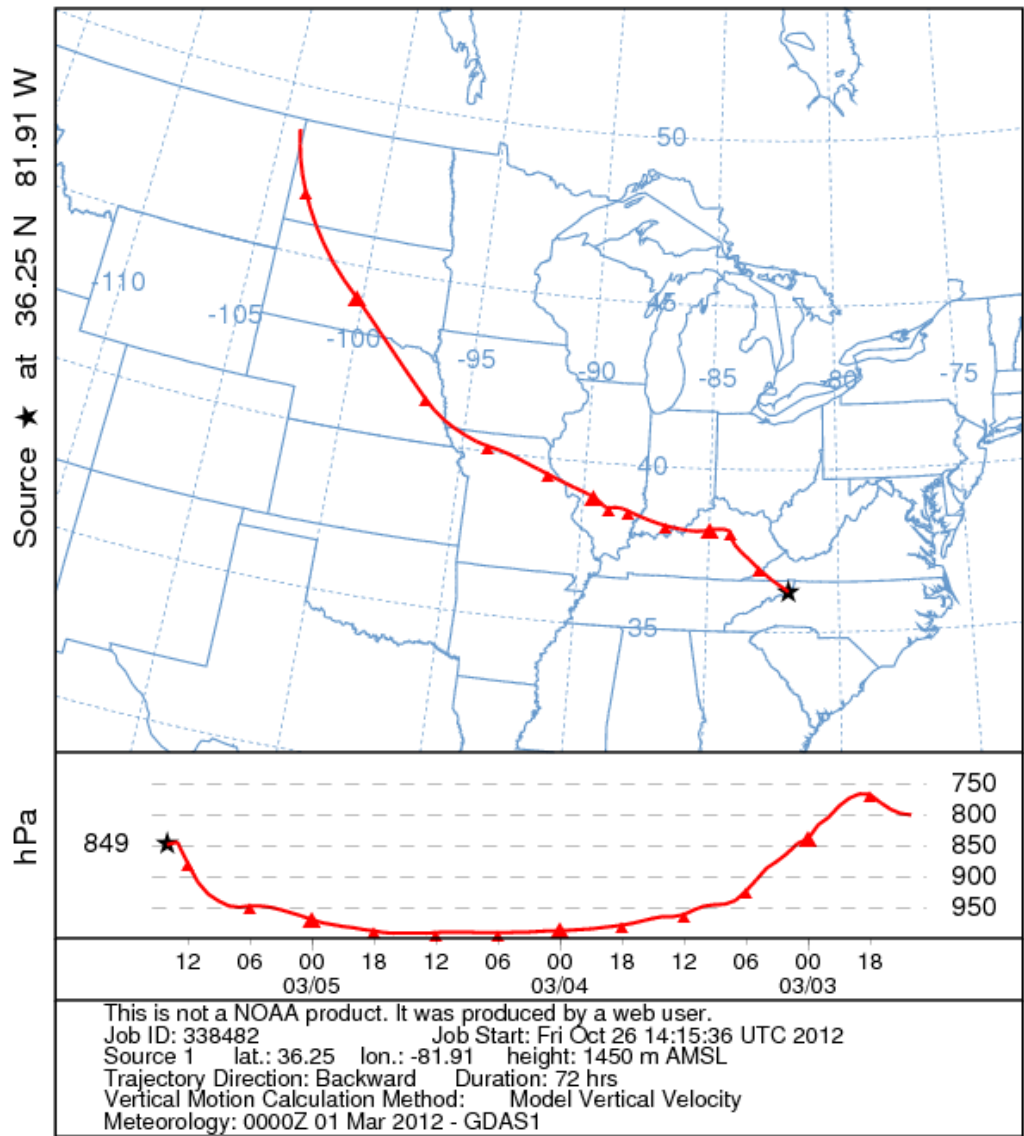


Figure 3.20. NOAA HYSPLIT backwards air trajectory for the Alberta Clipper event. Northwest flow occurs before air rises to the 849 hPa level at event maturation over Poga Mt., North Carolina.

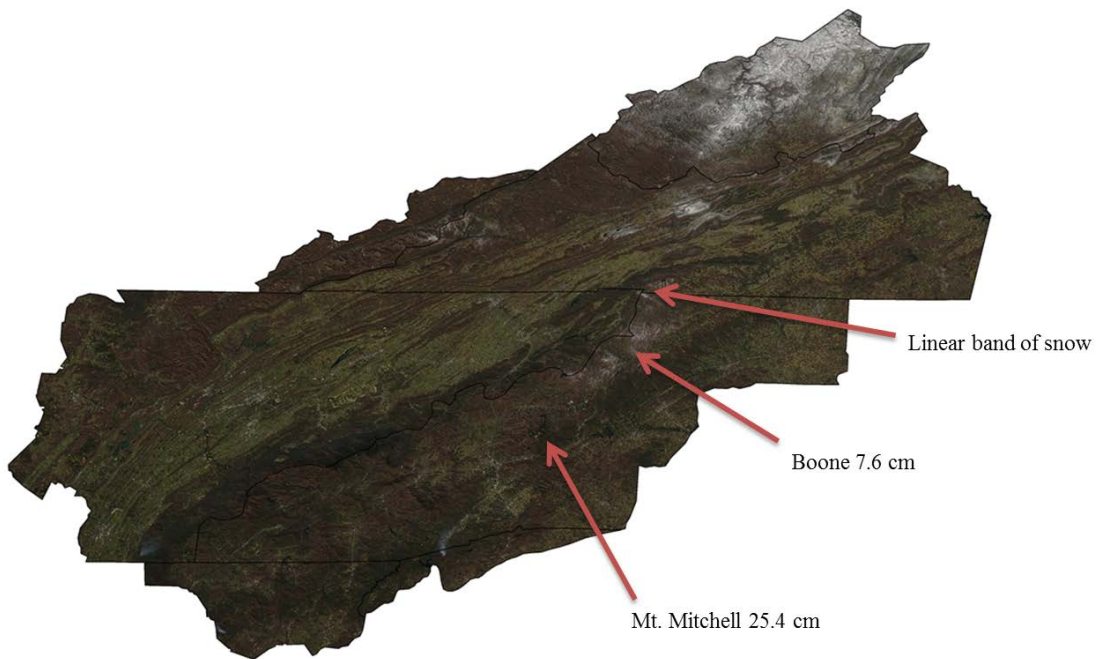


Figure 3.21. Aqua MODIS true color image from the day after event maturation, 6 March 2012, tile H11V05. Though the majority of southeastward tracking clippers exhibit a broad spatial pattern of snow cover, this Alberta Clipper was characterized by significant melting before sensor overpass. Accumulations were presumably more extensive on the previous day, though cloud cover prevented any visible reflection of the snow. Some accumulations are visible in NW North Carolina.

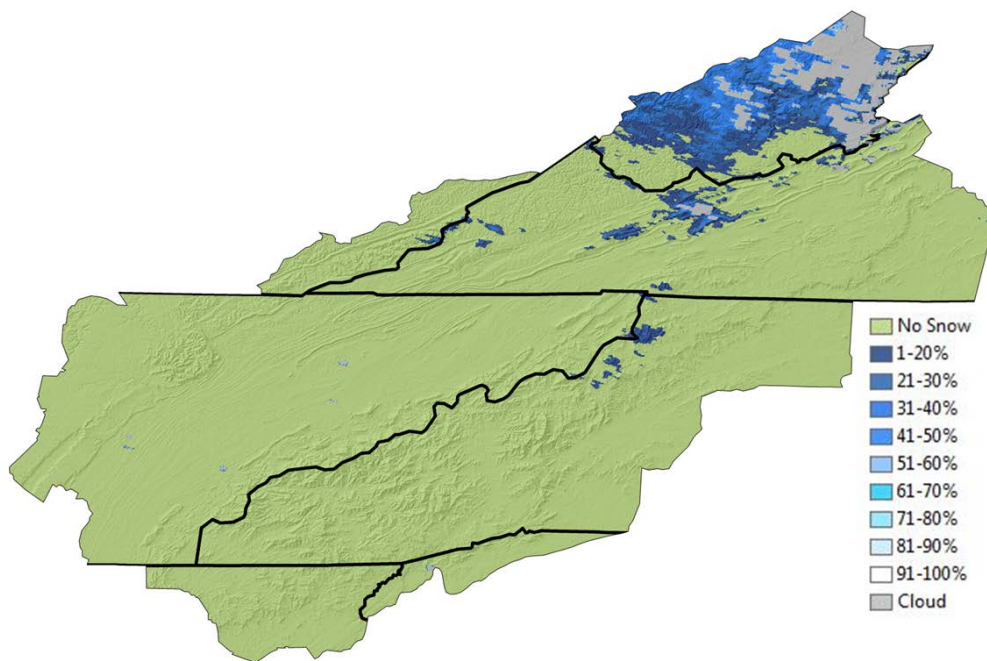


Figure 3.22. Aqua MODIS FSC map displaying less than 50% snow cover values, tile H11V05. Snow cover was limited to portions of NW North Carolina and southern West Virginia on the day after event maturation.

Gulf Surface Wave or Weak Low (Non-U)

While the Non-U category includes multiple synoptic classes, this discussion focuses on the 10 February 2011 gulf surface wave (GU) due to its unique snowfall pattern. This weak disturbance moved along the Gulf but did not turn northward up the East Coast like a Miller system. The HYSPLIT event trajectory reveals predominately northwesterly low-level flow before reaching Poga Mt. at event maturation (Figure 3.23). There is no associated eastern trajectory from this event, which may be a contributing factor towards the favored mountain locations. Gulf moisture via isentropic lifting was the dominant contributor to snowfall development west of the SAM in contrast to the Miller systems, where the Atlantic provides a secondary source of available moisture and is fed into the system.

Accumulations were variable between mountain and valley locations. While Poga Mt. observed only 2.54 cm of event total snowfall, Mt. LeConte in the Great Smoky Mountains further west recorded 12.7 cm. The Mt. Mitchell COOP station observed 10.2 cm of snowfall associated with this disturbance. Boone observed zero snow accumulation associated with this event, suggesting that mountain slopes were favored spots for snowfall while the valley locations experienced much less observable precipitation. The surface map from event maturation hour displays a low moving off the coast of North Carolina and a developing anticyclone further to the west in the central portion of the U.S (Figure 3.24). Snowfall development may have solely occurred as a result of isentropic lifting and in association with orographic lifting on mountain slopes leaving the mountain valleys snow free.

Daily average air temperature at the Mt. Mitchell COOP station was -8.9°C , so the snowpack was preserved at the higher elevations above the freezing level in the snow maps. Air temperature from event maturation at Poga Mt. was slightly higher at -6°C , and the

average air temperature in Boone for the date of image acquisition was -4.7°C . Any snowfall would likely be preserved as snow cover, visible in the MODIS snow maps. The true color snow map displays very little snow cover, with mountain ridges being the sole location for favored accumulations (Figure 3.25).

One interesting observation is the continuous snow cover occurring across lowland portions of Tennessee when compared to the mountain locations, explained by the event trajectory wavering across this area in the lead up to maturation hour. A continuous band of snow cover occurs in the FSC map along the western portion of the North Carolina, Tennessee border, though 0% FSC is present along the eastern side. Visible snow cover is slightly more continuous in the true color product when compared to the FSC performance. The FSC snow map shows a maximum in the 1-20% class, with only the highest mountain tops observing near 100% FSC. The remaining FSC classes 21-90% fall across a steep gradient surrounding the peaks and ridges, since there were very little snow covered pixels beyond the mountain slopes (Figure 3.26). Light accumulations across the entire study area are evident in the FSC snow map, which is useful for developing the synoptic perspective from this event.

NOAA HYSPLIT MODEL
 Backward trajectory ending at 0400 UTC 10 Feb 11
 GDAS Meteorological Data

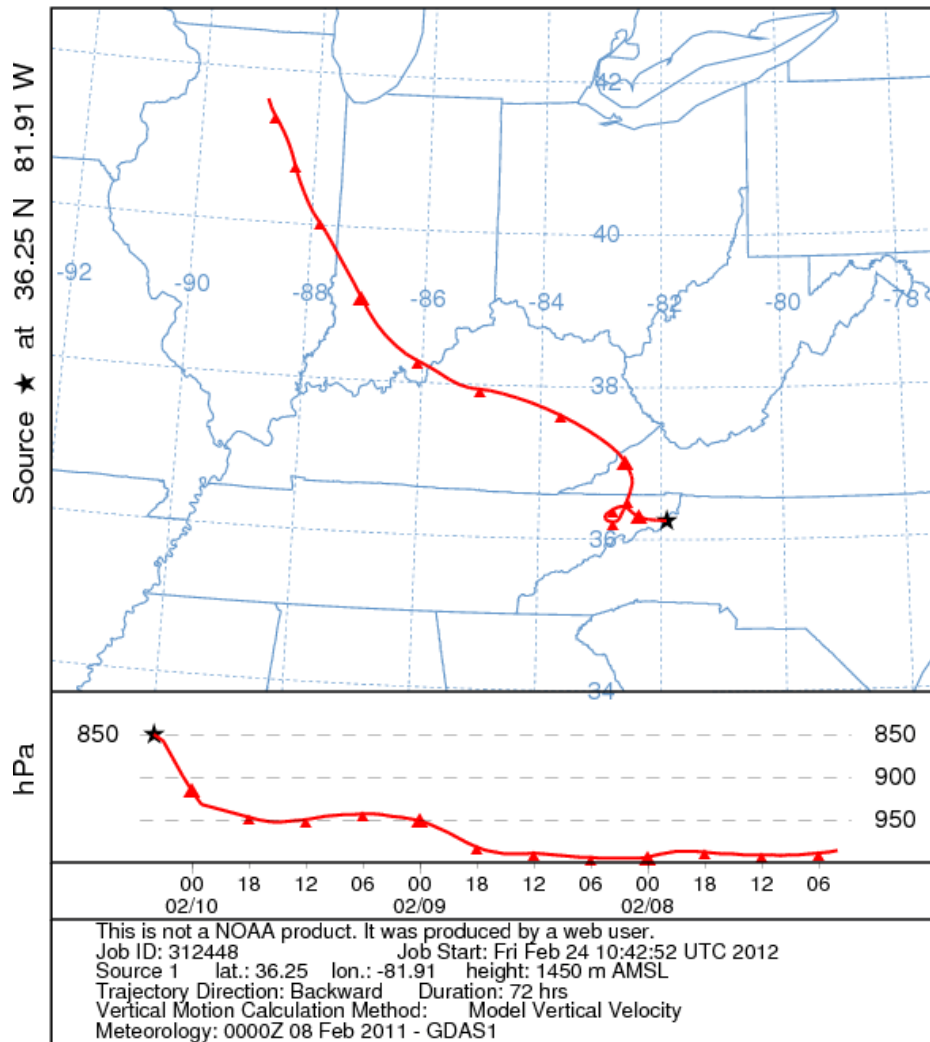


Figure 3.23. NOAA HYSPLIT backwards air trajectory for the 10 February 2011 gulf surface wave ending at Poga Mt., North Carolina. Shallow low level flow occurred until the 18 hours preceding event maturation, rising to 850 hPa.

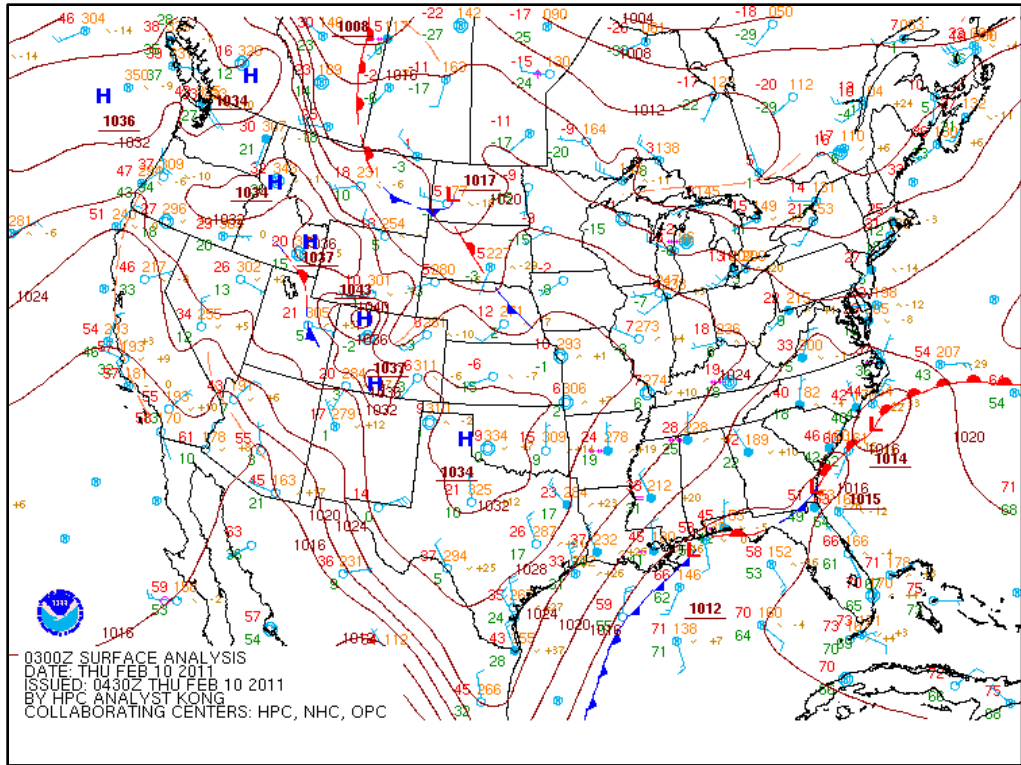


Figure 3.24. NOAA surface analysis near event maturation. A weak surface wave is present across the gulf region.

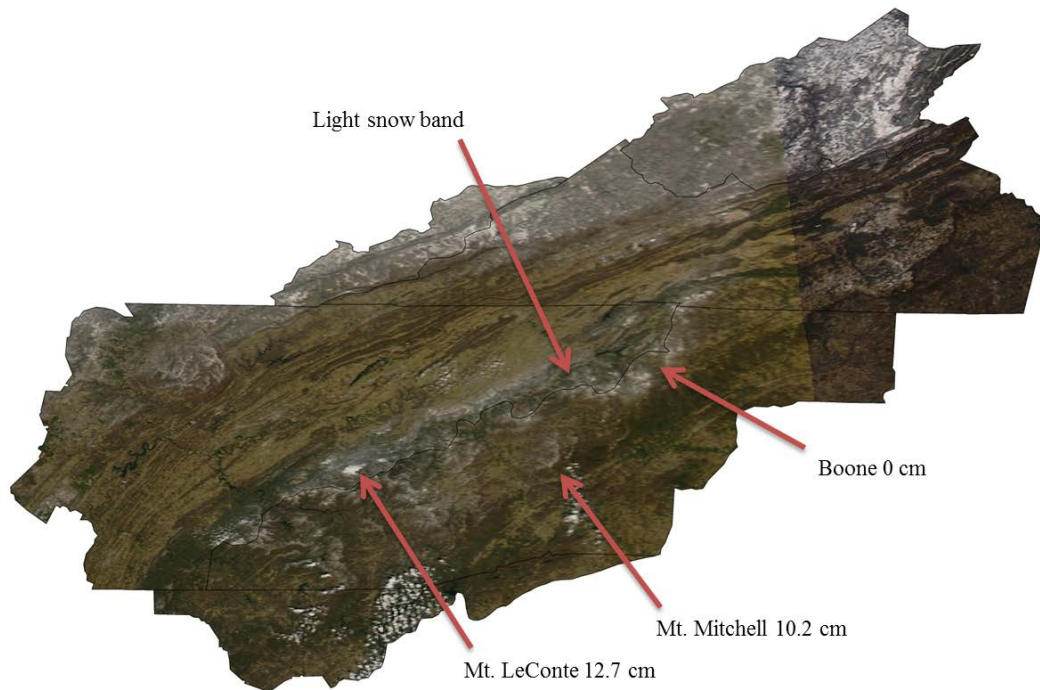


Figure 3.25. Aqua MODIS true color image from day of event maturation and ending on 10 February 2011, tile H11V05. SAM snow cover is visible across the ridge top locations. An outer band of snow occurs on the western periphery of the SAM and extends beyond the study area boundary.

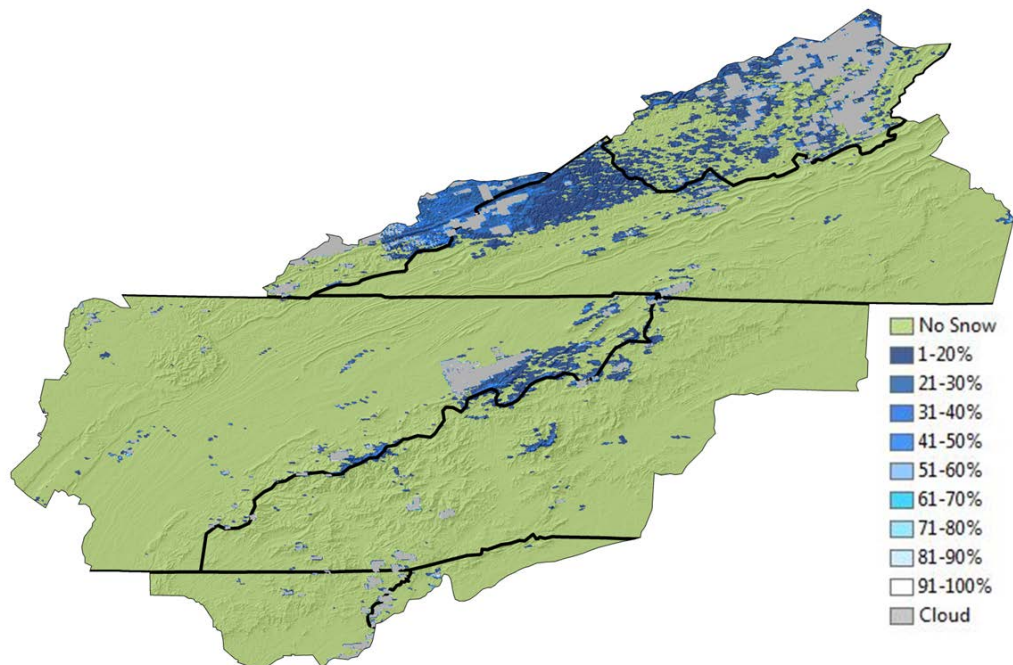


Figure 3.26. MODIS FSC map from day of event maturation and ending on 10 February 2011, tile H11V05. Minimal snow cover is detected, and most pixel values fall within the 1-40% classes. The high elevation ridges of western North Carolina and eastern Tennessee are visible as well as western portions of Virginia.

Northeastward Tracking Low Passing to the North with NW Upslope Flow(NE-U)

During northeastward tracking lows, the region is frequently in the warm sector, but is subject to a rapid temperature fall immediately behind a cold frontal passage. Thus, chances are increased for the MODIS snow maps to adequately capture the snow in this event class. One difficulty with the NE-U systems is that snow extents are much less expansive compared to the previous events, so accumulations can be more difficult to discern. During the 22 February 2009 NE-U event, the dominate flow pattern occurred in a shallow layer from the northwest before rising to 849 hPa at maturation hour (Figure 3.27). The surface maps reveal the cold frontal passage occurring behind the surface low, so temperatures at lower elevations may have been more marginal immediately during the snowfall, making accumulation more difficult preceding the cold front (Figure 3.28).

Poga Mt. received 4.3 cm of snowfall with an average air temperature from the two hours surrounding event maturation of -4.7°C . The majority of the snow cover in the true color snow map occurs in portions of Avery County, North Carolina near Beech Mt., and Sugar Mt. Poga Mt. is included in this band of snowfall since temperatures were ideal for the persistence of the snow pack after the cold frontal passage. Boone did not record any snowfall associated with the event, and temperatures were marginal for any trace snow to accumulate at -0.8°C . Mt. LeConte only recorded 7.6 cm of snowfall, while Mt. Mitchell observed slightly higher snowfall at 8.9 cm. Both peaks experienced roughly 1-2 cm of NW upslope flow accumulation after the cold frontal passage adding to the storm snowfall totals. Average daily air temperature recorded at the Mt. Mitchell COOP station was -5°C , so temperatures in the valley locations would have made accumulations more difficult.

The snow maps confirm the findings in the in-situ observations. Visible reflection of the snow in the true color snow map is limited to high areas within the Great Smoky Mountains and along the Black Mountain Range (Figure 3.29). A small border portion of snow cover exists in the vicinity of Roan Mt., which continues further into the North Carolina high country, but is nonexistent in the area immediately surrounding Boone. FSC cover maxima occur in the 1-20% class due to the lighter accumulations during this event. FSC values continue to progressively level off approaching 50%, while values from 51-100% equally occur as the minimum snow cover extents (Figure 3.30). These values suggest that snowfall development occurred only in specific locations where temperatures were low enough behind the cold front in combination with available moisture for precipitation. Ideal locations were primarily located across the ridges and mountain tops in the southwestern and northwestern portions of North Carolina, while central valley locations in the mountains experienced virtually no snowfall.

NOAA HYSPLIT MODEL
 Backward trajectory ending at 1100 UTC 22 Feb 09
 GDAS Meteorological Data

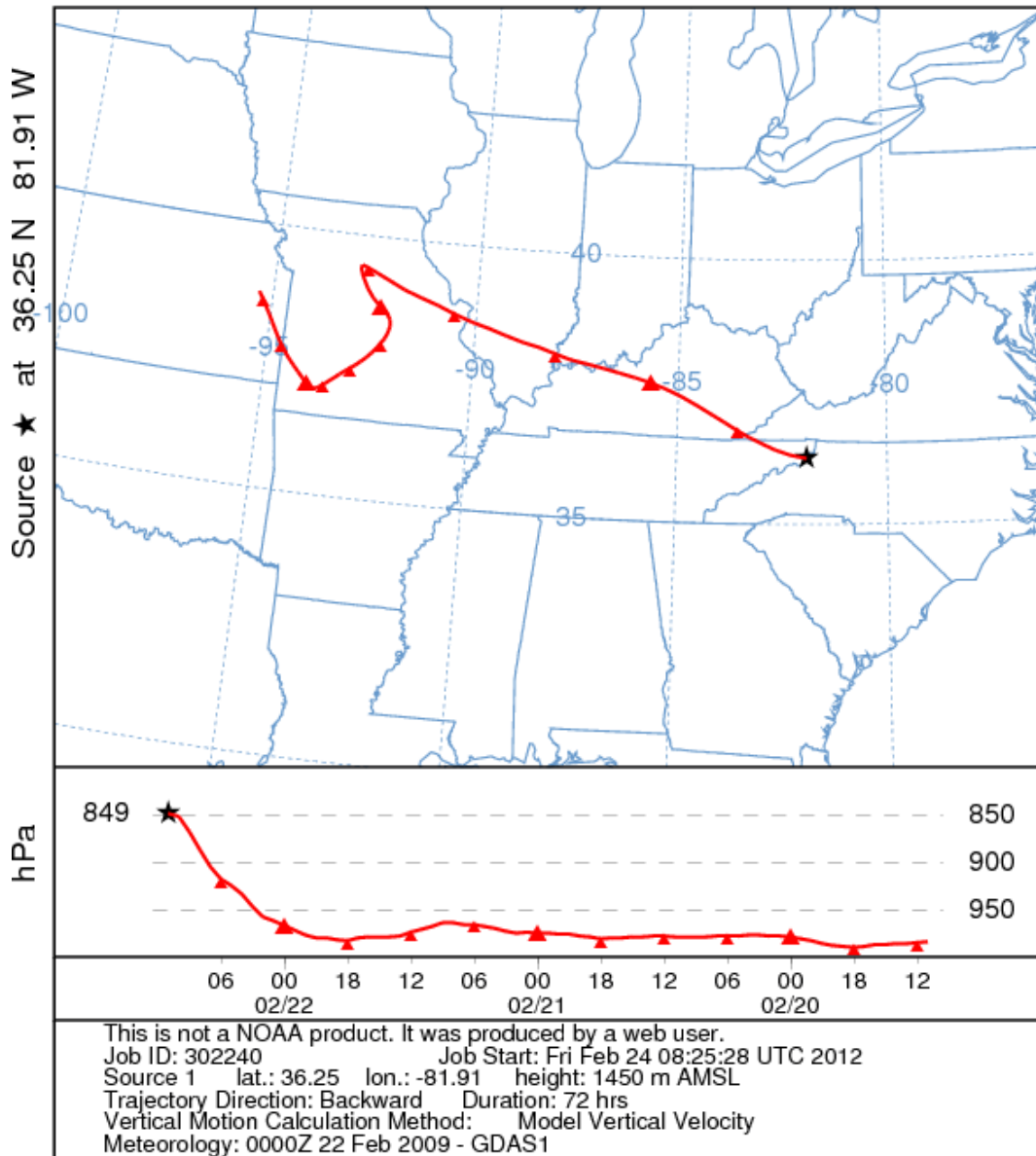


Figure 3.27. NOAA HYSPLIT backwards air trajectory for the 22 February 2009 northeastward tracking low event. Shallow NW flow is present in the lead up to event maturation, contributing to upslope flow after the frontal passage.

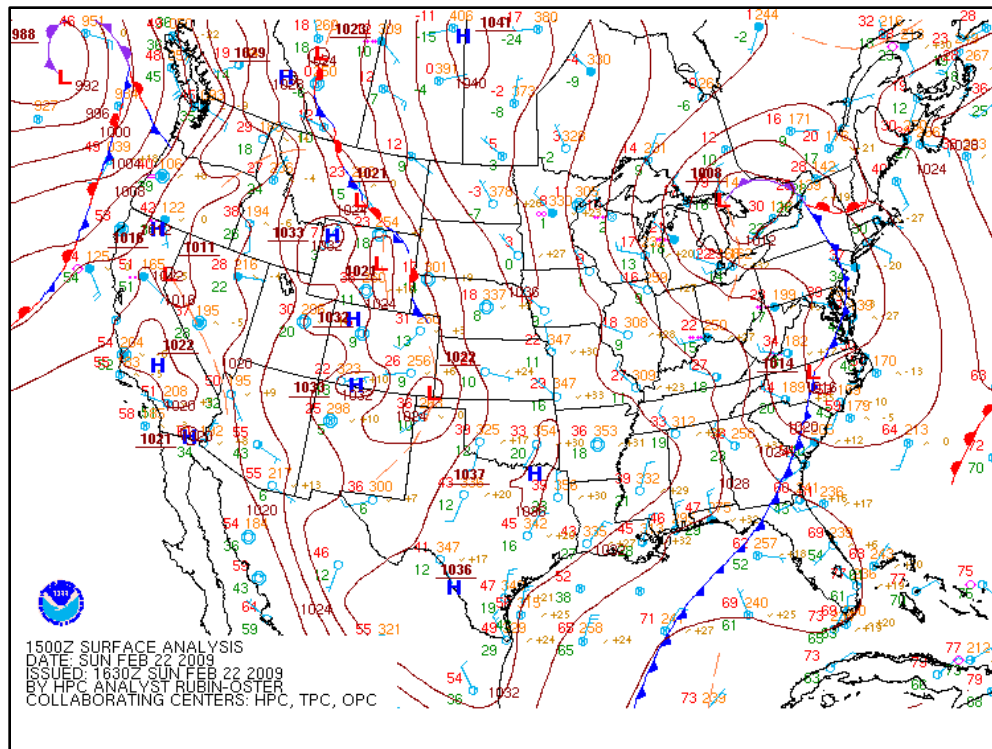


Figure 3.28. NOAA surface analysis at 1500 UTC near event maturation hour. Cold frontal passage associated with the northeastward tracking surface low is located in the central portion of North Carolina.

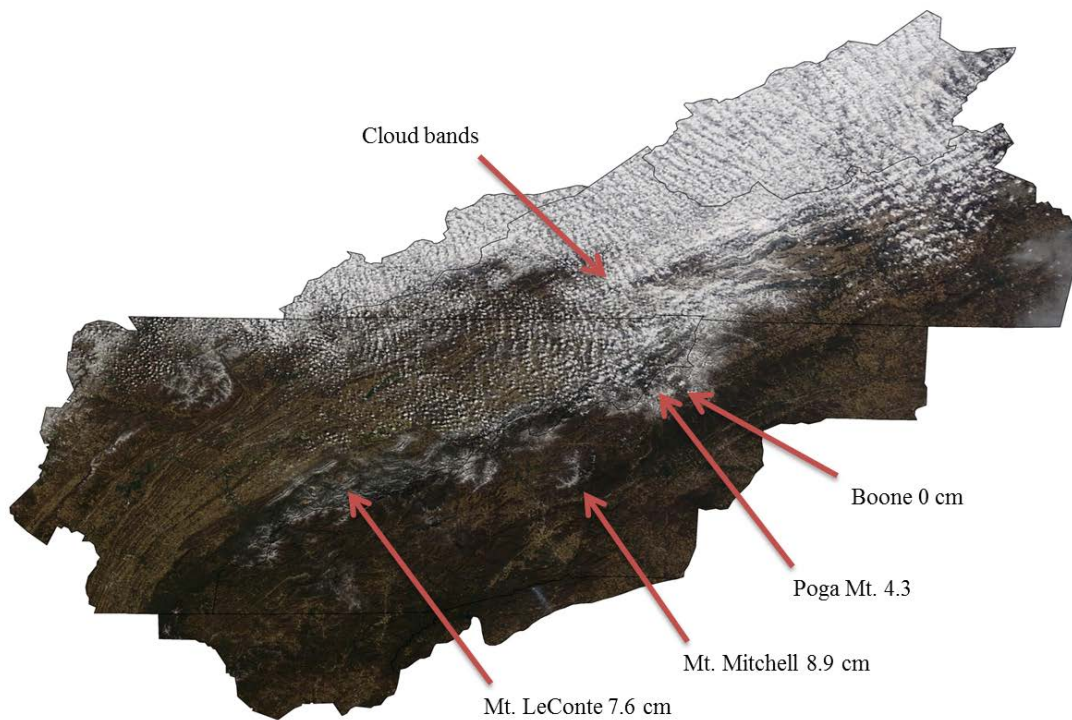


Figure 3.29. Terra MODIS true color image from the day after event maturation, 23 February 2009, tile H11V05. Cloud bands prevent some northern snow from view, however portions of the Great Smoky Mountains, Mt. Mitchell, and the Blue Ridge of NW North Carolina present a clear snow surface.

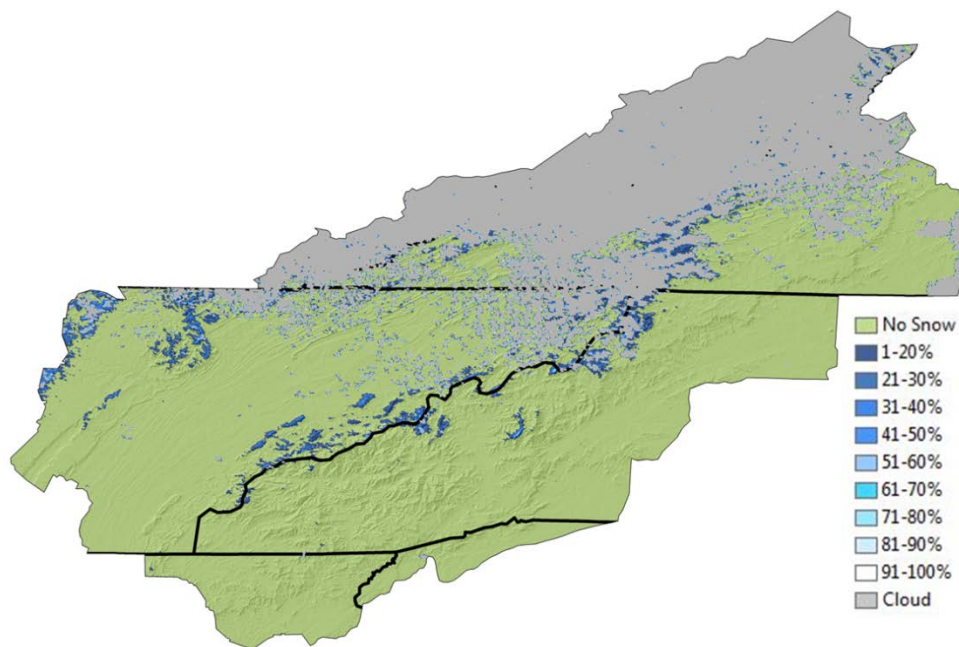


Figure 3.30. Terra MODIS FSC map. The snow map algorithm is very conservative with cloud cover over northern portions of the study area, tile H11V05. Snow cover over the southwestern peaks is still visible, though the most continuous area of snow likely occurs beneath the cloud, further north in association with the northeastward tracking low.

NW Upslope Flow in Absence of Frontal or Surface Features (U)

An extended NWFS event occurred 26 February 2008, producing a signature pattern of snow cover isolated to windward, high elevation peaks and ridges along the North Carolina-Tennessee border. This event formed in the presence of a deep upper level trough over portions of the Mississippi Valley and continued for over 24 hours (Holloway 2008). The majority of the SAM is non-snow covered during this event. Lower elevations along the snow covered area are typically comprised of 1-40% FSC, while areas of 81-100% FSC become more common at isolated high points found within the surrounding lower values of FSC (Figure 3.31). Areas surrounding Great Smoky Mountains National Park exhibit a more continuous snow cover pattern which continues south through the Balsam Range. Gaps with no snow occur across the Asheville valley where snow cover begins to build across the Black

Mountain Range. Snow cover continues along the border from Roan Mt. into Avery and Watauga counties, though low lying areas are typically snow free since the image acquisition date occurred one day after event ending. The snow cover becomes more widespread around Mt. Rogers, Virginia.

The surface map for the event maturation hour displays NW flow occurring as wraparound from a low pressure system centered off the coast of Maine. This system is further fed by clockwise flow from the approaching high pressure to the west, causing snowfall to cease by event end (Figure 3.32). Moisture is available along portions of eastern Tennessee and towards the North Carolina border, as well. In addition, a cold frontal passage is located off the coast line indicating the presence of cold air and ideal low temperatures for preserving the snow after the event. The HYSPLIT trajectory indicates continuous low level flow occurred around the 950 hPa level until the air parcel reached southeastern Kentucky and began to rise to 840 hPa (Figure 3.33). Available moisture was supplied as the parcel extended southward along the western shore of Lake Michigan.

By ending hour on 28 February, Poga Mt. recorded 21 cm of event total snowfall compared to the COOP observer station at Mt. Mitchell which only observed 10.2 cm of snowfall associated with the upslope event. Mt. LeConte, at the high end of the accumulation, observed 55.9 cm total snowfall by event end. Poga Mt. data indicated a relatively high level of humidity at 91.4% in addition to the NW wind direction, providing ideal conditions for shallow moist layers to undergo precipitation development as convection occurs. One curious finding is the small snowfall totals observed at Mt. Mitchell, especially when compared to snowfall at Mt. LeConte. Snow extent in the true color snow map favored a widespread area in the Smoky Mountains further to the west, suggesting the presence of

greater spillover from the windward slopes (Figure 3.34). Snow cover is still visible along the slopes of Mt. Mitchell, but is more limited to the high elevations. In general, Mt. Mitchell lies further downwind of the border, providing a further travel distance for low level flow to encounter the mountain barrier when compared to Mt. LeConte. Snow in the vicinity of Poga Mt. is more widespread compared to the low valleys surrounding Mt. Mitchell. In this case, the snow maps are useful for delineating the boundary of snow accumulation from the event across different portions of the SAM.

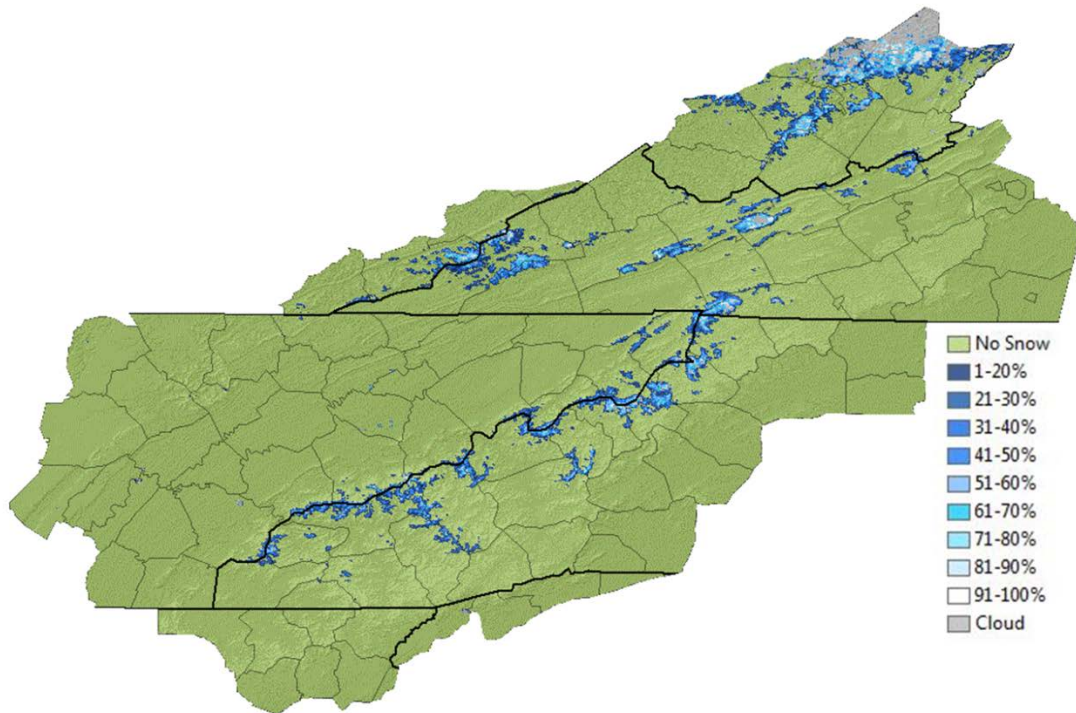


Figure 3.31. Terra MODIS FSC map from 28 February 2008, two days after event maturation, tile H11V05. Clear sky conditions provide a good view of the snow cover, idealized for high elevation and windward slopes.

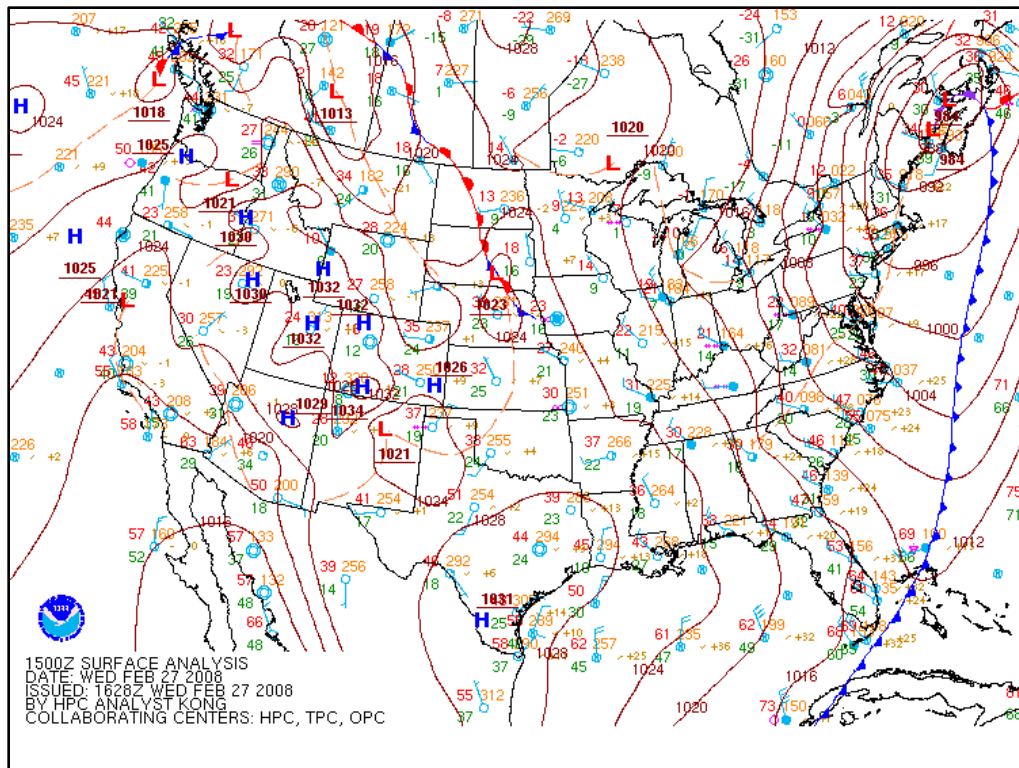


Figure 3.32. NOAA surface map for conditions near event maturation hour at 1500 UTC on 27 February 2008. Low level northwest flow occurs as wraparound from a surface cyclone off the coast of Maine, leaving the SAM in the cold sector.

NOAA HYSPLIT MODEL
 Backward trajectory ending at 1100 UTC 27 Feb 08
 GDAS Meteorological Data

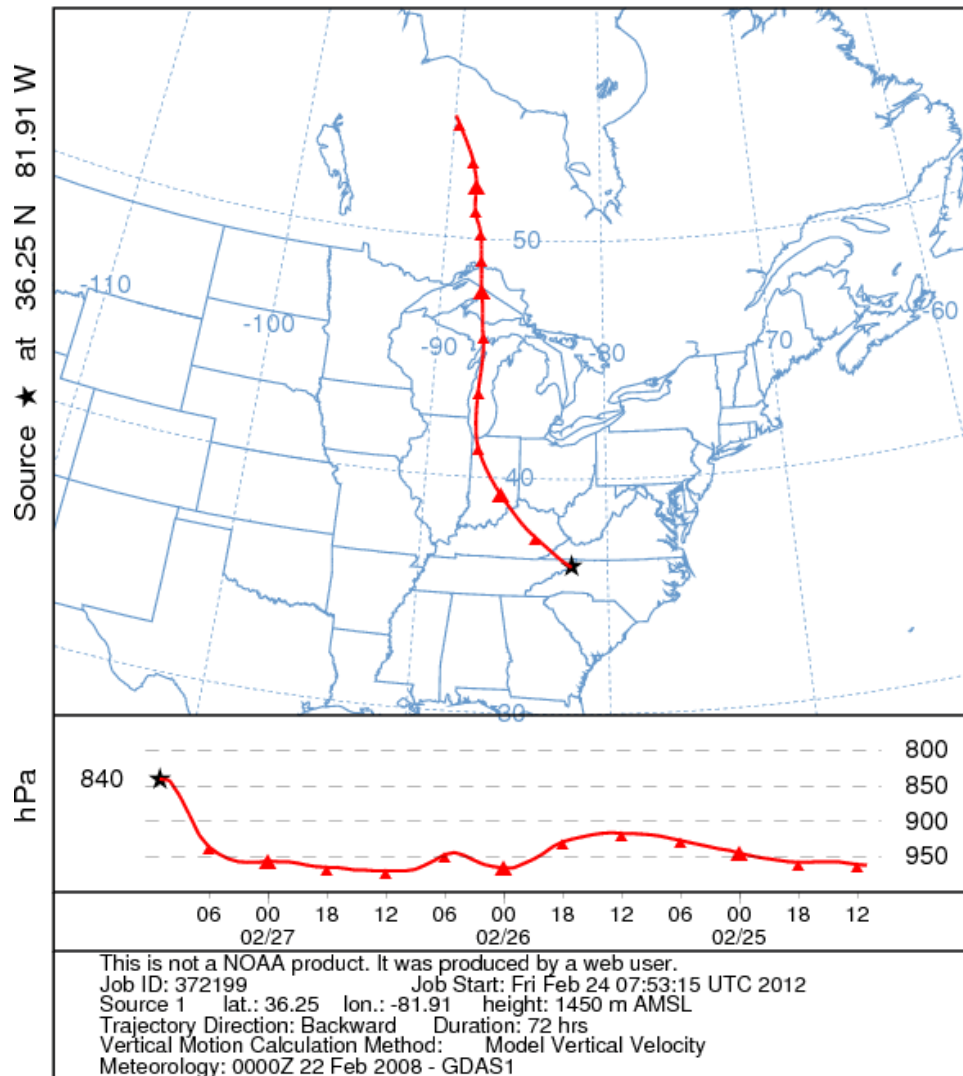


Figure 3.33. NOAA HYSPLIT backwards air trajectory for the 26 February 2008 NWFS (U) event. Upslope flow occurred in absence of other surface or frontal features occurred rising to 840 hPa.

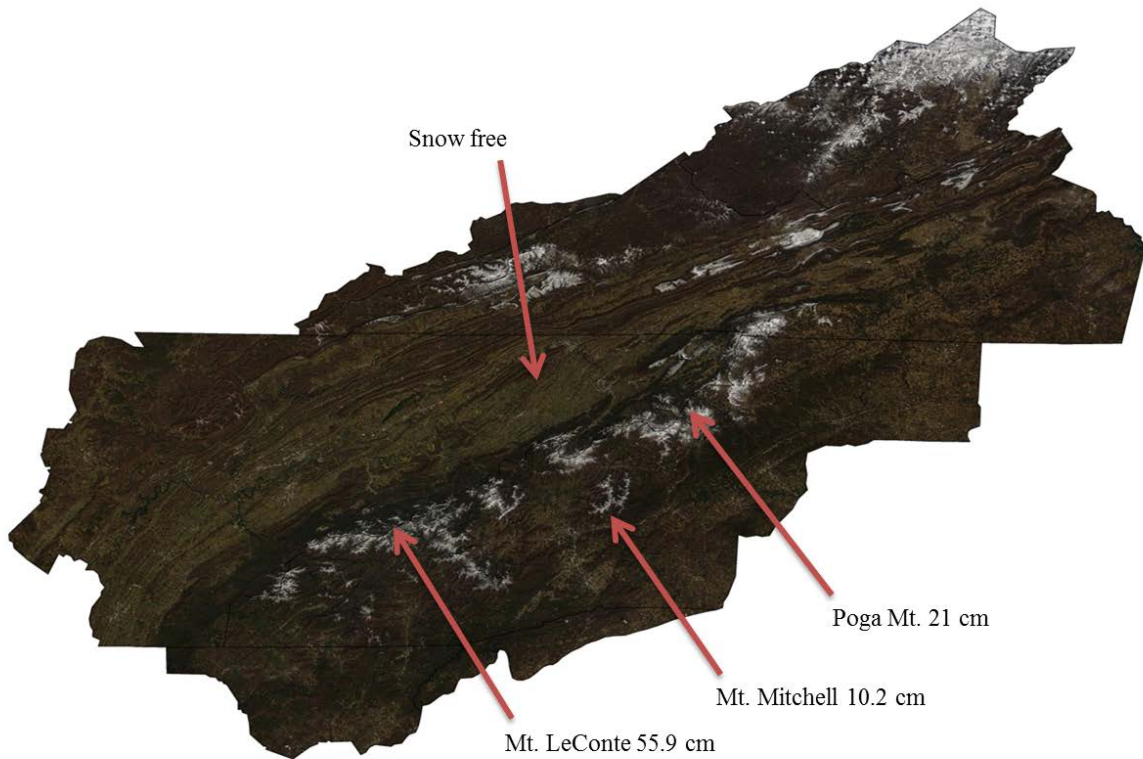


Figure 3.34. Terra MODIS true color image from 01 March 2008, tile H11V05. Clear skies are present with no cloud cover. The snow surface is visible across all major high elevation peaks and ridges in the SAM. Valleys and low elevation areas are snow free.

Leeward Surface Cyclone with NW Upslope Flow (LC-U)

Surface cyclones develop between the lee of the Appalachians and the Atlantic Coast where snow cover is highly limited in terms of raw pixel counts in the snow maps. The LC-U class contains the second lowest measurable snow extents out of all the event types. An early season lee cyclone occurred 28 October 2008 with visible snow cover favoring the high elevation areas of northwestern North Carolina and southwestern Virginia. The event trajectory indicates northwest flow occurring in the lead up to event maturation and would have contributed to NWFS occurring in conjunction with the rotation of the lee cyclone (Figure 3.35). The surface map confirms the presence of NW flow occurring at event maturation as wraparound when the surface cyclone tracked up the Atlantic Coast. The SAM

is completely within the cold sector during this event, indicating that limited moisture was the contributing factor to the small snowfall totals (1,536 km²) that were observed (Figure 3.36).

Poga Mt. observed 5.6 cm snowfall with an average air temperature from the two hours surrounding event maturation hour of -3 °C. Liquid water equivalents were recorded at 0.22 mm, indicating low density snow. Unrimed dendrites from limited moisture content may have contributed towards the observed spatial pattern in this event since the accumulation area would be located further downwind of the already small snowfall totals that were observed.

Conditions were very similar atop Mt. Mitchell where the COOP station reported 10.2 cm snowfall from the event and the average air temperature for the day was -4.4 °C. Conditions were milder in Boone where snow accumulated 0.3 cm, and the average daily air temperature was recorded at 3.3 °C. Any snowfall would have likely melted in the valley locations that exhibited similar conditions, and this characteristic is evident in the true color snow map where only Roan Mt. and high elevations of Avery and Watauga County in North Carolina have observable snow cover. Further west, Mt. LeConte recorded 3.8 cm and snow cover was quite limited in the true color snow map across the Smoky Mountains and other portions of southwestern North Carolina. Snow cover on the highest peaks is still visible, however (Figure 3.37).

FSC performance was quite limited, and roughly half of the snow cover fell within the 1-20% class. 10% of the snow cover fell within the 21-30% class, while the remaining classes all contained less than 10% of the snow. In terms of the total study area, FSC never characterized greater than 1% of the entire study area for each class. This result highlights the

extremely restrictive nature of snow cover in the LC-U class (Figure 3.38). In addition, extensive leaf cover is still present across much of the region during the fall season. High elevations with little to no leaf cover in the canopy may have presented easier conditions for detecting the snow whereas low lying valleys may have presented more of an obstacle with already trace accumulations. This case study presents useful conditions for determining how the synoptic and environmental conditions may affect future performance in the MODIS snow maps during very light accumulation events.

NOAA HYSPLIT MODEL
 Backward trajectory ending at 1300 UTC 28 Oct 08
 GDAS Meteorological Data

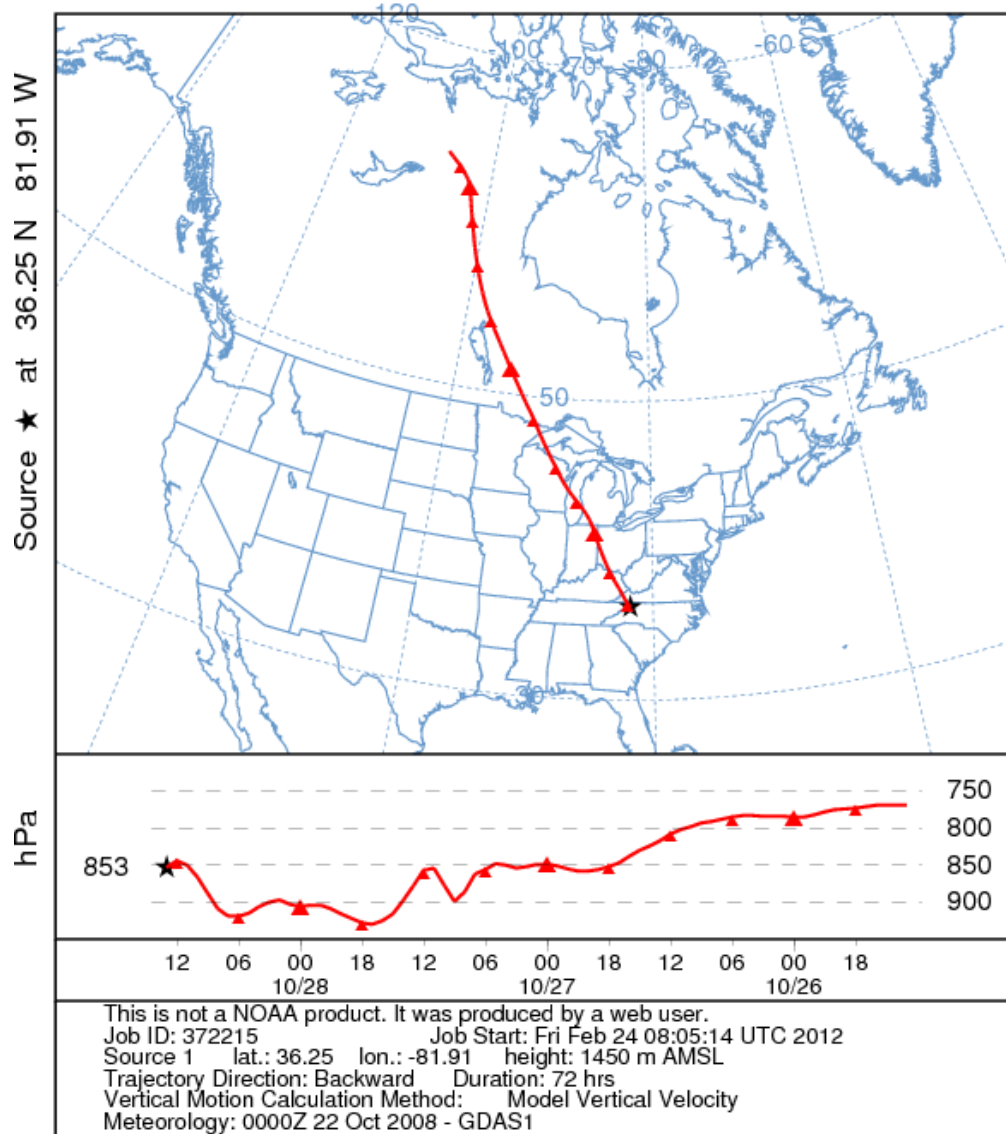


Figure 3.35. NOAA HYSPLIT backwards air trajectory for the leeward surface cyclone on 28 October 2008.

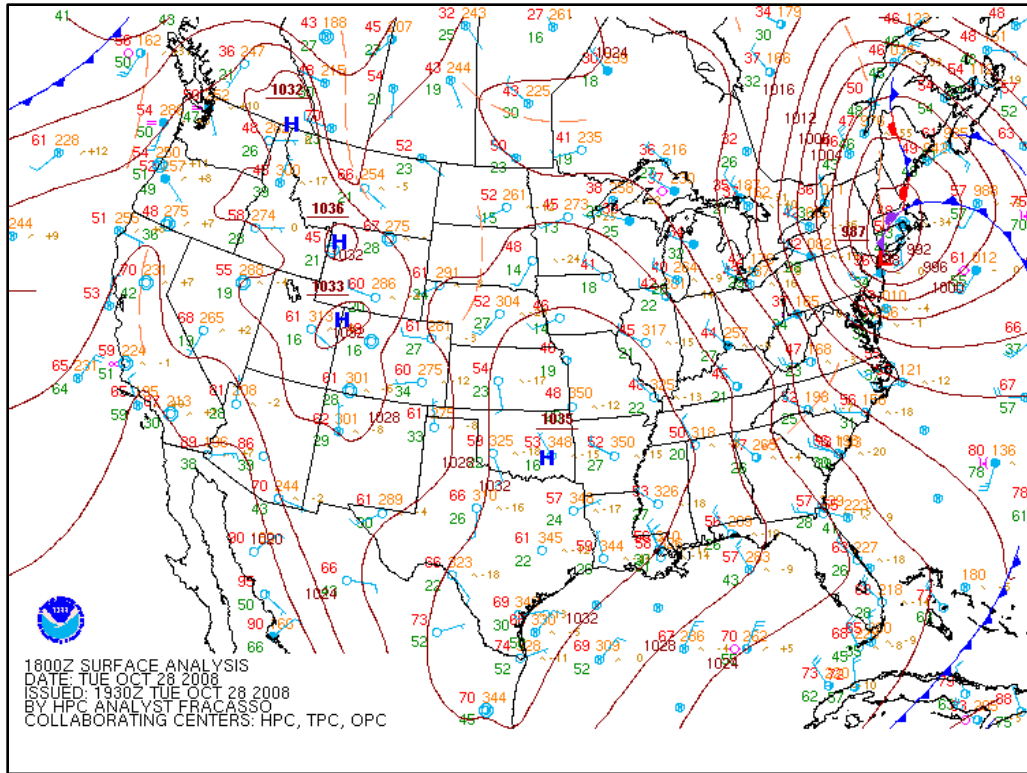


Figure 3.36. NOAA surface map for event maturation hour at 1800 UTC on 28 October 2008. A leeward surface cyclone is present further north over portions of New England, with wraparound flow occurring from the NW over the SAM.

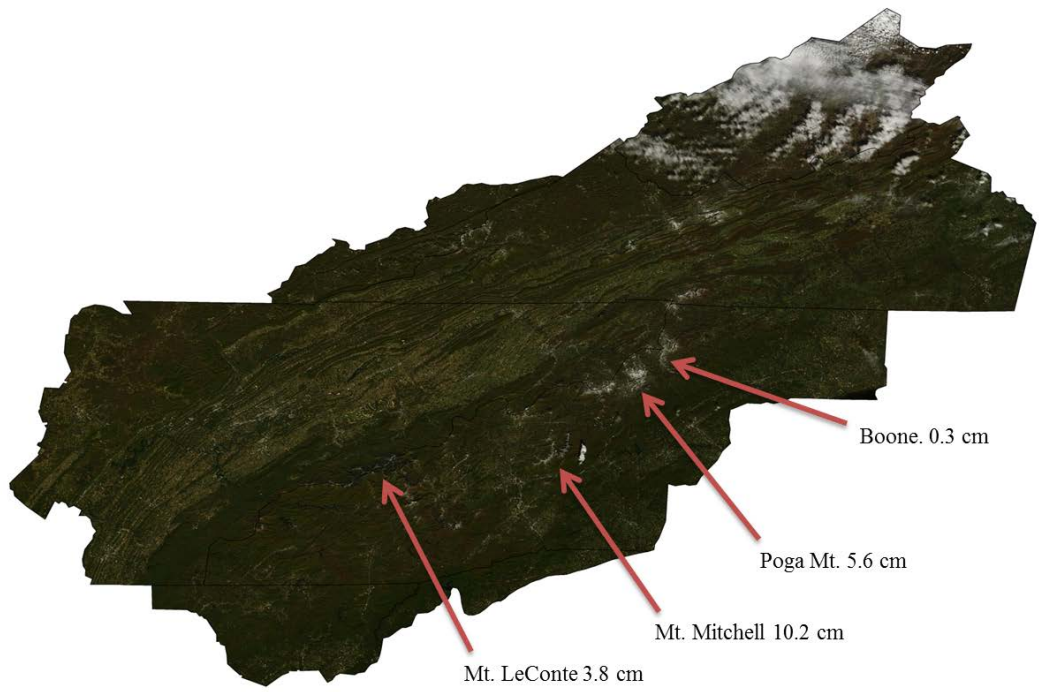


Figure 3.37. Minimal snow cover associated with the leeward surface cyclone in the Terra MODIS true color image from 29 October 2008, tile H11V05.

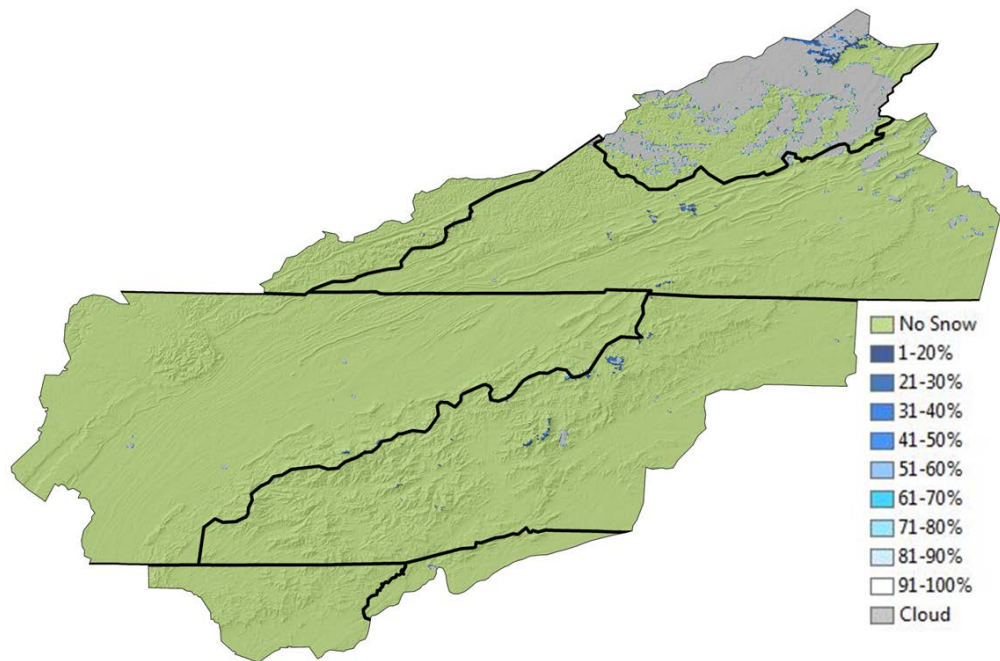


Figure 3.38. Terra MODIS FSC map from 29 October 2008, tile H11V05. Minimal values of FSC limit observations of the snow extent across the SAM. Isolated locations include the highest elevations of the Black Mountain Range and portions of Avery County in NW North Carolina.

Upper Level Cutoff Low with NW Upslope Flow (CL-U)

The final case study represents the most minimal snow extent associated with any synoptic class. A 500 mb cutoff low typically moves across the region, often slowly, and allows a surface cyclone to develop inland of the coast. These systems are unique in that they develop inland, pass over the southern Appalachian region, and move northeast unlike the Miller systems which tend to track towards the coast. The only upper level cutoff low to occur during the study period that was suitable for analysis using the MODIS snow maps occurred on 29 November 2011, and the imagery was acquired on 1 December 2011 under clear conditions. The event trajectory reveals flow beginning at the 1,000 hPa level over northern Mississippi and wavering in an easterly direction before turning northeastward and rising to 843 hPa at Poga Mt., North Carolina. The trajectory tracked across portions of northern Georgia into South Carolina, before crossing the North Carolina mountains (Figure 3.39). The surface map provides further insight into the presence of the surface low that tracked further to the north across the eastern seaboard and the associated cold front during event maturation hour (Figure 3.40).

Poga Mt. observed 9.4 cm of snowfall under low temperatures (-1.3 °C) during event maturation while Boone recorded 3.3 cm snowfall at more marginal average temperatures (7.2 °C). These data help to explain the visible reflectance of the snow cover in the true color map which displays more extensive snow across the mountain peaks of Avery and Watauga Counties in northwestern North Carolina. This pattern continues further north into the higher elevation portions of southwestern Virginia. Snow cover is practically nonexistent in the southwestern portions of the region, where only a few notable peaks are visible. The true color snow map was acquired two days after the event maturation, so it is reasonable that

some melting would occur in the valleys, particularly with similar temperatures compared to those observed in Boone for this event.

Temperatures were below freezing at the Mt. Mitchell COOP station at $-6.1\text{ }^{\circ}\text{C}$, and snowfall totals reached 5.1 cm. The ridge along the Black Mountain range where Mt. Mitchell is located stands out among the snow free areas in the true color snow map (Figure 3.41). Further west, Mt. LeConte observed 8.9 cm total snowfall which stands out as the sole high elevation location receiving snow accumulation in that area. The cutoff low provides a stark contrast to the spatial patterns observed in the true color product from other event types like the Miller systems where the region is predominately white. Knowledge of the topography and geographic distribution of the region is necessary to determine which peaks received snow when solely using the true color snow map.

Snow extent using the FSC map was $1,858\text{ km}^2$, and the majority of snow covered pixels fell within the 1-20% FSC class covering approximately $1,522\text{ km}^2$. The few remaining snow covered areas were marked by 21-90% FSC with 91-100% occurring on the mountain peaks and highest slopes (Figure 3.42). This event is notable due to the easily visible FSC and minimal amount of cloud cover two days after the event maturation. The FSC values are not surprising given the trend for maximum pixel values to occur in the lower range of percent snow covered area. One distinguishing factor during this cutoff low is the tendency for the spatial pattern of FSC values to fall within northwestern portions of North Carolina. While somewhat brief in this discussion, case studies provide a useful opportunity for linking in-situ observations of meteorological data, HYSPLIT backwards air trajectories, and surface maps with the spatial patterns of snow observed in the MODIS products. The upper level cutoff low provides a good example of this process.

NOAA HYSPLIT MODEL
 Backward trajectory ending at 2100 UTC 29 Nov 11
 GDAS Meteorological Data

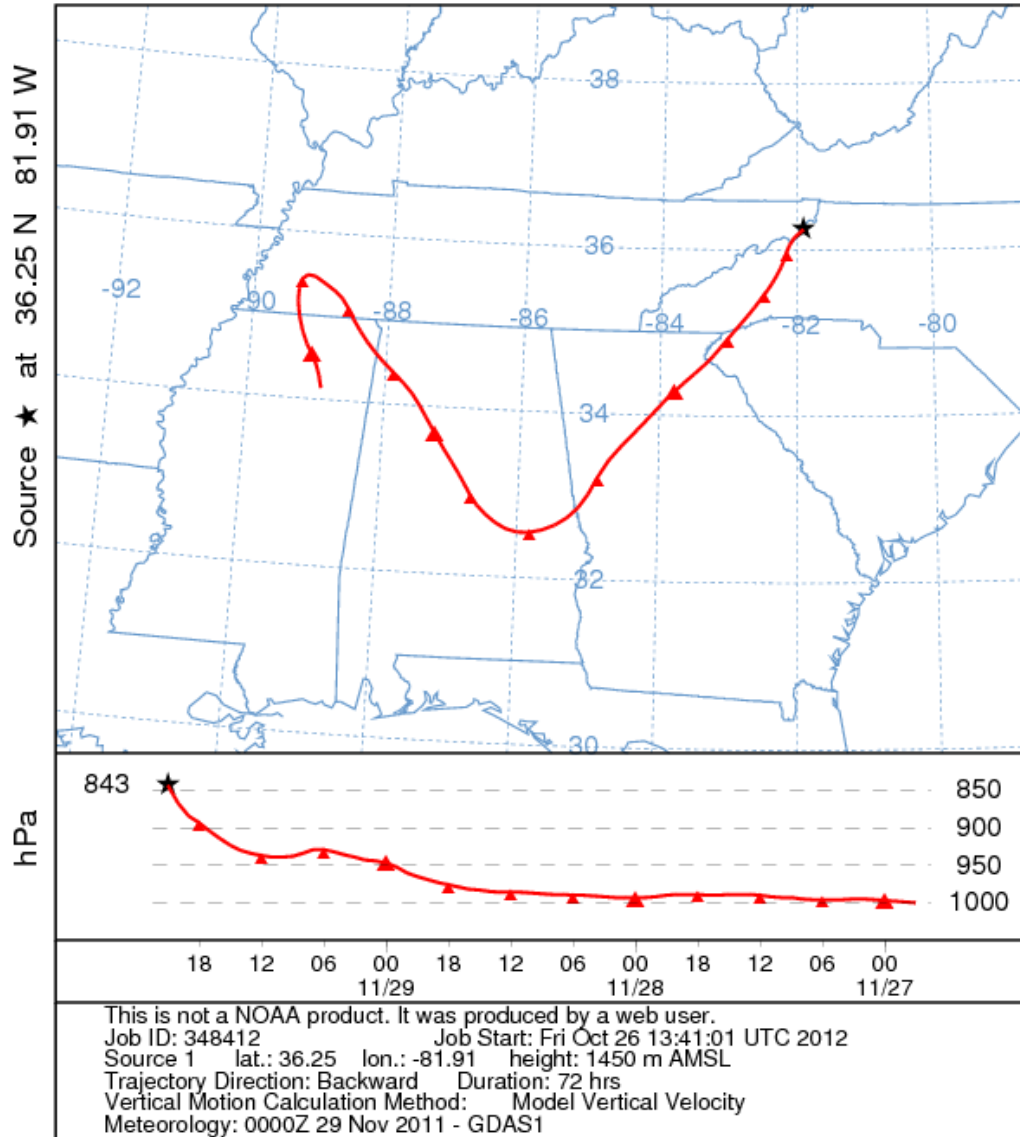


Figure 3.39. NOAA HYSPLIT backwards air trajectory for the 29 November 2011 upper level cutoff low. The event trajectory crosses portions of Mississippi, Alabama, and Georgia before ending at Poga Mt., North Carolina.

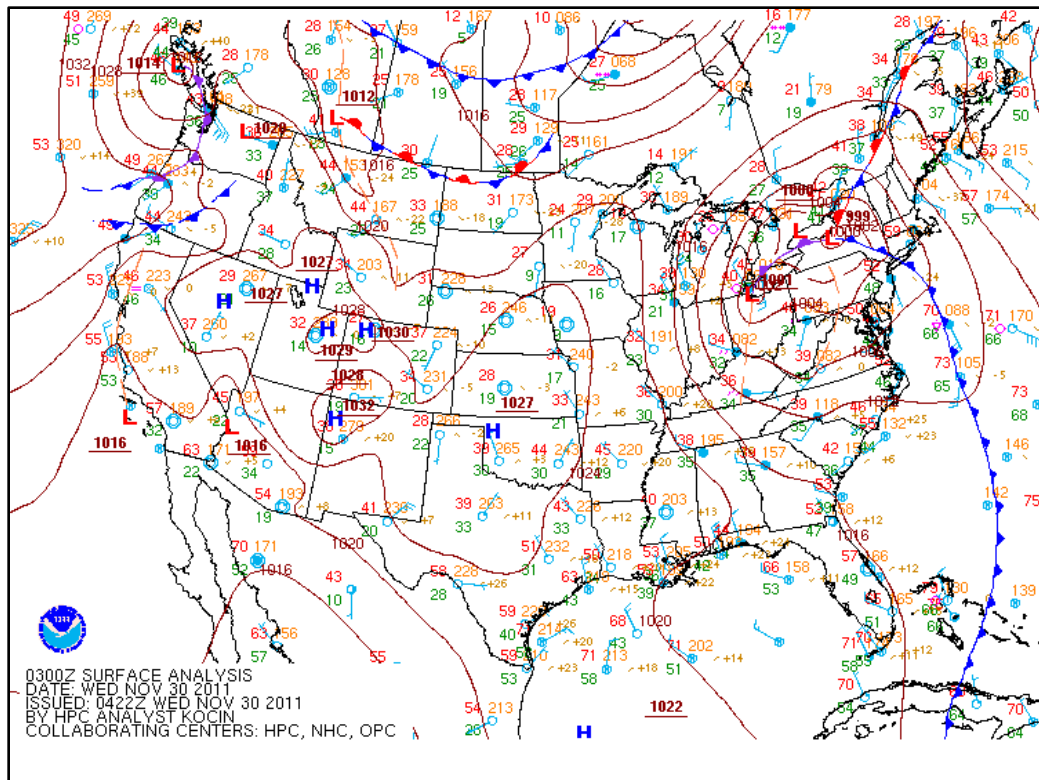


Figure 3.40. NOAA surface analysis near event maturation hour at 0300 UTC on 30 November 2011. A cold front is located off the east coast, leaving the SAM in the cold sector. Surface level low pressure is located further north over central New York.

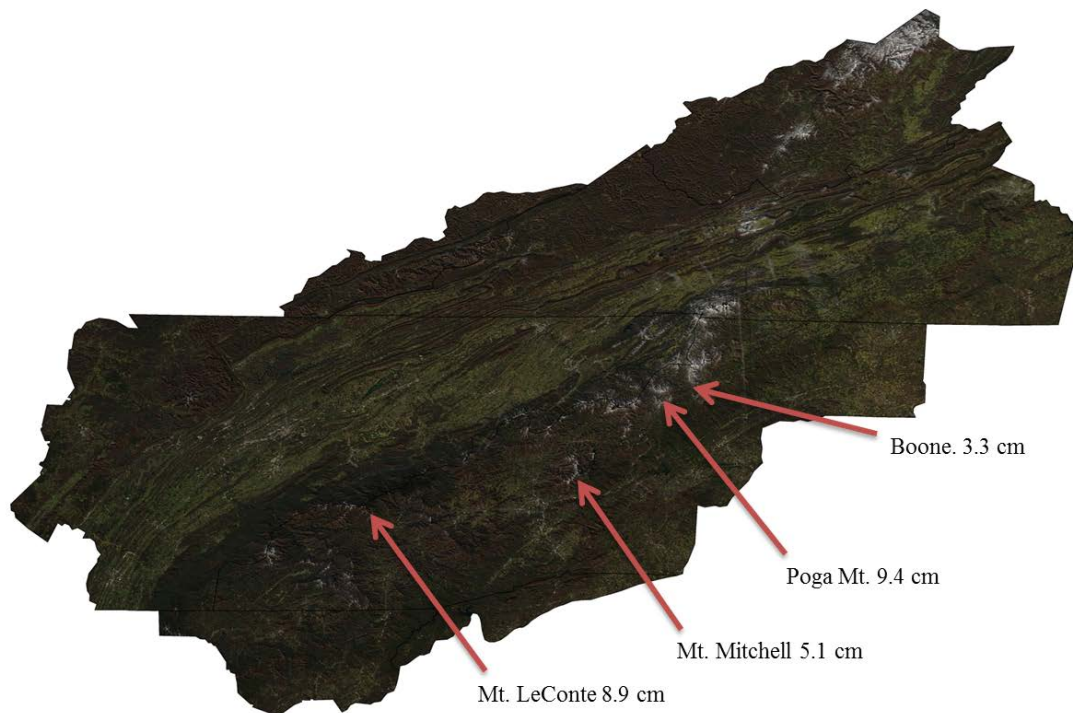


Figure 3.41. Aqua MODIS true color image with very little visible snow cover associated with the upper level cutoff low class, tile H11V05.

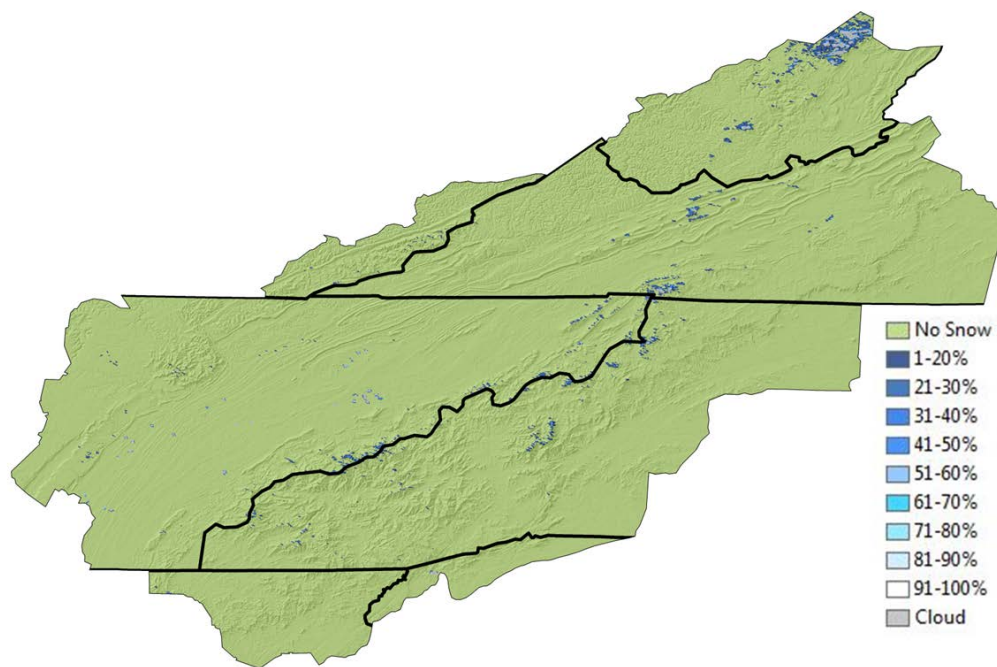


Figure 3.42. Aqua MODIS FSC map on 01 December 2011, tile H11V05. Snow cover is barely visible and strictly favors the highest elevation areas of the SAM.

Chapter 4

Summary and Conclusion

This thesis investigated the satellite and surface perspectives of snow extent in the SAM by examining 1) the suitability of the MODIS snow cover products for measuring snow cover in a mid-latitude mountain environment, and 2) the atmospheric circulation leading to specific snow cover patterns associated with synoptic classes from October 2006 to April 2012. The MODIS suitability analysis produced in this study is used to quantify the amount and quality of available snow mapping products for delineating snow extents among the 122 snowfall events in the SAM during the period. A manually derived event classified database from Poga Mt., North Carolina was used to assess in-situ observations of meteorological data in context with the FSC from each individual event.

Suitability of the MODIS Snow Cover Products in Mid-latitude Mountain Environments

Few studies using the MODIS snow mapping products have detailed a procedure for delineating mountain snow cover on an individual event basis. The majority of these studies have focused in mountain regions with large seasonal snowfall totals, seasonally continuous spatial coverage of snow, and where the impetus for conducting research is to quantify the amount of snowmelt runoff in the hydrologic cycle. The suitability analysis of the MODIS snow products created for this thesis revealed that MODIS is particularly suited to synoptic or atmospheric applications in snow mapping. MODIS adequately captured the snow in 51% of the total synoptic events (n=122) that occurred during the study period. Of these events, 63 were considered suitable for analysis using the MODIS snow maps while 59 of the events were not included due to limitations of the sensor. The likelihood of obtaining a suitable image for mapping the snow cover from individual snowfall events drastically increased when event maturation and ending hours were incorporated into this method.

Several major findings uncovered in the suitability assessment are readily transferrable to other mountain regions seeking to conduct similar studies linking the synoptic-scale circulation with the associated snow cover pattern. First, this method produced a highly conservative estimate of FSC values during each snowfall event due to the amount of cloud cover. FSC values are likely underestimated for the Miller A/B cyclones, the clipper systems, and for NWFS where heavy cloud banding is quite common. Continuation of future assessments would likely reveal higher FSC values under clear conditions.

Second, this assessment concluded that the climatological winter season (DJF) provides the best opportunity for acquiring MODIS data due to the greater sample size of events as well as the extension of the period for acquiring an image up to five days after event

maturation. This is an important factor in future work that may use remote sensing data for highlighting synoptic perspectives of individual events. The number of suitable MODIS images varied little between individual snow years over the study period, a result that is influenced by the sample size of events occurring each year.

This investigation revealed that MODIS is better suited to mapping the spatial pattern of snow cover from the heavy events, a conclusion that insinuates higher accumulation totals are also related to the greatest spatial extent of the snow. MODIS successfully mapped 89% of the upper quartile events from Poga Mt., while less than 50% were captured for the lightest events. When these events were broken down by synoptic class, Miller A/B cyclones, southeastward tracking clippers, and NWFS in absence of surface or frontal features provided the best opportunity to successfully measure snow extent in the MODIS data. The presence of incoming strong high pressure after event end during these events certainly helps conditions where clear skies are ideal for acquisition of a suitable image.

The results of this suitability analysis provide a model for assessing mountain snow cover in other mid-latitude regions where snow is ephemeral, melt onset between events is common, and dense forest cover presents a major obstacle to detecting snow from the ground. Adequate snow mapping in these regions requires a sensor network that collects data at sub-daily resolutions in order to capture changes to the snow occurring on the order of hours to days. The amount and quality of the MODIS snow maps analyzed in this study are useful for assessing the nature of synoptic-scale events on a temporal basis, particularly related to the timing of event onset, maturation, and ending. This suitability analysis may be used in future work to assess the persistence of snow cover in these regions and quantify the rate of ablation in mountain snow packs.

Fractional Snow Cover Variability in the SAM

One of the most interesting findings to emerge from this thesis is the statistically significant difference in snow extent between the Gulf/Atlantic Low (M*-U) systems and NWFS (U) events. Differences between snow extents from the other synoptic classes were also tested, but low sample sizes limited the ability to make conclusive assessments about mean snow extents. Theoretically, one would expect to see a slight variation in snow extent between all of the event types, which would suggest a variation of multi-scaled atmospheric processes leading to snowfall development. Instead, differences were most noticeable between the M*-U and U systems. Differences between the other synoptic event types may be more difficult to discern since the snow cover patterns exhibit similar characteristics in terms of spatial variability. Alternatively, these differences may be more easily quantified as future sample sizes of events increase.

On average, FSC maxima occurred in the 1-20% category for each synoptic class and tended to progressively decline in every category from 21-100%. 100% FSC in the SAM was usually limited to isolated areas at higher elevations depending on the specific event trajectory. One exception is the M*-U systems where FSC values increased from 50-100% displaying more widespread regional snow cover. In-situ observations indicating a high degree of confidence in near 100% FSC were often contrasted with the reality of the snow maps which tended to show reduced values.

The limitation of 100% FSC values among the synoptic classes is not surprising given the topographic variability and changes in land cover type across short distances in the SAM. Dense canopy cover and steep slopes limited FSC performance when meteorological conditions indicated near 100% snow cover whereas open areas and pasture in the lower

valleys were responsible for the increase in FSC values. Individual snowfall events from the southeastward tracking clipper systems (SE-U) showed considerable variation in FSC performance, with some events occurring near the total maximum of snow extent, and others occurring near the minimum of the range, consistent with the observation that some of these systems are especially fast moving.

Additionally, windward slopes performed better than leeward slopes when examining FSC during the Upslope (U) events. More research is needed to assess processes of the cloud microphysical environment and at the mesoscale in relation to the snow cover pattern. In some cases with particularly limited moisture and low temperatures, spillover effects may have influenced the downwind accumulation, skewing FSC measurements on the leeward sides. However, a high degree of riming is indicative of higher fall speeds associated with greater upslope accumulations favoring the windward side. In conjunction with previous research highlighting variability at these scales, snow accumulation between windward and leeward slopes is less clear cut than are suggested by the MODIS data.

When analyzed in context with in-situ observations and trajectory analyses from individual synoptic events, MODIS data support the hypothesis that atmospheric circulation holds a major influence on associated snow cover patterns.

Implications

Integration of remotely sensed MODIS and in-situ COOP field data provides a unique method for improving modern snow mapping techniques. Not only can studies build upon previous work incorporating sensor platforms to make knowledge contributions in atmospheric and cryospheric research, but related studies also have the simultaneous benefit

of providing validation for current sensors and making recommendations for future algorithm improvements. Snow mapping has seldom been included in synoptic approaches to further understand the spatial patterns of snowfall related to broader circulation regimes.

Additionally, remote sensing domains benefit from the inclusion of data from various sensor platforms within interdisciplinary research fields. Increasing accuracy is a consistent objective within the academic and operational communities, who collect earth observation data at given spatial and temporal resolutions with varying precision.

This research has the advantage of producing results that contribute to GIScience research objectives outlined by the University Consortium for GIS (UCGIS 2013). Snow mapping involves multiple techniques which directly advance the use of scale, visualization, and remotely acquired data networks. Results produced here are useful for scientists incorporating data within a GIS environment since methods are reproducible for other research questions related to the patterns and processes of mid-latitude mountain snowfall.

Little has been done to advance snow mapping techniques in mountain environments, and the small body of work that does exist has tended to focus on validation efforts of sensors or solely used in-situ data networks for analysis of snow cover. A hybrid study incorporating the two approaches is presented here. This research produced a model for developing explicit linkages between synoptic-scale atmospheric circulation regimes and resulting snow cover patterns across high elevation areas where processes are still largely unknown. The extent and patterns of the snow cover are a result of the multi-scale atmospheric processes that occur throughout the event duration within these circulation regimes. Therefore, it is important to use snow cover patterns as a way to further understand how the process of synoptic circulation affects the spatial variability of snowfall. These improvements are

important for continuing long term assessments of climate change, locally in the SAM, and in context with broader patterns of global changes to snow cover. A continuation of snow mapping techniques will add to the availability of consistent data records from the 1950s to present and can be used to address future questions related to the persistence of snow cover in context with future climate change.

Limitations

Several limitations impacted the results of this thesis. Major obstacles for adequately detecting the snow cover with the MODIS snow maps include persistent cloud cover, dense forest canopy, and ephemeral snow. MODIS cannot effectively measure the snow extent on a day to day basis when all three conditions are present. The twice daily availability of the snow maps drastically improves the likelihood of obtaining a clear surface view, especially considering the repeat pass times of other sensors that may only map the region every 16 days. In addition, FSC performance as a measure of areal coverage cannot be validated by using point based measurements of meteorological data including snow depth or snowfall. Other satellite data using various cell sizes must be incorporated for comparison purposes to assess the performance accuracy of the snow maps. These problems are particularly important when undertaking studies in areas like the SAM where higher elevation sites within a 500m pixel may be snow covered, but lower portions of the same pixel are snow free. Sub-pixel classification of snow cover is necessary to better discriminate between snow-covered and snow-free forests. This study assumed that the MODIS snow maps were already highly accurate based on algorithm refinements in the literature, even though cloud cover likely reduced the FSC performance in several of the synoptic classes.

The short time period of the manually event classified synoptic data resulted in an even smaller sample size of available MODIS data that were included in the analysis (e.g., leeward surface cyclones LC-U, n=4). In fact, the upper level cutoff lows were excluded from discussion for this reason (n=1). This problem limited the amount of conclusions that can be drawn from using the MODIS snow maps for specific synoptic classes. The major solution to this problem is to increase the sample size of events as future snowfall patterns develop. In turn, the amount of suitable imagery will also increase. Another solution is to extend the study period into preceding years when MODIS data are still available, though further complications arise when considering the lack of meteorological data on a specific event basis before 2006. Though 122 total events were included in this analysis, snow cover was quantified in 63 of the events due to limitations of the sensor. Conclusions drawn here are quite promising based on the results from measurements in the snow maps of event types with larger sample sizes (e.g., Miller A/B cyclones (M*-U), southeastward tracking clippers (SE-U), NWFS (U)).

The manually derived event database from Poga Mt., North Carolina was particularly useful for comparing upper and lower quartiles of snow extent between synoptic classes with meteorological data, but does not adequately capture snow event data from other portions of the SAM. Future research should seek to make similar comparisons with snowfall event data from other high elevation stations in order to determine correlations between specific snowfall parameters and snow extent on a region-wide basis. For example, snowfall data from Mt. LeConte and Mt. Mitchell would be particularly useful for expanding the analysis further across the region. The Poga Mt. data do indicate that atmospheric circulation significantly influences snow cover patterns, and particularly with the heavy events, but this

relationship should be tested with a higher resolution and spatial coverage of meteorological event data.

Future Work

Current findings in this thesis have opened the door for future applications of snowfall research using MODIS data in the SAM. Foremost is the need to increase sample sizes of snowfall events in the MODIS imagery. Greater sample sizes will provide more robust results that can be applied to numerous related research questions. For example, one major question that could employ MODIS data is to determine how hemispheric circulation patterns (teleconnections) including the AO and ENSO influence the persistence of snow cover in the SAM. Quantifying these processes would enable further assessments of how climate change may affect future conditions in the SAM at longer time frames and provide valuable context for explaining local processes at global scales. Exploring correlations between the AO and ENSO indices with snow cover pixels or other FSC data would be a good starting point for assessing these trends, especially since six years of MODIS data have already been collected for the region.

Likewise, the MODIS snow maps could be used on a daily basis to measure seasonal days of snow cover in the SAM, providing year to year evaluations of consistency and change over time. Another question is to determine how the days of snow cover vary from year to year in context with the number of snowfall events. This method would require downloading the snow maps for every day of the season and provide a single measurement of snow cover on a daily basis. Comparisons could also be made between peak and valley locations within the SAM in an effort to quantify the variation in snow cover or pixel values

between high elevation and low lying areas. This type of study would complement the objectives of other work seeking to improve the availability of meteorological data from a denser network of weather stations and aid in capturing local topographic effects of snowfall development.

Given the amount of ephemeral snow in the SAM, another curiosity is the duration of mountain snow cover in a given season. A daily time series of individual pixel values across the highest peaks would be an interesting way to assess high elevation snow cover patterns in locations without in-situ observations. A major consideration of this method is that most summits of the major peaks fall within one or two 500 m MODIS pixels, so identifying the specific cells using GIS point data is an important step in this process. Mt. LeConte, Mt. Mitchell, Roan Mt., and Mt. Rogers would all serve as suitable locations to develop this project. This method would also require that the snow maps be downloaded for every day of the season. The true color images would make a good addition to the time series in order to develop 3D visualizations of mountain snow cover using DEM and terrain data that could be displayed in mountain visitor centers.

Seasonal animations used in educational settings would greatly benefit the public awareness of snowfall processes and lead to enhanced understanding of the societal impacts in the SAM. MODIS data should continue to be employed as a means for assessing mid-latitude mountain snow cover. The snow maps offer promising results for developing idealized snow cover extents from specific synoptic classes that can be used to improve future forecasting scenarios, mitigating the negative human impacts of snow.

List of Abbreviations and Acronyms

AO – Arctic Oscillation

AR4 – Fourth Assessment Report

ASL – Above Sea Level

CoCoRaHS – Community Collaborative Rain, Hail, and Snow Network

COOP – Cooperative Observer

CRONOS – Climate Retrieval and Observations Network of the Southeast

CL-U – Upper level cutoff lows with upslope flow after maturation

DJF – December, January, February; Northern Hemisphere climatological winter

ENSO – El Niño-Southern Oscillation

FSC – Fractional Snow Cover

GCM – Global Circulation Model

HYSPLIT – Hybrid Single Particle Lagrangian Integrated Trajectory

IPCC – Intergovernmental Panel on Climate Change

LC-U – Leeward surface cyclones with upslope flow after maturation

MAM – March, April, May; Northern Hemisphere climatological spring

MOD10A1 – MODIS Terra Daily Snow Cover Maps

MODIS – Moderate Resolution Imaging Spectroradiometer

M*-U – Miller cyclones with upslope flow after maturation

MYD10A1 – MODIS Aqua Daily Snow Cover Maps

NASA – National Aeronautics and Space Administration

NE-U – Northeastward tracking lows with upslope flow after maturation

NOAA – National Oceanic and Atmospheric Administration

Non-U – Non upslope flow, including gulf surface waves

NSIDC – National Snow and Ice Data Center

NWP – Numerical Weather Prediction

NWS – National Weather Service

SAM – Southern Appalachian Mountains

SE-U – Southeastward tracking clippers with upslope flow after maturation

SLE – Snow Liquid Equivalent

SNOTEL – Snowpack Telemetry

SON – September, October, November; Northern Hemisphere climatological fall

SWE – Snow Water Equivalent

U – NW upslope flow in absence of surface or frontal features

X-U – Unclassified with upslope flow after maturation

Bibliography

- Ackerman, S. A., K. I. Strabala, W. P. Menzel, R. A. Frey, C. C. Moeller, and L. E. Gumley, 1998: Discriminating clear sky from clouds with MODIS. *Journal of Geophysical Research*, **103:24**, 32141-32157.
- Barnett, T. P., J. C. Adam, and D. P. Lettenmaier, 2005: Potential impacts of a warming climate on water availability in snow-dominated regions. *Nature*, **438**, 303-309.
- Barry, R. G., 1985: *The cryosphere and climate change*. Chapter 6. In: M. C. MacCracken and F. M. Luther, eds., *Detection of CO₂-Induced Climatic Change*. DOE/ER-0235, U. S. Dept. of Energy, Washington, D. C., 109-148.
- Barry, R. G., 2002: The role of snow and ice in the global climate system: a review. *Polar Geography*, **26:3**, 235-246.
- Birkeland, K. W., and C. J. Mock, 1996: Atmospheric Circulation Patterns Associated with Heavy Snowfall Events, Bridger Bowl, Montana, USA. *Mountain Research and Development*, **16:3**, 281-286.
- Bishop, M. P., and Coauthors, 2004: Global Land Ice Measurements from Space (GLIMS): Remote Sensing and GIS Investigations of the Earth's Cryosphere. *Geocarto International*, **19:2**, 57-84.
- Chang, E. M., 2009: Diabatic and Orographic Forcing of Northern Winter Stationary Waves and Storm Tracks. *Journal of Climate*, **22**, 670-688.
- Choudhury, B. J., and A. T. C. Chang, 1979: Two-stream theory of reflectance of snow. *IEEE Transactions on Geoscience and Remote Sensing*, **17:3**, 63-68.
- Christensen, N. S., A. W. Wood, N. Voisin, D. P. Lettenmaier, and R. N. Palmer, 2004: The Effects of Climate Change on the Hydrology and Water Resources of the Colorado River Basin. *Climatic Change*, **62**, 337-363.
- Cohen, J., and D. Rind, 1991: The Effect of Snow Cover on the Climate. *Journal of Climate*, **4**, 689-706.
- Cohen, J., J. Foster, M. Barlow, K. Saito, and J. Jones, 2010: Winter 2009-2010: A case study of an extreme arctic oscillation event. *Geophysical Research Letters*, **37**, L17707, doi: 10.1029/2010GL044256.
- Colby, J., 1991: Topographic normalization in rugged terrain. *Photogrammetric Engineering & Remote Sensing*, **57:5**, 531-537.
- Diaz, H. F., M. Grosjean, and L. Graumlich, 2003: Climate Variability and Change in High Elevation Regions: Past, Present and Future. *Climatic Change*, **59**, 1-4.

- Doesken, N. J., and A. Judson, 1997: *The Snow Booklet: A Guide to the Science, Climatology, and Measurement of Snow in the United States*. Colorado Climate Center: Fort Collins, CO.
- Dore, A. J., T. W. Choularton, D. Fowler, and A. Crossley, 1992: Orographic enhancement of snowfall. *Environmental Pollution*, **75**, 175-179.
- Dozier, J., T. H. Painter, K. Rittger, and J. E. Frew, 2008: Time-space continuity of daily maps of fractional snow cover and albedo from MODIS. *Advances in Water Resources*, **31**, 1515-1526.
- Elsasser, H., and R. Bürki, 2002: Climate change as a threat to tourism in the Alps. *Climate Research*, **20**, 253-257.
- EOSDIS (Earth Observing System Data and Information System), 2009: Earth Observing System ClearingHouse (ECHO) / Reverb Version 10.X [online application]. Greenbelt, MD: EOSDIS, Goddard Space Flight Center (GSFC) National Aeronautics and Space Administration (NASA). [<https://wist.echo.nasa.gov/api/>]
- Fitzharris, B. B., 1976: An avalanche event in the seasonal snow zone of the mount cook region, New Zealand. *New Zealand Journal of Geology and Geophysics*, **19:4**, 449-462.
- Foster, J. L., D. K. Hall, and A. C. Chang, 1987: Remote Sensing of Snow. *Transactions of the American Geophysical Union*, **68:32**, 682-684.
- Foster, J., M. Owe, and A. Rango, 1983: Snow Cover and Temperature Relationships in North America and Eurasia. *Journal of Climate and Applied Meteorology*, **22**, 460-469.
- Francis, J. A., and S. J. Vavrus, 2012: Evidence linking Arctic Amplification to extreme weather in mid-latitudes. *Geophysical Research Letters*, **39**, L06801, doi: 10.1029/2012GL051000.
- Francis, J. A., W. Chan, D. J. Leathers, J. R. Miller, and D. E. Veron, 2009: Winter Northern Hemisphere weather patterns remember summer Arctic sea-ice extent. *Geophysical Research Letters*, **36**, L07503, doi: 10.1029/2009GL037274.
- Frei, A., M. Tedesco, S. Lee, J. Foster, D. Hall, R. Kelly, and D. A. Robinson, 2012: A review of global satellite-derived snow products. *Advances in Space Research*, **50**, 1007-1029.
- Fuhrmann, C. M., D. K. Hall, L. B. Perry, and G. A. Riggs, 2010: Spatial Patterns of Snow Cover in North Carolina: Surface and Satellite Perspectives. *Proceedings of the 67th Eastern Snow Conference*, Jiminy Peak Mountain Resort, Hancock, MA, USA.
- Goodge, G., and G. Hammer, 1993: Special Weather Summary, in *Climatological Data, North Carolina: March 1993*. Asheville, NC: National Climatic Data Center.
- Graybeal, D. Y., and D. J. Leathers, 2006: Snowmelt-Related Flood Risk in Appalachia: First Estimates from a Historical Snow Climatology. *Journal of Applied Meteorology and Climatology*, **45**, 178-193.

- Hall, D. K., and G. A. Riggs, 2007: Accuracy assessment of the MODIS snow products. *Hydrological Processes*, **21**, 1534-1547.
- Hall, D. K., G. A. Riggs, and V. V. Salomonson, 1995: Development of Methods for Mapping Snow Cover Using Moderate Resolution Imaging Spectroradiometer Data. *Remote Sensing of Environment*, **54**, 127-140.
- Hall, D. K., J. L. Foster, V. V. Salomonson, A. G. Klein, and J. L. Chien, 2001: Development of a technique to assess snow-cover mapping errors from space. *IEEE Transactions on Geoscience and Remote Sensing*, **39:2**, 432-438.
- Hall, D. K., G. A. Riggs, and V. V. Salomonson, 2001: Algorithm Theoretical Basis Document (ATBD) for the MODIS Snow and Sea Ice-Mapping Algorithms. <http://modis-snow-ice.gsfc.nasa.gov/atbd.html>.
- Hall, D. K., G. A. Riggs, V. V. Salomonson, N. DiGirolamo, and K. Bayr, 2002: MODIS snow-cover products. *Remote Sensing of Environment*, **83**, 181-194.
- Hall, D. K., R. J. Kelly, J. L. Foster, and A. Chang, 2005: Estimation of Snow Extent and Snow Properties. *Encyclopedia of Hydrological Sciences*, 811-829.
- Hall, D. K., and G. A. Riggs, 2013, updated daily: MODIS/Terra Snow Cover daily L3 Global 500m Grid V005. Boulder, Colorado USA: *National Snow and Ice Data Center*. Digital media.
- Hall, D. K., C. M. Fuhrmann, L. B. Perry, G. A. Riggs, D. A. Robinson, and J. L. Foster, 2010: A Comparison of Satellite-Derived Snow Maps with a Focus on Ephemeral Snow in North Carolina. *Proceedings of the 67th Eastern Snow Conference*, Jiminy Peak Mountain Resort, Hancock, MA, USA.
- Hardie, A. V., 1960: Special Weather Summary, in *Climatological Data, North Carolina: March 1960*. Asheville, NC: National Climatic Data Center.
- Holloway, B., 2008: A Comparison of Two Northwest Flow Snowfall Events from the 2007-2008 Winter Season. *NOAA/National Weather Service*, Greer, South Carolina. [www.erh.noaa.gov/gsp/localdat/cases/jan_feb_2008_nwfs/comparison.html].
- Hooker, B. L., and B. B. Fitzharris, 1999: The correlation between climatic parameters and the retreat and advance of Franz Josef Glacier, New Zealand. *Global and Planetary Change*, **22**, 39-48.
- IPCC, 2007: Climate Change 2007: The Physical Science Basis. Contribution of Working Group 1 to the Fourth Assessment Report of the Intergovernmental Panel on Climate Change. [Solomon, S., D. Qin, M. Manning, Z. Chen, M. Marquis, K. B. Averyt, M. Tignor, and H. L. Millers (eds.)]. Cambridge University Press, Cambridge, United Kingdom and New York, NY, USA.
- Kawagoe, S., S. Kazama, and P. R. Sarukkalige, 2009: Assessment of snowmelt triggered landslide hazard and risk in Japan. *Cold Regions Science and Technology*, **58**, 120-129.

- Keighton, S., and Coauthors, 2009: A collaborative approach to better understanding northwest flow snowfall in the southern Appalachians. *Bulletin of the American Meteorological Society*, **90**, 979-991.
- Kelly, G. M., L. B. Perry, B. F. Taubman, and P. S. Soulé, 2012: Synoptic classification of 2009-10 precipitation events in the Southern Appalachian Mountains. *Climate Research*, In press.
- Kelly, R. E., A. T. Chang, L. Tsang, and J. L. Foster, 2003: A Prototype AMSR-E Global Snow Area and Snow Depth Algorithm. *IEEE Transactions on Geoscience and Remote Sensing*, **41:2**, 230-242.
- Kingsmill, D., A. White, D. Gottas, and P. Neiman, 2008: Spatial variability of the snow level across the northern California Sierra Nevada. Extended Abstracts, 13th Conf. on Mountain Meteorology, Whistler, B.C., Canada, Amer. Meteor. Soc., 6A.3. [http://ams.confex.com/ams/13MontMet17AP/techprogram/paper_140814.htm.]
- Klein, A. G., D. K. Hall, and G. A. Riggs, 1998: Improving snow cover mapping in forests through the use of a canopy reflectance model. *Hydrological Processes*, **12**, 1723-1744.
- Klein, A. G., and A. C. Barnett, 2003: Validation of daily MODIS snow cover maps of the Upper Rio Grande River Basin for the 2000-2001 snow year. *Remote Sensing of Environment*, **86**, 162-176.
- Kocin, P. J., and L. W. Uccellini, 1990: Snowstorms along the northeastern coast of the United States, 1955 to 1985. *Meteorological Monograph No. 44*, American Meteorological Society, **22**, 280 pp.
- Koenig, U., and B. Abegg, 1997: Impacts of Climate Change on Winter Tourism in the Swiss Alps. *Journal of Sustainable Tourism*, **5:1**, 46-58.
- Lackmann, G., 2011: *Midlatitude Synoptic Meteorology: Dynamics, Analysis, and Forecasting*. American Meteorological Society, 345 pp.
- Laternser, M., and M. Schneebeli, 2002: Temporal trend and spatial distribution of avalanche activity during the last 50 years in Switzerland. *Natural Hazards*, **27**, 201-230.
- Lee, L. G., and P. D. Moore, 2009: The 18-20 December 2009 Winter Storm. *NOAA/National Weather Service*, Greer, South Carolina. [www.erh.noaa.gov/gsp/localdat/cases/2009/18-20DecemberWinterStorm/18-20DecemberWinterStorm.html].
- Messerli, B., and J. D. Ives, 1997: *Mountains of the World: A Global Priority*. 1st Edition. CRC Press, 510 pp.
- Messerli, B., D. Viviroli, and R. Weingartner, 2004: Mountains of the World: Vulnerable Water Towers for the 21st Century. *Ambio Special Report*, Royal Swedish Academy of Sciences, **13**, 29-34.

- Miller, D. K., 2012: Near-Term Effects of the Lower Atmosphere in Simulated Northwest Flow Snowfall Forced over the Southern Appalachians. *Weather and Forecasting*, **27**, 1198-1216.
- Miller, J. E., 1946: Cyclogenesis in the Atlantic Coastal Region of the United States. *Journal of Meteorology*, **3**, 31-44.
- Millsaps, S. A., and P. A. Groothuis, 2003: The economic impact of the North Carolina ski areas on the economy of North Carolina, 2002-2003 season. Final report prepared for the North Carolina Ski Areas Association by Appalachian State University, 17 pp.
- Minder, J. R., D. R. Durran, and G. H. Roe, 2011: Mesoscale controls on the mountainside snow line. *Journal of the Atmospheric Sciences*, **68**, 2107-2127.
- Mote, T. L., D. W. Gamble, S. J. Underwood, and M. L. Bentley, 1997: Synoptic-Scale Features Common to Heavy Snowstorms in the Southeast United States. *Weather and Forecasting*, **12**, 5-23.
- Mote, P. W., A. F. Hamlet, M. P. Clark, and D. P. Lettenmaier, 2005: Declining mountain snowpack in western North America. *Bulletin of the American Meteorological Society*, **86**, 39-49.
- NASA (National Aeronautics and Space Administration), cited 2013: The Landsat Program. [<http://www.landsat.gsfc.nasa.gov>]
- NC CRONOS (North Carolina, Climate Retrieval and Observation Network of the Southeast), State Climate Office, cited 2012: [www.nc-climate.ncsu.edu/cronos]
- Neiman, P. J., F. M. Ralph, G. A. Wick, J. D. Lundquist, and M. D. Dettinger, 2008: Meteorological Characteristics and Overland Precipitation Impacts of Atmospheric Rivers Affecting the West Coast of North America Based on Eight Years of SSM/I Satellite Observations. *Journal of Hydrometeorology*, **9**, 22-47.
- Niziol, T. A., 1987: Operational Forecasting of Lake Effect Snowfall in Western and Central New York. *Weather and Forecasting*, **2**, 310-321.
- NOAA (National Oceanic and Atmospheric Administration), cited 2012: Hydrometeorological Prediction Center (HPC), U.S. Surface Analysis. [<http://www.hpc.ncep.noaa.gov>]
- NOAA (National Oceanic and Atmospheric Administration), cited 2013: U.S. National Ice Center Products. [<http://www.natice.noaa.gov/products/>]
- Nolin, A. W., and S. Liang, 2000: Progress in Bidirectional Reflectance Modeling and Applications for Surface Particulate Media: Snow and Soils. *Remote Sensing Reviews*, **18**, 307-342.
- NSIDC (National Snow and Ice Data Center), cited 2013. [<http://www.nsidc.org>]

- NWS (National Weather Service), cited 2008: Killer Flooding in Carter County of Extreme East Tennessee. [<http://www.srh.noaa.gov/mrx/hydro/cflood/doeflood.php>]
- Orsolini, Y. J., and N. G. Kvamstø, 2009: Role of Eurasian snow cover in wintertime circulation: Decadal simulations forced with satellite observations. *Journal of Geophysical Research*, **114**, D19108, doi: 10.1029/2009JD012253
- Painter, T. H., K. Rittger, C. McKenzie, P. Slaughter, R. E. Davis, and J. Dozier, 2009: Retrieval of subpixel snow covered area, grain size, and albedo from MODIS. *Remote Sensing of Environment*, **113**, 868-879.
- Pavelsky, T. M., S. Sobolowski, S. B. Kapnick, and J. B. Barnes, 2012: Changes in orographic precipitation patterns caused by a shift from snow to rain. *Geophysical Research Letters*, **39**, doi: 10.1029/2012GL052741
- Pederson, G. T., and Coauthors, 2011: The Unusual Nature of Recent Snowpack Declines in the North American Cordillera. *Science*, **333**, 332-335.
- Perry, L. B., 2006: *Synoptic Climatology of Northwest Flow Snowfall in the Southern Appalachian Mountains*. Ph.D. Dissertation, University of North Carolina at Chapel Hill.
- Perry, L. B., and C. E. Konrad, 2006a: Relationships between NW flow snowfall and topography in the southern Appalachians, USA. *Climate Research*, **32**, 35-47.
- Perry, L. B., and C. E. Konrad, 2006b: Synoptic Patterns Associated with the Record Snowfall of 1960 in the Southern Appalachians. *Proceedings of the 63rd Eastern Snow Conference*, Newark, Delaware, USA.
- Perry, L. B., C. E. Konrad, and T. W. Schmidlin, 2007: Antecedent Upstream Air Trajectories Associated with Northwest Flow Snowfall in the Southern Appalachians. *Weather and Forecasting*, **22**, 334-352.
- Perry, L. B., D. K. Miller, S. E. Yuter, L. G. Lee, and S. J. Keighton, 2008: Atmospheric Influences on New Snowfall Density in the Southern Appalachian Mountains, USA. *Proceedings of the 65th Eastern Snow Conference*, Fairlee (Lake Morey), Vermont, USA.
- Perry, L. B., D. Hotz, S. Keighton, C. Konrad, L. Lee, G. Dobson, and D. K. Hall, 2010a: Overview of the 2009-2010 snow season in the southern Appalachian Mountains. *Proceedings of the 67th Eastern Snow Conference*, Jiminy Peak Mountain Resort, Hancock, MA, USA.
- Perry, L. B., C. E. Konrad, D. G. Hotz, and L. G. Lee, 2010b: Synoptic classification of snowfall events in the Great Smoky Mountains, USA. *Physical Geography*, **31**, 156-171.
- Perry, L. B., S. J. Keighton, L. G. Lee, D. K. Miller, S. E. Yuter, and C. E. Konrad, 2013: Synoptic influences on snowfall event characteristics in the southern Appalachian Mountains. In preparation for *Weather and Forecasting*.

- Pinto, J. G., T. Brücher, A. H. Fink, and A. Krüger, 2007: Extraordinary snow accumulations over parts of central Europe during the winter of 2005/06 and weather-related hazards. *Weather, Royal Meteorological Society*, **62:1**, 16-21.
- Platnick, S., M. D. King, S. A. Ackerman, W. P. Menzel, B. A. Baum, J. C. Riédi, and R. A. Frey, 2003: The MODIS Cloud Products: Algorithms and Examples from Terra. *IEEE Transactions on Geoscience and Remote Sensing*, **41:2**, 459-473.
- Ramsay, B. H., 1998: The interactive multisensor snow and ice mapping system. *Hydrological Processes*, **12**, 1537-1546.
- Rasmussen, R., and Coauthors, 2012: How well are we measuring snow? The NOAA/FAA/NCAR winter precipitation test bed. *Bulletin of the American Meteorological Society*, **93**, 811-829.
- Raleigh, M. S., K. Rittger, C. E. Moore, B. Henn, J. A. Lutz, and J. D. Lundquist, 2013: Ground-based testing of MODIS fractional snow cover in subalpine meadows and forests of the Sierra Nevada. *Remote Sensing of Environment*, **128**, 44-57.
- Riggs, G. A., and D. K. Hall, 2002: Reduction of Cloud Obscuration in the MODIS Snow Data Product. *Proceedings of the 59th Eastern Snow Conference*, Stowe, Vermont, USA.
- Riggs, G. A., and D. K. Hall, 2012: Improved Detection of Snow Cover on Mountains with Revised MODIS Snow Algorithm. Poster presented at the 69th Eastern Snow Conference, Claryville (Frost Valley), New York, June 2012.
- Riggs, G. A., D. K. Hall, and V. V. Salomonson, 2006: MODIS Snow Products User Guide to Collection 5. *NASA Goddard Space Flight Center*.
- Rittger, K., T. H. Painter, and J. Dozier, 2012: Assessment of methods for mapping snow cover from MODIS. *Advances in Water Resources*, **51**, 367-380.
- Robinson, D. A., 1993: Monitoring Northern Hemisphere snow cover. *Snow Watch '92: Detection Strategies for Snow and Ice. Glaciological Data Report. GD-25*, National Snow and Ice Data Center, 1-25.
- Robinson, D. A., and A. Frei, 2000: Seasonal Variability of Northern Hemisphere Snow Extent Using Visible Satellite Data. *Professional Geographer*, **52:2**, 307-315.
- Robock, A., 1980: The Seasonal Cycle of Snow Cover, Sea Ice and Surface Albedo. *Monthly Weather Review*, **108**, 267-285.
- Salomonson, V. V., and I. Appel, 2004: Estimating fractional snow cover from MODIS using the normalized difference snow index. *Remote Sensing of Environment*, **89**, 351-360.
- Schultz, D. M., D. S. Arndt, D. J. Stensrud, and J. W. Hanna, 2004: Snowbands during the Cold-Air Outbreak of 23 January 2003. *Monthly Weather Review*, **132**, 827-842.

- Scott, D., B. Jones, and J. Konopek, 2007: Implications of climate and environmental change for nature-based tourism in the Canadian Rocky Mountains: A case study of Waterton Lakes National Park. *Tourism Management*, **28**, 570-579.
- Seager, R., Y. Kushnir, J. Nakamura, M. Ting, and N. Naik, 2010: Northern Hemisphere winter snow anomalies: ENSO, NAO and the winter of 2009/10. *Geophysical Research Letters*, **37**, L14703, doi: 2010GL043830.
- Şorman, A. Ü., Z. Akyürek, A. Şensoy, A. A. Şorman, and A. E. Tekeli, 2007: Commentary on comparison of MODIS snow cover and albedo products with ground observations over the mountainous terrain of Turkey. *Hydrology and Earth System Sciences*, **11**, 1353-1360.
- Steiger, R., and M. Mayer, 2008: Snowmaking and Climate Change. *Mountain Research and Development*, **28:3**, 292-298.
- Sugg, J. W., 2012: Land cover effects on snow classification in the Southern Appalachian Mountains. Poster presented at the 67th Annual Meeting of the Southeastern Division of the Association of American Geographers (SEDAAG), Asheville, NC, October, 2012.
- Sugg, J. W., L. B. Perry, and D. K. Hall, 2012: Satellite and surface perspectives of snow extent in the Southern Appalachian Mountains. *Proceedings of the 69th Eastern Snow Conference*, Claryville (Frost Valley), New York, USA. In Press.
- Tang, B., B. Shrestha, Z. Li, G. Liu, H. Ouyang, D. R. Gurung, A. Giriraj, and K. S. Aung, 2013: Determination of snow cover from MODIS data for the Tibetan Plateau region. *International Journal of Applied Earth Observation and Geoinformation*, **21**, 356-365.
- Tekeli, A. E., Z. Akyürek, A. A. Şorman, A. Şensoy, and A. Ü. Şorman, 2005: Using MODIS snow cover maps in modeling snowmelt runoff process in the eastern part of Turkey. *Remote Sensing of Environment*, **97**, 216-230.
- Tekeli, A. E., A. Şensoy, A. Şorman, Z. Akyürek, and Ü. Şorman, 2006: Accuracy assessment of MODIS daily snow albedo retrievals with *in situ* measurements in Karasu basin, Turkey. *Hydrological Processes*, **20**, 705-721.
- UCGIS, University Consortium for Geographic Information Science, 2002: *Research Agenda*. www.ucgis.org/priorities/research/
- UW-Madison SSEC (University of Wisconsin-Madison, Space Science and Engineering Center), cited 2012: MODIS Today. [ge.ssec.wisc.edu/modis-today/index.php]
- Vuille, M., B. Francou, P. Wagnon, I. Juen, G. Kaser, B. G. Mark, and R. S. Bradley, 2008: Climate change and tropical Andean glaciers: Past, present and future. *Earth-Science Reviews*, **89**, 79-96.
- Warren, S. G., 1982: Optical Properties of Snow. *Reviews of Geophysics and Space Physics*, **20:1**, 67-89.

Watanabe, M., and T. Nitta, 1998: Decadal Changes in the Atmospheric Circulation and Associated Surface Climate Variations in the Northern Hemisphere Winter. *Journal of Climate*, **12**, 494-510.

Wiscombe, W. J., and S. G. Warren, 1980: A Model for the Spectral Albedo of Snow. I: Pure Snow. *Journal of the Atmospheric Sciences*, **37**, 2712-2733.

Zängl, G., 2005: The impact of lee-side stratification on the spatial distribution of orographic precipitation. *Quarterly Journal of the Royal Meteorological Society*, **131:607**, 1075-1091.

Appendix A

Events suitable for analysis using the MODIS products.

Date	Satellite	Best Acquisition Date	Synoptic Class
12/7/2006	myd	8-Dec	U
12/26/2006	myd	27-Dec	X-U
1/9/2007	myd	10-Jan	SE-U
1/25/2007	myd	26-Jan	X-U
1/28/2007	myd	29-Jan	LC-U
2/6/2007	myd	8-Feb	SE-U
2/9/2007	mod	10-Feb	U
2/14/2007	myd	15-Feb	MBS-U
2/17/2007	myd	18-Feb	SE-U
3/4/2007	myd	6-Mar	U
11/15/2007	myd	16-Nov	U
12/16/2007	myd	17-Dec	MBN-U
1/1/2008	mod	3-Jan	MBN-U
1/17/2008	mod	18-Jan	MAB
1/19/2008	mod	20-Jan	X-U
2/14/2008	mod	14-Feb	LC-U
2/26/2008	mod	28-Feb	U
2/29/2008	mod	1-Mar	NEb
3/8/2008	mod	9-Mar	MAB-U
3/20/2008	mod	20-Mar	NE-U
3/24/2008	myd	25-Mar	U
10/28/2008	mod	29-Oct	LC-U
11/18/2008	mod	18-Nov	U
11/20/2008	myd	20-Nov	SE-U
12/5/2008	myd	7-Dec	U
12/13/2008	mod	13-Dec	U
1/18/2009	mod	21-Jan	SE-U
2/3/2009	mod	5-Feb	SE-U
2/22/2009	mod	23-Feb	NE-U
3/1/2009	mod	3-Mar	MAB-U
4/6/2009	mod	9-Apr	NE-U
10/18/2009	mod	19-Oct	U

Cont.

Date	Satellite	Best Acquisition Date	Synoptic Class
12/18/2009	myd	22-Dec	MABu
1/2/2010	myd	3-Jan	U
1/7/2010	myd	10-Jan	NE-U
1/29/2010	myd	31-Jan	MAB
2/3/2010	myd	3-Feb	MA-U
2/10/2010	myd	11-Feb	MBS-U
2/12/2010	mod	14-Feb	MA-U
2/15/2010	mod	19-Feb	MBN-U
2/24/2010	mod	26-Feb	MA-U
3/3/2010	mod	5-Mar	MA-U
11/5/2010	myd	6-Nov	U
12/4/2010	mod	9-Dec	X-U
12/12/2010	myd	14-Dec	NE-U
12/15/2010	mod	15-Dec	U
12/25/2010	myd	28-Dec	MA-U
1/7/2011	mod	9-Jan	SE-U
1/11/2011	mod	14-Jan	MABN-U
1/21/2011	myd	22-Jan	NE-U
1/26/2011	myd	27-Jan	MBS-U
1/28/2011	mod	29-Jan	SE-U
2/10/2011	myd	10-Feb	GU
3/10/2011	mod	12-Mar	NE-U
4/1/2011	mod	3-Apr	U
11/17/2011	mod	18-Nov	LC-U
11/29/2011	myd	1-Dec	CL-U
12/27/2011	myd	28-Dec	NE-U
1/2/2012	myd	4-Jan	U
1/14/2012	mod	14-Jan	SE-U
2/11/2012	myd	12-Feb	U
2/19/2012	mod	20-Feb	MABu
3/5/2012	myd	6-Mar	SE-U

Appendix B

Events unsuitable for analysis using MODIS products.

Date	Suitable for Analysis	Reason	Event Type
11/12/2006	N	cloud	LC-U
11/19/2006	N	time	U
1/21/2007	N	cloud	GU
1/23/2007	N	cloud	U
2/1/2007	N	cloud	GU
2/2/2007	N	cloud	NE-U
2/4/2007	N	cloud	X-U
3/16/2007	N	cloud	U
4/7/2007	N	cloud	LC-U
4/15/2007	N	cloud	MAB-U
11/23/2007	N	cloud	U
12/5/2007	N	cloud	SE-U
12/7/2007	N	cloud	X
12/19/2007	N	cloud	X-U
1/14/2008	N	cloud	NE-U
1/15/2008	N	cloud	U
1/24/2008	N	cloud	LC/SE-U
2/19/2008	N	cloud	U
3/5/2008	N	no snow	NE-U
4/13/2008	N	cloud	U
4/14/2008	N	cloud/nosnow	U
4/29/2008	N	cloud	SE-U
11/15/2008	N	cloud	NE-U
12/1/2008	N	cloud	NE-U
12/12/2008	N	modisdown	X-U
1/2/2009	N	modisdown	X
1/7/2009	N	modisdown	NE-U
1/8/2009	N	modisdown	X-U
1/13/2009	N	modisdown	NE-U

Cont.

Date	Suitable for Analysis	Reason	Event Type
2/2/2009	N	cloud	X-U
11/26/2009	N	no snow	NE-U
11/30/2009	N	no snow	NE-U
12/5/2009	N	cloud	MA-U
1/4/2010	N	cloud	U
1/25/2010	N	cloud	U
1/26/2010	N	cloud	U
2/5/2010	N	cloud	MBS
2/6/2010	N	cloud	MBS-U
2/28/2010	N	cloud	U
3/2/2010	N	cloud	MA
3/8/2010	N	cloud	X-U
3/22/2010	N	cloud/no snow	CL-U
12/1/2010	N	cloud	U
12/16/2010	N	cloud	SF
1/5/2011	N	cloud	X
1/10/2011	N	cloud	GU
1/24/2011	N	cloud	X
2/8/2011	N	cloud	NE-U
3/6/2011	N	cloud	MA
3/25/2011	N	-	U
4/2/2011	N	no snow	SE-U
4/5/2011	N	no snow	NE-U
10/1/2011	N	no snow	CL-U
10/29/2011	N	no snow	MAB-U
12/7/2011	N	cloud	LC-U
1/13/2012	N	cloud	NE-U
1/14/2012	N	cloud	U
2/8/2012	N	cloud	X-U
4/23/2012	N	cloud	CL-U

Biographical Information

Johnathan Sugg was born in Birmingham, AL, on October 17th, 1985. He attended Forest Hill Elementary, Liberty Middle School, and graduated from Freedom High School in Morganton, NC in May 2004. The following August, he entered Appalachian State University and received a Bachelor of Science degree in Geography in May 2008. In the fall of 2008, he accepted a position working as a GIS Specialist. In August 2011, he began work toward a Master of Arts in Geography at Appalachian State University, and was awarded the degree in May 2013. His permanent address is 2698 Lakeridge Ct., Nebo, NC 28761. His parents are Anne Gaillard Sugg and Wendell Arthur Sugg.